
Since January 2020 Elsevier has created a COVID-19 resource centre with free information in English and Mandarin on the novel coronavirus COVID-19. The COVID-19 resource centre is hosted on Elsevier Connect, the company's public news and information website.

CHAPTER

# 53

# Eye

*Leandro Teixeira, Richard R. Dubielzig*
**University of Wisconsin-Madison, Madison, WI, USA**

OUTLINE



*Haschek and Rousseaux's Handbook of Toxicologic Pathology, Third Edition.*
http://dx.doi.org/10.1016/B978-0-12-415759-0.00053-4

# 1. INTRODUCTION

This chapter presents a comprehensive description of pathological processes affecting the ocular tissues in the most commonly used laboratory animals, and their correlations with human diseases of interest in toxicology. Also presented are detailed descriptions of the structure and function of the different ocular tissues, the most advanced techniques applied in the toxicological evaluation of the eye, useful animal models of human disease, and known mechanisms of ocular toxicity. The introductory sections of the chapter also feature such essential topics as ocular embryology, an overview of clinical ophthalmic evaluation, and eye-specific techniques of tissue processing. A glossary of terms is found at the end of the chapter.

# 2. BIOLOGICAL AND ANATOMIC FEATURES UNIQUE TO THE MAMMALIAN EYE

## 2.1. Unique and Challenging Characteristics of Ocular Tissues

Evaluation of ocular tissues with the goal of assessing toxicity or evaluating the efficacy of a treatment or substance has many challenges that are shared with evaluation of non-ocular tissues. That said, there are many challenges facing the eye pathologist that are different from those facing the generalist.

The eye pathologist must understand the special requirements of tissue sampling, trimming, fixation, and histologic processing for eye specimens as a class, and also for distinctive eye specimens from particular species. For example, it is customary to trim the eyes of dogs, cats, and rabbits in the vertical plane to sample the retina above and below the optic nerve. In contrast, primate eyes are trimmed in the horizontal plane, with the goal of sampling the optic papilla, the fovea, and the pupil in the same section. Small rodent eyes often are best prepared if not trimmed at all, allowing the experienced histotechnician to trim into the block until a section is obtained that samples the optic nerve and pupil together. From the biologic and anatomic perspectives, the eye has several special characteristics that must be considered when evaluating ocular tissues.

## 2.2. Optical Clarity of Ocular Tissues

Perhaps the most obvious and also unique trait is the need for optical clarity that is absolutely essential if the cornea, aqueous chambers, lens, vitreous body, and inner retina are to function properly. Of course, optical clarity cannot be evaluated on a stained histology slide, so the pathologist must become aware of the changes in morphology in tissue sections that predict the existence of changes in optical clarity *in vivo*. One must also be aware that clinical evaluation may be a more sensitive means for detecting these changes than microscopic examination. Three common examples that illustrate this dilemma are corneal edema, cloudy aqueous humor, and cataract.

Corneal edema causes the cornea to thicken and become translucent, thus seriously impacting vision and predisposing to further corneal damage. The normal optical clarity of the cornea is dependent on an exacting arrangement of cells, collagen, and non-collagenous matrix in the corneal stroma. Therefore, the morphologist must rely on very subtle changes in the staining properties of various corneal tissues and on the quality of stromal changes (which are a predictable form of artifact) to assess the hydration status of the cornea.

Protein in the aqueous is a common cause of a cloudy appearance. This finding is best appreciated by slit-lamp examination. The

ophthalmologist observes the light traversing the aqueous, and any protein in the aqueous creates an effect known as aqueous flare; however, this effect is not appreciable to the histologist. Since aqueous flare is the hallmark of the clinical diagnosis of uveitis, there is often a disconnection between the clinical diagnosis of uveitis and the extent of uveal lesions that can be appreciated by histopathologic examination.

Cataract, or opacity of lens tissue, is a common endpoint following toxicant exposure. The lens is organized to have both optical clarity and a highly specified optical refractivity. As in the cornea, the optical properties of the lens depend on the spacing of cytoplasmic proteins. Some but not all of the changes that are seen with cataract have morphologic correlates that are appreciable when examining routine tissue sections. Frustratingly, many other structural features of cataract cannot be distinguished from artifact, so the ocular clinical exam is more likely to rule out cataract than will a microscopic analysis of the lens. That said there are also instances where microscopy can detect morphology changes in lens fibers that might not be detected clinically. For example, the authors have diagnosed lens fiber swelling in rodent eyes in several studies in which no clinical evidence of cataract was observed.

## 2.3. Structural Rigidity and Maintenance of Optical Focus

In order for the eye to focus light effectively, several structural characteristics need to be preserved. The size and rigidity of the globe have to be precisely matched with the refractive properties of the curved corneal surface and the location of the suspended lens such that light passing through the various ocular tissues is focused exactly on the retinal layer containing the photoreceptor outer segments. These properties are acquired during development and must be maintained in dynamic fashion throughout life if the function of the eye is to remain intact. In general, these properties depend on a precise balance in the production of molecules that help regulate the deposition and degradation of extracellular matrix. The pathologist, who views a static snapshot of heavily processed ocular anatomy, is only partially able to judge the likely integrity of optical focus and the preservation of such characteristics as the size and rigidity of the globe.

## 2.4. Immune Privilege and the Eye

In order to maintain all the characteristics of optical clarity and precise interrelationships among the ocular tissues, a strict control of the ocular inflammatory response is essential. Whereas other tissues can overcome the effects of limited inflammation because of built-in redundancy, the function of the eye is dependent on maintaining exact structural relationships and physiological homeostasis, which are not easily preserved in the face of even minor and transient inflammation. The tissues of the eye are replete with built-in cytokines and immune regulatory factors which, alone or in combination, have the effect of downregulating inflammation. Among these, the secretion of transforming growth factor-beta 2 (TGF-β2) and interleukin-6 (IL-6) by the anterior uveal epithelium and corneal endothelial cells play a major role. In addition, the anterior chamber-associated immune deviation (ACAID) phenomenon is designed such that antigens presented in the anterior chamber are captured by intraocular antigen-presenting cells (APCs) which transfer them directly to the blood stream (via the trabecular meshwork) and present them to the spleen (Figure 53.1). In the spleen, these eye-derived APCs selectively rest on the marginal zone and stimulate the production of T-regulatory cells ($T_{reg}$), which in turn suppress the initial activation of Th1 and Th2 effector cells, inducing tolerance to ocular antigens. The critical roles that these distinctive immunologic mechanisms play in ocular tissues have to be carefully considered when interpreting inflammation and immunologic properties in studies of ocular pathology. The potency of these novel immune regulatory pathways may obscure the relationship between cause and effect in the eye to a much greater extent than may be evident in other tissues.

## 2.5. Embryology and Interpretation of Ocular Tissue Changes

Table 53.1 offers timelines for the comparative embryological development of the dog, mouse, and human. Since toxicologic pathologists use numerous different animals as test systems, we will refer the reader to the literature regarding embryology for select species. It is worthy of

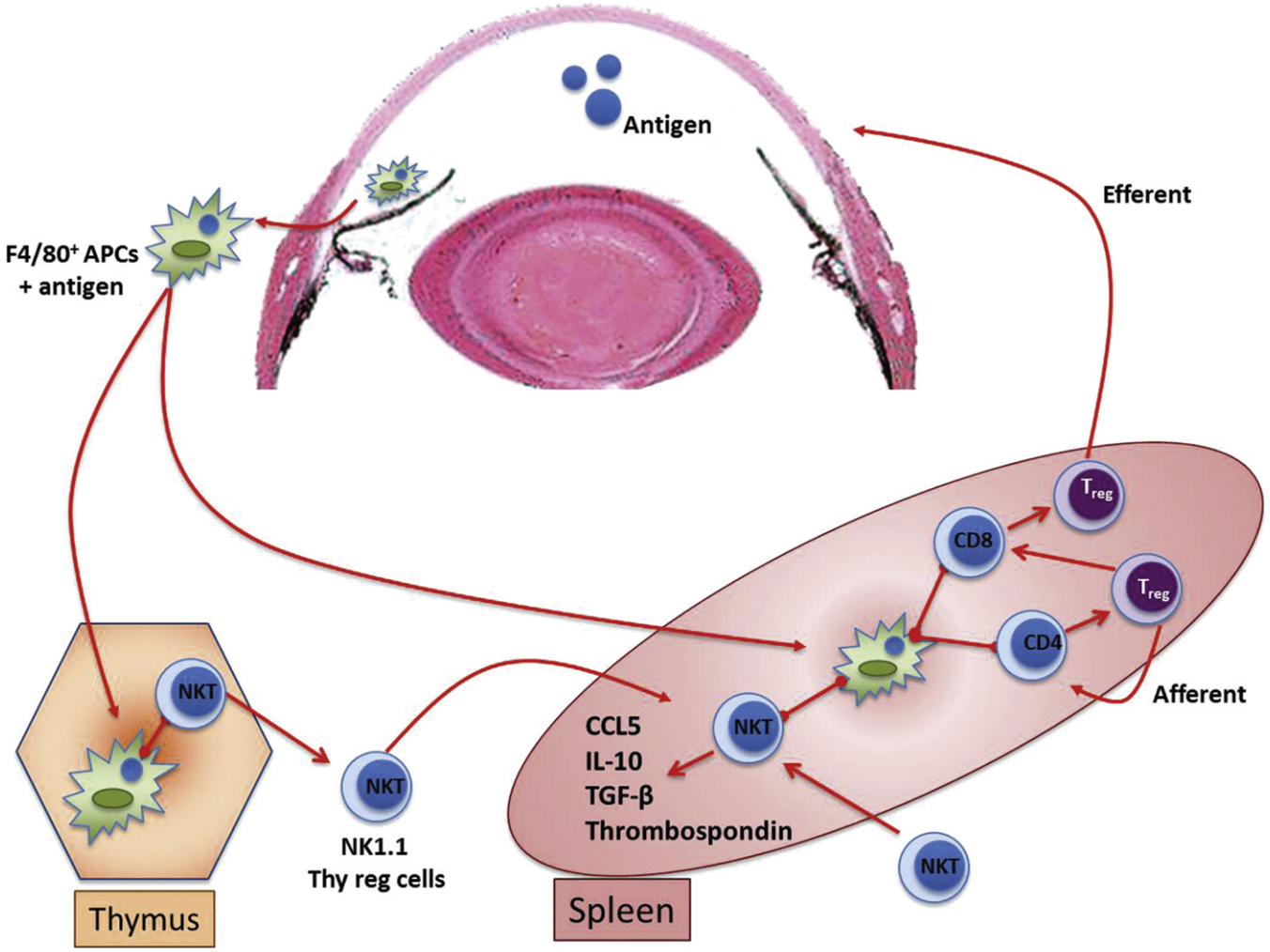


FIGURE 53.1 Anterior chamber-associated immune deviation (ACAID) system. Intraocular antigen (blue circles) is phagocytized by indigenous F4/80$^{+}$ antigen-presenting cells (APCs [pale green stellate shapes]), which leave the eye through the trabecular meshwork and scleral veins. These cells present antigens to lymphocytes residing in the secondary lymphoid organs. In the spleen, APCs selectively home to the marginal zone where they recruit natural killer T cells (NKT) and produce an environment rich in thrombospondin, transforming growth factor-beta (TGF-β), interleukin-10 (IL-10), and chemokine C-C motif ligand 5 (CCL5). This environment will in turn recruit CD4+ and CD8+ T-cells specific for ocular-derived antigens that, after interacting with the eye-derived APCs, will be transformed into CD4+ and CD8+ regulatory T cells ($T_{reg}$). The CD4+ $T_{reg}$ (afferent $T_{reg}$) will inhibit the activation and transformation of naïve T cells into $T_H1$ effector cells in the secondary lymphoid organs, and CD8+ $T_{reg}$ (efferent $T_{reg}$) will inhibit the expression of a $T_H1$ response in the peripheral tissues, including the eye. In the thymus, APCs carrying ocular antigens interact with NKT cells, transforming them into NK1.1 Thy regulatory cells that migrate to the spleen and help in the transformation of CD4+ and CD8+ T cells into $T_{reg}$ cells.

attention that, in experiments where the development of the eye is a central issue, the zebrafish offers an excellent model system as progression from a fertilized egg to a fully differentiated eye occurs in approximately 72 hours post-fertilization, which presents a very attractive time-saving model.

### *Tissue Derivation of Ocular Structures*

Developmentally, the tissues of the eye are derived from multiple progenitor sources, with substantial contributions from the neural crest, mesoderm, neuroectoderm (neural tube epithelium), and surface ectoderm. Endoderm does not contribute to the formation of the eye.

**TABLE 53.1** Sequence of Ocular Development

| Human (approximate postfertilization age) | | | Day post-fertilization | | |
|---|---|---|---|---|---|
| **Month** | **Week** | **Day** | **Mouse** | **Dog** | **Developmental events** |
| 1 | 3 | 22 | 8 | 13 | Optic sulci present in forebrain |
| | 4 | 24 | 9 | 15 | Optic sulci convert into optic vesicles |
| | | | 10 | 17 | Optic vesicle contacts surface ectoderm |
| | | 26 | | | Lens placode begins to thicken |
| | | | | | Optic vesicle surrounded by neural crest mesenchyme |
| 2 | 5 | 28 | 10.5 | | Optic vesicle begins to invaginate, forming optic cup |
| | | | | | Lens pit forms as lens placode invaginates |
| | | | | | Retinal primordium thickens, marginal zone present |
| | | 32 | 11 | 19 | Optic vesicle invaginated to form optic cup |
| | | | | | Optic fissure delineated |
| | | | | | Retinal primordium consists of external limiting membrane, proliferative zone, primitive zone, marginal zone, and internal limiting membrane |
| | | | | | Oculomotor nerve present |
| | | 33 | 11.5 | 25 | Pigment in outer layer of optic cup |
| | | | | | Hyaloid artery enters through the optic fissure |
| | | | | | Lens vesicle separated from surface ectoderm |
| | | | | | Lens surrounded by intact basement membrane (lens capsule) |
| | | | | | Retina: inner marginal and outer nuclear zones |
| | | | 11.5 | 29 | Basement membrane of surface ectoderm intact |
| | | | | | Primary lens fibers form |
| | | | | | Trochlear and abducens nerves appear |
| | | | | | Lid folds present |
| | 6 | 37 | 12 | | Edges of optic fissure in contact |
| | | | 12 | 30 | Tunica vasculosa lentis present |
| | | | | | Lens vesicle cavity obliterated |

(*Continued*)

**TABLE 53.1** Sequence of Ocular Development—cont'd

| Human (approximate postfertilization age) | | | Day post-fertilization | | |
|---|---|---|---|---|---|
| **Month** | **Week** | **Day** | **Mouse** | **Dog** | **Developmental events** |
| | | | | | Ciliary ganglion present |
| | | 41 | 12 | 32 | Posterior retina consists of nerve fiber layer, inner neuroblastic layer, transient fiber layer of Chievitz, proliferative zone, outer neuroblastic layer, and external limiting membrane |
| | | | 17 | 32 | Eyelids fuse (dog) |
| | 7 | | | | Anterior chamber beginning to form |
| | | | 12.5 | 40 | Secondary lens fibers present |
| | | 48 | 14 | 32 | Corneal endothelium differentiated |
| | 8 | 51 | | | Optic nerve fibers reach the brain |
| | | | | | Optic stalk cavity is obliterated |
| | | | | | Lens sutures appear |
| | | | | | Acellular corneal stroma present |
| | | 54 | | 30–35 | Scleral condensation present |
| | 9 | 57 | 17 | 40 | First indication of ciliary processes and iris |
| | | | | | Extraocular muscles visible |
| | | | | — | Eyelids fuse (occurs earlier in the dog) |
| | 10 | | | 45 | Pigment visible in iris stroma |
| | | | | | Ciliary processes touch lens equator |
| | | | | | Rudimentary rods and cones appear |
| | | | | 45–1P | Hyaloid artery begins to atrophy to the disc |
| 3 | 12 | | | — | Branches of the central retinal artery form |
| 4 | | | | 51 | Pupillary sphincter differentiates |
| | | | | | Retinal vessels present |
| | | | | 56 | Ciliary muscle appears |
| | | | | — | Eye axis forward (human) |
| — | | | | 56 | Tapetum present (dog) |
| | | | | 2–14 P | Tunica vasculosa lentis atrophies |
| | | | | | Short eyelashes appear |
| 5 | | | | 40 | Layers of the choriod are complete with pigmentation |
| 6 | | | | — | Eyelids begin to open, light perception |

**TABLE 53.1** Sequence of Ocular Development—cont'd

| Human (approximate postfertilization age) | | | Day post-fertilization | | |
|---|---|---|---|---|---|
| **Month** | **Week** | **Day** | **Mouse** | **Dog** | **Developmental events** |
| | | | | 1 P | Pupillary dilator muscle present |
| 7 | | | | 1–14 P | Pupillary membrane atrophies |
| | | | | 1–16 P | Rod and cone inner and outer segments present in posterior retina |
| | | | | 10–13 P | Pars plana distinct |
| 9 | | | | 16–40t P | Retinal layers developed |
| | | | | 14 P | Regression of pupillary membrane, TVL, and hyaloid artery nearly complete |
| | | | | | Lacrimal duct canalized |

*Table reproduced from Handbook of Toxicologic Pathology, 2nd Ed. W. M. Haschek, C. G. Rousseaux and M. A. Wallig, eds. (2002) Academic Press, Table. 1, p 541–42, with permission.*

Furthermore, many of the types of cellular differentiation in ocular tissues represent completely unique pathways for the germ layer of origin that manifest through several surprising differentiation pathways.

The surface ectoderm gives rise to multiple epithelial structures in and around the eye. The lens is the primary intraocular derivative, while the epithelium of the cornea is the only other major eye component arising from this embryonic layer. Periocular tissues that evolve from the surface ectoderm include the conjunctiva, the lacrimal gland, the adnexal glands (e.g., sebaceous [meibomian] glands in the eyelids), and the epidermis of the eyelids.

The neural ectoderm gives rise to the optic vesicle and optic cup. This embryonic layer thus is responsible for the formation of the intraocular neural and neural-like tissues: the retina and retinal pigment epithelium (RPE), pigmented and non-pigmented epithelial layers of the ciliary body, and the optic nerve fibers (i.e., axons) and glia. Neural ectoderm is also the source for the posterior epithelium as well as the dilator and sphincter muscles of the iris.

The neural crest, which arises from the surface ectoderm located immediately adjacent to the tips of the folds of neural ectoderm, is responsible for producing many ocular tissues. Major elements include the corneal keratocytes (corneal stromal cells), the endothelium of the cornea, the trabecular meshwork, the stroma and melanocytes of the uvea, the ciliary muscle, the fibroblasts of the sclera, the vitreous, and the optic nerve meninges. It is also involved in formation of the orbital connective tissues and nerves, the extraocular muscles, and the sub-epidermal layers of the eyelids.

The connective tissues of the eye once were thought to be derived from mesoderm. However, it has been shown more recently that most mesenchymal derivatives in the head and neck region are derived from the cranial neural crest.

## *Major Steps in Ocular Differentiation*

### OPTIC VESICLE STAGE

The embryonic plate is the earliest stage in which ocular differentiation can be found. The edges of the neural plate thicken to form the neural folds. The elevating neural folds then fuse to form the neural tube, which becomes surrounded by mesoderm and detaches from the surface epithelium. The site of the optic groove or optic sulcus is in the cephalic neural folds on either side of or parallel to the neural groove. Just before the rostral (anterior) portion of the neural tube closes completely, neural ectoderm grows outward from the neural tube and toward the surface ectoderm on either side to form the spherical optic vesicles.

The optic vesicles are connected to the forebrain by the optic stalks. At this stage,

a thickening of the surface ectoderm (lens plate) begins at the opposite (i.e., superficial) end of the optic vesicles, which are expanding towards the surface.

#### OPTIC CUP STAGE

As the optic vesicle invaginates to produce the optic cup, the original superficial wall of the spherical optic vesicle inverts to assume a position located parallel near the inner wall. The invagination of the ventral surface of the optic stalk and of the optic vesicle occurs simultaneously and creates a groove, the optic (embryonic) fissure. The margins of the optic cup then grow around the optic fissure. At the same time, the lens plate invaginates and separates from the surface ectoderm to form first a cup and then a hollow sphere known as the lens vesicle, which lies free in the rim of the optic cup.

The optic fissure allows the vascular mesoderm to enter the optic stalk and eventually to form the hyaloid vascular system of the vitreous cavity. As invagination is completed, the optic fissure narrows and closes leaving one small opening at the rostral (anterior) end of the optic stalk through which the hyaloid artery passes.

At this stage, the ultimate general pattern of the eye has been determined. Further development of the eye consists in differentiation of the individual optic structures. In general, in all mammalian species differentiation of the optic structures occurs more rapidly in the caudal (posterior) than in the rostral (anterior) segment of the eye during the early stages, and more rapidly in the anterior segment during the later stages of gestation.

### *Summary Principles of Ocular Embryology*

The retina and retinal pigment epithelium (RPE) are derived from neuroectoderm. This origin is expected, given the essentially neural nature and function of these closely related layers. It is more surprising that the neural tube also gives rise to the ciliary and iris epithelium as well as the iris sphincter and dilator muscles. The lens is derived from surface ectoderm, but it is so highly specialized that it has little similarity to any other tissues of ectodermal origin (Figure 53.2).

One must always keep in mind that the vitreous and aqueous humors of the eye are in fact tissues and not simply gels. If the morphologist forgets the embryologic origin of these uniquely derived ocular tissues, it is difficult to comprehend the patterns of reaction – in terms of both structural changes and protein expression – that eye tissues undertake in response to disease processes.

### *Developmental Abnormalities*

The embryology of the eye is complex and involves numerous inductive relationships in which one component works by proximity to stimulate a developmental event in another component, often one derived from a different germ layer. Ocular developmental abnormalities are common in humans, domestic animals, and laboratory animals. They can be a part of hereditary disease processes passed on from generation to generation, or they can be the result of exposure to teratogenic compounds that affect development of the eye *in utero* without affecting the genome. In either case, ocular abnormalities can be limited to the eye or periocular tissues, but they are often part of systemic syndromes where the effect on ocular tissues is but one of many lesions induced in multiple organ systems. Toxicity studies often need to evaluate for either genotoxic or teratogenic potential, and evaluation of the developing eye in treated embryos has a role in modern toxicologic pathology. Although the mouse model is most often used for this assessment, the zebrafish model has many potential advantages, including the rapid pace of embryonic development, the transparency of fish embryos throughout the period of ocular embryogenesis, and the large numbers of offspring.

The most common ocular developmental problems encountered in both the teratogenic and genetic scenarios are lesions that involve inductive phenomena such as closure of the optic fissure, separation of the lens vesicle, or replacement of the primary vitreous. Congenital cataract or abnormalities of lens size or position are other fairly frequent problems that may be observed in developmental toxicity studies (Figure 53.3). We provide a list of known teratogenic substances affecting the eye in Table 53.2.

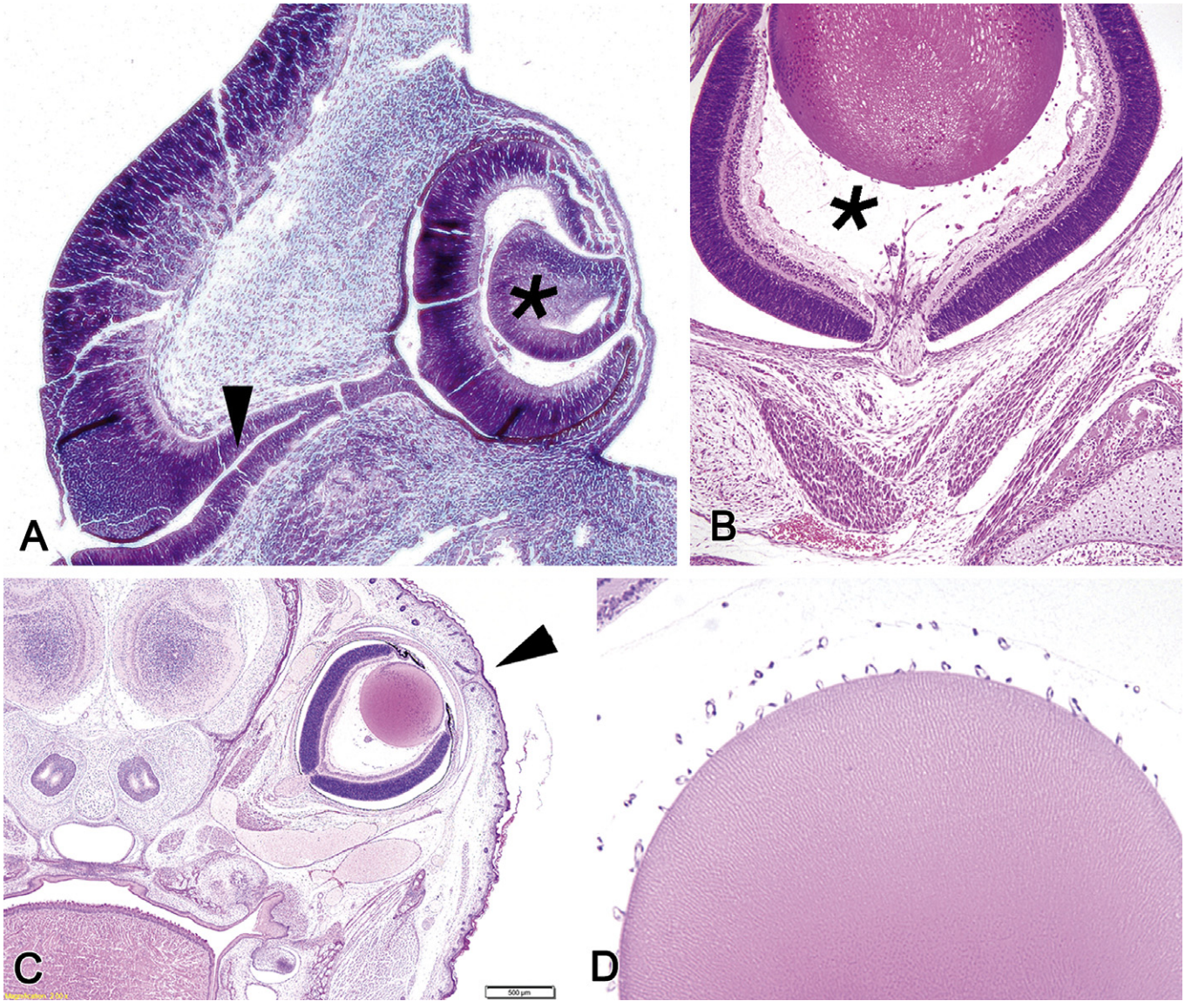


FIGURE 53.2 Embryology of the mammalian eye. (A) Developing eye from a mid-term (gestational day 128) equine embryo showing the developing neuroretina (thick C-shaped layer lining the deep portion of the globe and encircling the lens vesicle), lens vesicle (*) and the optic stalk (or primitive optic nerve [arrowhead]). (B) Near-term mouse fetus showing the primary vitreous (*) between the lens (pale eosinophilic orb at the top) and retina (thick multi-laminar layer at the bottom). (C) Near-term mouse fetus showing the fused eyelids; the arrowhead points to the cleft where the palpebrae (eyelids) will eventually separate. (D) Lens from a near-term mouse fetus showing the *tunica vascularis lentis* (as small, regularly spaced capillary cross-sections along the posterior [upper] edge of the lens). (A) Periodic acid-Schiff stain (PAS), 100×; (B) H&E, 200×; (C) H&E, 40×; (D) H&E, 200×.

## 3. TOXICOLOGICAL, CLINICAL, AND PATHOLOGICAL EVALUATION OF THE EYE

### 3.1. Animal Models

In preclinical drug development, animal test systems are the backbone of hazard identification and risk assessment (see *Pathology in Non-Clinical Safety Assessment*, *Chapter 24*). While *in vitro* test systems are being used increasingly to probe relevant questions, none of the current methods for culturing ocular tissues can mimic the whole animal setting in performing these safety assessment functions.

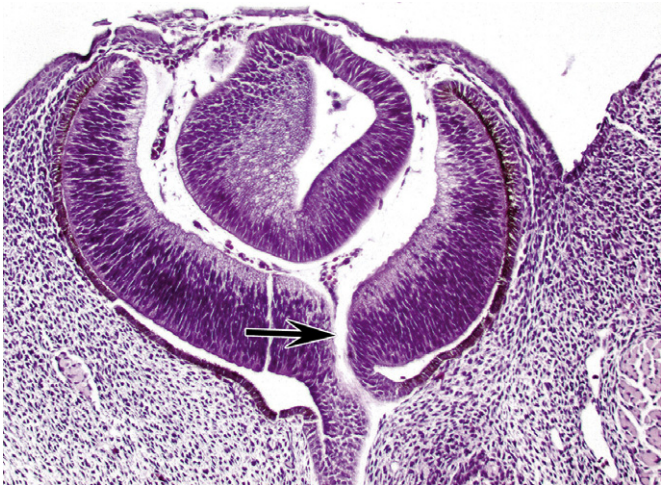

FIGURE 53.3 Normal architecture of the optic fissure and optic nerve. Developing eye of a mid-term horse embryo (gestational day 128) showing the optic fissure (arrow) with mesenchyme extending into the area of the primary vitreous beneath the lens vesicle. The retinal pigmented epithelium (RPE) appears as a thin pigmented layer beneath the thick retinal primordium. H&E, 100×.

When choosing the most appropriate animal test system in an ocular toxicity experiment, many factors need to be considered.

1. **The model should be well characterized.** The animal species that are commonly used as models in ocular toxicologic pathology are rodents (mouse, rat), rabbits, and larger animals (dog, non-human primate). Although less common in the past, zebrafish are gaining popularity rapidly as models for ocular toxicologic pathology studies. Although there may be specific reasons to choose some other species, the bias is to use an animal model is founded in the large mass of historic data with well-characterized background changes and expected variations for these mammalian species. Husbandry characteristics, including their potential effects on ocular health, are well defined. Standard operating procedures and handling protocols are familiar and proven.
   Cats are a favorite species used in basic vision science experiments, so there is abundant experience and data on how the cat eye functions. Cats are not often used in toxicologic vision science. Given the familiarity with the eye and central visual pathways in this species, one might ask if cats are in fact underused in ocular toxicity research.
2. **The model should be appropriate for the experimental question.** Although small rodents have incalculable value as test models in toxicologic pathology, the small size of the rodent eye and the relatively large size of the lens often preclude the use of such models when certain in-life procedures are a part of the experimental design. Some examples of procedures that are either unachievable or achievable only with great effort and/or risk in rodents are intraocular injections, sampling of aqueous or vitreous, tonometry, fundoscopy, and conventional surgery (e.g., glaucoma filtration procedures). On the other hand, the small eye size in rodents makes it possible to sample the entire eye by making serial or short-interval step sections through the globe. Other in-life procedures, like optical coherence tomography (OCT) and fluorescein angiography, can be employed successfully in small rodent eyes, although the technical skill needed for working with such small specimens must be honed over time by painstaking practice.
3. **The model should be anatomically appropriate.** The usual species of interest when evaluating the impact of ocular toxicants to the visual system is the human. While eyes of vertebrates share many more similarities than differences regarding structure and function, many experimental hypotheses are most reliably answered using an animal model that best represents the anatomic and functional properties of the human situation. Largely for this reason, in toxicologic vision protocols the non-human primate is almost a default favorite as the animal model of choice. The species with the most historical data and accumulated experience are rhesus macaques (*Macaca mulatta*) and cynomolgus monkeys (*Macaca fascicularis*). Unique anatomic features in the monkey eye that are almost identical to traits in the human eye are the presence of a cone-rich retina with a fovea, the number and distribution of ganglion cells, the structure and physiology of the aqueous

drainage system, the robust accommodation system, and the anatomy of the optic nerve. Also important is the tear film biology and the anatomy of the lids, including the adnexal glands and conjunctiva. The neurobiology of vision as assessed by visual-evoked potentials (VEP) and non-invasive imaging procedures of the brain is also optimally tested in the non-human primate.

4. Since rodents, rabbits, and dogs are also commonly used for ocular toxicity testing, some **anatomic variations in these species** should receive consideration prior to selecting an animal system for modeling the human eye. Albino rodents present many challenges with regard to their appropriateness in ocular toxicologic pathology. They are prone to retinal phototoxicity, which typically presents as marked retinal atrophy (Figure 53.4) and blindness, and also exhibit drug distribution differences relative to pigmented eyes. The differences in drugs distribution are usually associated with drug binding by melanin, so they can be very difficult to characterize. Many rodent strains have heritable retinal degeneration as a background finding (e.g., the *rd* gene), so retinal morphology is substantially abnormal even in the control groups. Rabbits have distinctive tear biology owing to the lipid-rich secretions of the large Harderian gland, which protect the ocular surfaces without frequent blinking. However, this characteristic variation might impact topical drug distribution, absorption, and efficacy. Rabbits also have a unique retinal vasculature and optic nerve morphology which might impact glaucoma research if the optic nerve is the target tissue (Figure 53.5). Dogs and cats have a tapetum lucidum behind a large portion of the retina above the optic nerve. This reflective layer functions to enhance dim light vision but may complicate procedures like fluorescein angiography or OCT. The RPE cells in the tapetal zone do not have melanin pigment. There are instances where substance toxicity specifically affects the tapetum. Since this region is absent in humans, such tapetal toxicants likely have no biological significance in humans.
5. **The model should be useful for both acute and chronic studies.** It is not efficient to use animal models where aging is an important part of the testing strategy if the animal in question takes 10 years or longer to age. Laboratory rodents achieve advanced age in 2 years, making them useful for chronic studies.
6. **The model should be cost-effective.** Small rodents provide obvious cost efficiency, although careful consideration should be given to the likelihood of success if certain protocols and procedures are to be employed. It may end up being cheaper to conduct an experiment on a non-human primate if the vision scientist can more easily translate the necessary procedures and resulting data for human risk assessment.
7. **The model should be appropriate for answering questions about efficacy.** Many animal models of disease have been developed to mimic aspects of particular human ophthalmologic diseases. These models may be useful in drug testing, particularly when evaluating molecule effectiveness. Some examples are provided below.
8. **Genetically engineered animal models.** Many current models of human disease are produced by manipulating the genome of test animals, usually mice. Models can be developed that mimic heritable ocular disease in humans if the mutant gene is known or if ocular phenotypes can be elicited by manipulating the tissue physiology or by altering gene expression. By way of example, a model of the human retinal condition Leber's congenital amaurosis can be produced in mice by removing the gene for retinal pigment epithelium-specific 65-kDa protein (RPE 65), the same gene responsible for the disease in humans. The mouse model then can be used in trials of gene replacement therapy. Likewise, overexpression of the gene responsible for the production of vascular endothelial growth factor (VEGF) can be induced locally in the RPE by linking expression of an installed gene with a protein native to the RPE, thus causing overstimulation of VEGF production. This model has been used to study choroidal neovascularization.

TABLE 53.2 Chemicals and Drugs Causing Eye Malformations

| Chemical | Animal | Malformation |
|---|---|---|
| Actinomycin | Rat | Anophthalmia, coloboma |
| Adenine | Rat | Anophthalmia, microphthalmia |
| Adrenalin (epinephrine) | Rat | Cataract |
| Alcohol | Mouse | Coloboma, open eye |
| | Rat | Anophthalmia, opaque lens |
| Alloxan | Mouse, rat | Microphthalmia |
| 6-Aminonicotinamide | Mouse | Microphthalmia, open eye, retinal folds |
| | Rat* | Lens vacuolation, retinal folds |
| Aminophenurobutane | Rat | Anophthalmia, microphthalmia, no optic nerve |
| Aminothiadiazole | Rat* | Anophthalmia, microphthalmia |
| Arsenic | Hamster | Anophthalmia |
| | Mouse | Anophthalmia, open eye |
| | Rat* | Anophthalmia, microphthalmia |
| 5-Bromodeoxyuridine | Mouse | Open eye |
| Cadmium | Hamster | Microphthalmia |
| | Mouse | Anophthalmia, microphthalmia |
| | Rat* | Anophthalmia, microphthalmia |
| Carbutamide | Mouse | Anophthalmia, microphthalmia, cataract |
| | Rat | Anophthalmia, no optic nerve |
| Chloraminophen | Mouse | Microphthalmia, no optic nerve |
| Chloroquine | Rat | Anophthalmia, microphthalmia |
| Congo red | Rat | Anophthalmia, microphthalmia |
| Cyclopamine | Rabbit | Cyclopia |
| Cyclophosphamide | Mouse | Aphakia, open eye |
| | Rabbit | Coloboma, microphthalmia, retinal folds |
| | Rat* | Cataract, exophthalmos, open eye |
| Cytosine arabinoside | Mouse | Retinal dysplasia |
| | Rat | Retinal dysplasia |
| Diphenylhydantoin | Mouse | Open eye |
| Dithiocarbamate | Rat* | Exophthalmos |
| 1-Ethyl-1-nitrosourea | Mouse | Anophthalmia, microphthalmia, exophthalmos |
| Ethylenedia-minetetraacetic acid | Rat* | Anophthalmia, microphthalmia |
| Ethylenethiourea | Rat | Coloboma, exophthalmos |
| Galactose | Rat | Anophthalmia, cataract |

**TABLE 53.2** Chemicals and Drugs Causing Eye Malformations—cont'd

| Chemical | Animal | Malformation |
|---|---|---|
| Glucagon | Rat | Glaucoma, microphthalmia |
| Griseofulvin | Rat | Anophthalmia |
| Hycanthone | Mouse | Microphthalmia |
| Hydrazine | Mouse, rat | Anophthalmia, microphthalmia |
| Hydrocortisone | Guinea pig | Open eye |
| Leucine | Rat | Anophthalmia, microphthalmia |
| Lithium | Rat | Anophthalmia |
| Methamphetamine | Mouse | Anophthalmia, microphthalmia |
| | Rabbit | Cyclopia |
| Mercury | Rat | Exophthalmos, microphthalmia, opaque cornea and lens |
| Niagara sky blue 6B | Rat* | Anophthalmia, microphthalmia |
| Ochratoxin A | Mouse | Anophthalmia, open eye |
| Perphenazine | Rat | Anophthalmia |
| Pesticides (aldrin, dieldrin, endrin) | Hamster | Open eye |
| Phthalic esters | Rat | Anophthalmia |
| Procarbazine | Rat | Anophthalmia, microphthalmia |
| Reserpine | Rat | Anophthalmia |
| Retinoic acid | Hamster | Microphthalmia |
| | Mouse, rat | Anophthalmia, exophthalmos, microphthalmia, open eye |
| Ribavirin | Hamster | Anophthalmia, microphthalmia, open eye |
| Rubidomycin | Rat | Anophthalmia, microphthalmia, |
| Rubratoxin | Mouse | Open eye |
| Saccharine | Rat | Lens necrosis, abnormal optic nerve |
| Salicylate | Rat | Open eye, retinals dysplasia |
| Serotonin | Mouse | Anophthalmia |
| | Rat | Anophthalmia |
| Streptonigrin | Rat* | Microphthalmia |
| Triparanol | Rat* | Anophthalmia, microphthalmia |
| Trypan blue | Mouse | Anophthalmia, microphthalmia, |
| | Rat* | Anophthalmia, microphthalmia, lens degeneration, abnormal optic nerve, retinal dysplasia |
| Urethane | Rat | Open eye, lens vacuolation |
| Vinblastine, vincristine | Hamster | Anophthalmia, microphthalmia, |
| | Mouse | Anophthalmia |
| | Rat* | Anophthalmia, microphthalmia, |

** 50% or more of the surviving fetuses have eye malformations.*

*Table reproduced from* Handbook of Toxicologic Pathology, *2nd Ed. W. M. Haschek, C. G. Rousseaux and M. A. Wallig, eds. (2002) Academic Press, Vol. 2, Table II, pp. 544–545, with permission.*

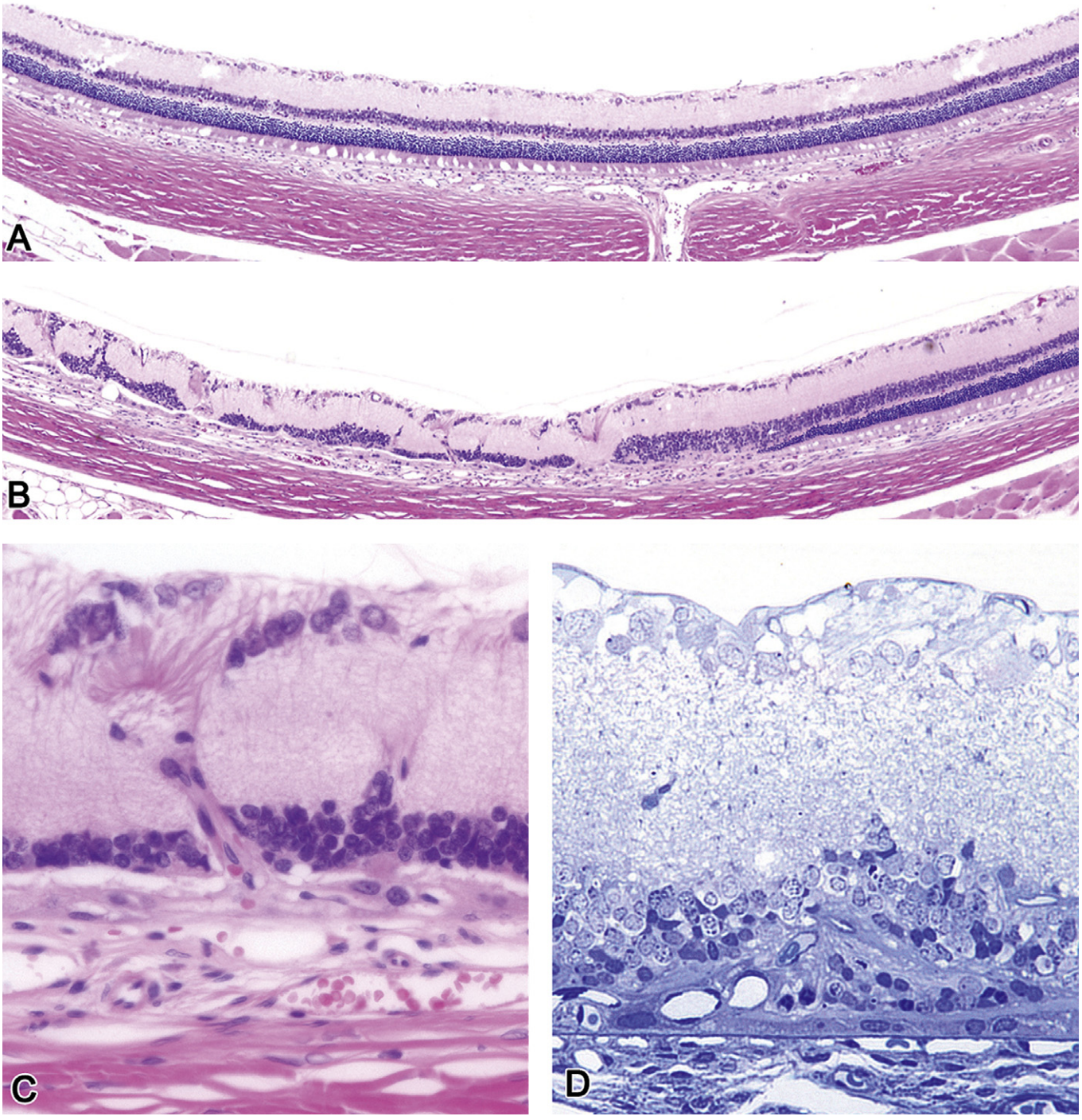


FIGURE 53.4 Chronic phototoxicity in an albino rat. (A) Normal retina, showing the distinct alternating layers of nuclei (dark bands) and cell processes (pale bands). (B) Segmental outer retinal atrophy caused by phototoxicity, indicated by variable loss of the nuclear bands (especially toward the left of the image). (C) Higher magnification of the affected retina showing vascular proliferation into the retina and focal displacement of retinal nuclei as part of the typical findings. (D) Plastic section of a similarly affected area showing outer retinal atrophy and vessels growing in the retinal pigment epithelial layer. (A, B) H&E, 50×; (C) H&E, 600×; (D) Toluidine blue, 600×.

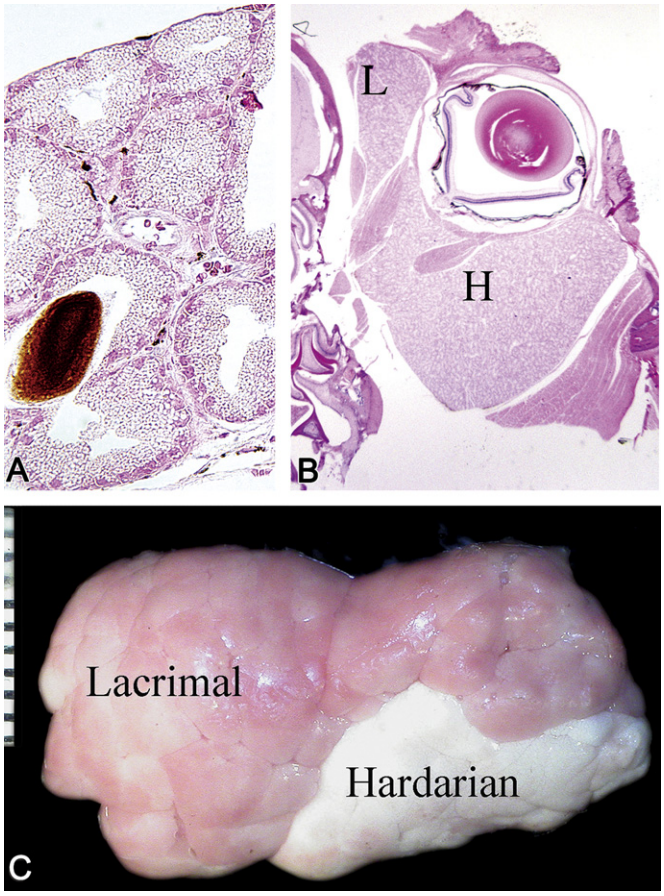


FIGURE 53.5 Normal architecture of the Harderian and lacrimal glands. (A) High magnification image of the Harderian gland from a mouse showing the lipid vacuoles within the acinar epithelium and secreted porphyrin pigment within the lumen. (B) Low-magnification view of the mouse globe *in situ* showing the relative sizes of the Harderian (H) and lacrimal (L) glands. (C) The lacrimal and Harderian glands dissected from the orbit of a rabbit showing the difference in color. Scale, 1 interval = 1 mm. (A) H&E, 200×; (B) H&E, 20×.

9. **Spontaneous animal models of human disease.** Animals are susceptible to ocular diseases that share many similarities to human eye diseases, and the treatments employed are nearly identical across species. The trouble is that the factors responsible for spontaneous animal eye diseases, like cataract, glaucoma, or keratoconjunctivitis sicca ("dry eye"), are not well understood, and there is no practical way of developing an affected group. Clinical trials in animal hospitals have been used in limited studies in veterinary ophthalmology research. Spontaneous heritable diseases in animals have been used very successfully as models of similar or identical human disease. The development of successful gene treatment of Leber's congenital amaurosis in humans was first achieved in a spontaneous dog model.

## 3.2. Clinical Ophthalmic Examination

The experimental endpoint in drug development often might be a measurement made by the clinician or an ophthalmic specialist rather than the pathologist. As an example, nonhuman primate models with induced high intraocular pressure (IOP) treated with IOP-lowering drugs can be monitored rapidly and quantitatively by measuring the IOP using a tonometer without the need to necropsy valuable animals. Some other examples where clinical or procedural measurements might be more important than histopathology are given below.

Many analytical procedures are available for the clinical examination of eyes in live animals. A few of the more common techniques are discussed here.

1. **Clinical assessment of optical clarity.** The slit lamp is used to evaluate the optical transparency of the cornea, aqueous, lens, vitreous, and retina. This property cannot be evaluated on a microscope slide.
2. **Evaluation of emmetropia.** Normal focus (emmetropia) requires the appropriate combination of ocular refraction by the lens and axial length of the globe. The quality of having an eye "in focus" can be evaluated by retinoscopy, a procedure using lenses to observe the pattern of fundic reflection. The morphologist is unable to make this determination.
3. **Evaluation of tear formation.** The Schirmer's tear test uses absorptive paper applied inside the conjunctival cul-de-sac to assess the production of tears. No comparable test can be done post-mortem, nor is this functional parameter subject to measurement by light microscopy.
4. **Evaluation of corneal sensation.** Sensory innervation to the eye is evaluated using an asthesiometer. This device quantifies minute differences in pressure applied directly to the corneal surface in the conscious animal, using the blink as an endpoint.
5. **Fundoscopy.** A well-designed non-clinical ocular toxicity study in which retinal effects are to be evaluated should include examination and photographic ocular imaging of the retina. Interpretation of data should rest with an individual who is both qualified and, ideally, masked to the identities of the treatment groups until the image interpretations are completed. When examining the fundus in the live animal, the clinician is essentially evaluating the gross pathology of the tissue. The advantage of fundoscopy is that the entire fundus is evaluated rather than a small (5-μm thick) section. Also, fundoscopic examination allows data collection at multiple points throughout the study, comparison between baseline images and post-treatment, retrospective analysis of data, and assessment of dose response changes and recovery of animals.
6. **Fluorescein angiography.** The small molecular size of fluorescein gives information about the integrity of the blood–retinal barrier in the living eye, which is not obtainable by other diagnostic means. The blood–retinal barrier in the eye is located in two places – the endothelial cell tight junctions in the retinal vessels, and the zonula adherens of the RPE cells. This barrier often breaks down in ocular inflammation; if introduced into the blood, fluorescein leakage will occur at points where the barrier is porous. The optic nerve can also leak when inflamed, even when it is not swollen. This property would not be apparent on color fundoscopic images alone.
7. **Electroretinogram (ERG).** It is not clear whether the functional integrity of the retina is better analyzed by morphology of the fixed eye or by examining the ERG in life. What is clear is that both techniques used together provide a much better indication of retinal function than does either procedure used alone.
8. **Other tests.** Multiple innovative modalities have been investigated of late for fundus examinations, and some are already used at least occasionally as in-life assessments during toxicological studies. Examples include spectral domain optical coherence tomography (sdOCT), confocal scanning laser ophthalmoscopy, scanning laser polarimetry, and adaptive optics imaging. Some of these will be described briefly later in the chapter, but the details are beyond the scope of this work. Readers seeking further information should examine the citations in the Suggested Reading list.

## 4. FUNDAMENTALS OF THE MORPHOLOGIC EXAMINATION OF OCULAR TISSUES

### 4.1. Tissue Fixation and Handling

Usually, intact globes will be fixed by immersion of the entire organ after removal of excess eyelids, muscle, and periorbital tissues. There are special circumstances where tissues adjacent

to the globe should be kept intact and sampled along with the globe. These might include cases where a surgical field is important (e.g., to define where a glaucoma device was oriented or when analyzing subconjunctival injections) or to evaluate the invasiveness of a tumors adjacent to the eye.

General considerations in the selection of fixatives for the eye will be considered first. Regardless of the fixative used, the volume of tissue to be fixed should be kept to a minimum, without sacrificing the integrity of the tissue's anatomic orientation. In most cases, not less than 10 times the volume of fixative should be used compared to the tissue to be fixed (i.e., 10 mL of solution per 1 g of tissue). The commonly used fixatives for ocular tissues destined for microscopic evaluation are discussed below.

1. **Formalin.** A common solution is neutral buffered 10% formalin (i.e., approximately 4% formaldehyde) in water. This most common of fixatives is cheap and effective as a general all-purpose fixative. Formalin has excellent tissue penetration, allowing large tissue fragments like whole globes to fix adequately by emersion. The aldehyde fixatives in general achieve tissue fixation by creating chemical crosslinkages from protein to protein. Formalin is a suitable preservative for gross anatomic pathology detail for photography and for selection of sites for light-microscopic examination, and it provides reasonable morphological detail in standard paraffin-embedded tissue sections used for light-microscopic examination, including most immunohistochemistry (IHC) procedures. Formalin is adequate but not ideal for both transmission and scanning electron microscopy (TEM and SEM, respectively), although it should never be the fixative of choice for protocols which call for TEM as a primary morphological endpoint. The most notable unfavorable quality of formalin fixation when used on ocular tissues is the less than adequate tissue rigidity, which can lead to folding and artifactual retinal detachments when paraffin sections are made.
2. **Bouin's solution.** This fixative incorporates picric acid, formaldehyde, and glacial acetic acid. The favorable qualities of Bouin's solution include excellent tissue rigidity, making it easy to maintain the shape of the globe during trimming and sectioning; this property prevents artifactual folding and substantially lessens retinal detachment in paraffin sections. The suitability of Bouin's solution for ocular IHC is unproven, and most technicians do not want to develop special IHC protocols for its use. Unfavorable qualities of Bouin's solution include the explosive nature of picric acid when dried, the ability of the fixative to corrode metal tissue-processing instruments, and the prohibitive safety requirements for handling or shipping. Bouin's solution also imparts an opaque yellow color to the tissue, making it harder to recognize landmarks for tissue trimming and unsatisfactory for purposes of gross photography. It is necessary to wash Bouin's-fixed tissues in copious amounts of 70% ethanol and water prior to processing. Bouin's fixative is not able to penetrate tissues as well as formalin, and it is totally unsuitable for TEM.
3. **Davidson's fixative.** This fluid contains formaldehyde, alcohol, and glacial acetic acid. Davidson's fixative is frequently used to fix globes in toxicologic pathology, as it has many favorable attributes; direct comparison with modified Davidson's solution (a variant of Davidson's solution) as a preservative for rat eyes indicates that Davidson's solution provides superior fixation to modified Davidson's solution. Tissue penetration is the same as formalin, and there is also improved tissue rigidity, thereby making it easy to maintain the shape of the globe and to prevent artifactual retinal detachment. Davidson's fixation in combination with paraffin embedding provides excellent retinal and lens preservation, the two ocular tissues for which achieving good morphologic preservation is most difficult. Davidson's fixative is unproven for ocular IHC, and technicians typically are reluctant to develop new techniques to optimize IHC for this solution. Unfavorable qualities of Davidson's fixative include the need to change the fixatives and wash the tissues, although some laboratories have not seen the need for complex washing protocols when using Davidson's. Tissues fixed with Davidson's

solution are opaque white; therefore, it may be difficult to recognize landmarks for tissue trimming, and gross photography is imperfect. It should not be used if TEM is a possible consideration.

4. **Glutaraldehyde.** This molecule has two aldehyde moieties. Therefore, it is an extremely effective crosslinking agent, but also will penetrate tissues at a much slower rate. In most cases, glutaraldehyde is combined with formaldehyde or paraformaldehyde, which will increase the speed of initial tissue penetration. Glutaraldehyde is the best fixative for TEM. It imparts excellent tissue rigidity and the native colors are preserved better than formalin, so site selection is easier when trimming. Unfortunately, glutaraldehyde has very poor tissue penetrating qualities, so tissues fixed should be no larger than 1 $mm^3$. Whole rodent globes can be fixed in glutaraldehyde, but large animal globes must be opened before surface fixation can commence. Whole body perfusion should be considered if large amounts of tissue need to be fixed en bloc. Glutaraldehyde does not preserve well on the shelf, so it should be stored frozen (at −20°C) and made up fresh before each use. To optimize the benefits of glutaraldehyde fixation, plastic embedding should be chosen rather than paraffin. Glutaraldehyde is very caustic when it contacts the skin.
5. **Frozen tissue processing.** When IHC is an essential procedure and fixed tissue provides inadequate preservation of labile antigens, or when preservation of enzymatic activity is needed for histochemistry, then tissues should be sectioned frozen on a cryostat. Tissues may be frozen without fixation or, more commonly, they may be fixed for a brief period (typically 30 minutes or less) in ice-cold formalin to improve cell morphology. Briefly, fixed specimens should be transferred to 20% sucrose in Dulbecco's phosphate-buffered saline for 15 minutes and then dipped three times into a 1 : 1 mixture of 20% sucrose : tissue freezing medium. Next, the sample should be oriented in a cryomold surrounded by 100% freezing medium, frozen by immersion in liquid nitrogen-cooled isopentane , and stored at −80°C until sectioning.

## 4.2. Trimming the Eye

The default plane of section for animal species other than non-human primates is the vertical section, which samples both the tapetal (typically dorsal [superior]) and non-tapetal (typically ventral [inferior]) portions of the retina. Exceptions are made in order to sample known or suspected lesions in the temporal or nasal aspect of the globe more effectively. The horizontal plane is the preferred default orientation in non-human primates because the fovea is lateral (temporal) to the optic nerve. In the extremely small eyes of rodents, trimming is to be avoided. Instead, the whole globe is submitted and oriented at the time of paraffin embedding. Rodent eyes are positioned in the vertical plane, and ideally should include a portion of the optic nerve (cranial nerve II).

Most rodent globes can be fixed and processed while intact, including periocular connective tissue and eyelids. However, these extraocular tissues may be removed if not interesting. It is more practical to fix and embed these smaller globes whole and step-section through the specimen until a central section that contains the optic nerve is obtained than to trim them before embedding. In contrast, eyes of species with larger globes (i.e. non-human primates, dogs) should not be processed whole. Instead, regions of interest from large eyes should be trimmed and then processed.

Select a standard technique for trimming globes of each species. This strategy will provide sections with a single orientation and similar morphological features; such standardization will speed the pathologist's histopathological analysis. Generally, the goal is to obtain a histological section that includes the optic nerve and passes through the pupil. Below are some techniques that are helpful in obtaining reproducible sections among animals and across studies.

- For large globes, make the initial trimming cut near the optic nerve. The lens is sectioned with a quick forceful cut while supporting the globe on the cutting board. A major advantage to this approach is that suitable sections for analysis may be obtained after facing only a few sections from the embedded tissue to reach the optic nerve. Another advantage is that the globe is cut close to the anatomic

center, which is appealing for the purpose of photography. The disadvantage is that the lens may be misplaced or damaged during trimming.
- To maximize the chances of preserving good lens morphology when trimming, make an initial off-center cut that avoids the lens. Subsequent step-sectioning once the tissue has been embedded in paraffin can be used to achieve a central cut through the lens and optic nerve. An advantage of this technique is that the lens is untouched during trimming and thus is less likely to be artifactually dislodged.
- Ensure the inclusion of lesions in the plane of section. The ideal strategy is to have the clinician indicate the location of a focal lesion in the globe with a careful clinical description and/or drawings or photographs, as well as some indication directly on the tissue with a suture or another tissue-marking technique. Gentle palpation of the globe often is valuable in detecting large localized lesions before sectioning. The orientation of the initial section can be changed in such a way as to sample the palpable lesion. "Candling" the globe by holding it in front of a bright light in a darkened room can help to localize an opaque focal lesion. Careful examination of the sectioned globe using a dissecting microscope also facilitates the identification of focal lesions. Additional steps may be indicated to sample a focal lesion. The primary calotte (i.e., an isolated portion of the globe) might be re-trimmed so that only the segment of the globe with the lesion is embedded. The histology technician is then instructed to step-section to a specified depth to sample focal lesions. This added step is sometimes essential to fully characterize discrete lesions.

## 5. EYELIDS

### 5.1. Structure, Function and Cell Biology

In mammals, the primary function of the eyelids is protection of the ocular surface against exposure or the risk of accidental trauma. The lids also have important functions in tear film formation and distribution (see below). In rodents, rabbits, and dogs, the upper and lower lids are fused at birth and separate only after retinal development is adequate for vision (between 12 and 15 days of age in the rat).

In the species commonly used in toxicologic pathology studies, the eyelid (palpebrum) is made up of a palpebral surface lined by conjunctiva, a specialized lid margin that contains meibomian (sebaceous) glands, and haired skin on the outer surface. The lid margin in mammals is supported by a firm dermal collagenous layer which, in the upper lids of non-human primates, forms a robust rigid structure called the tarsal plate. Carnivores and humans present an almond-shaped eye fissure, while most rodents and non-human primates have a round one. Lid closure is moderated by the circumferential orbicularis oculi muscle and levator palpebrae muscle, which raise the upper lid, along with the sympathetically innervated superior tarsal muscle, a smooth muscle (Figure 53.6). Cilia are long, wide hairs produced by specialized hair follicles near the mucocutaneous junction. Cilia are present in the eyelid margin of most species, but are absent in the cat and only present in the upper eyelid of dogs. Cilia form an outward curving tactical mesh in front of the eye that helps protect the cornea. Histologically, the pilosebaceous units of the eyelids are similar to the truncal hairs, but larger.

Of the species used in toxicologic pathology, the dog, cat, and rabbit possess a nictitating membrane (third eyelid). This structure presents as a large fold of conjunctiva that protrudes from the medial canthus over the corneal surface of the globe. It is supported by a curved, T-shaped plate of hyaline cartilage surrounded by elastin-rich stroma. At its base, the cartilage is surrounded by a mixed (seromucinous) gland, the gland of the third eyelid. Numerous small aggregates of lymphoid tissue are usually present underneath the conjunctival epithelium on the bulbar (inner) aspect of the third eyelid. In species with this structure, the third eyelid mechanically protects the cornea, aids in the tear distribution over the corneal surface, and contributes to 30–50% of the aqueous portion of the tear film via multiple very small ductules that enter the bulbar conjunctival surface near the fornix.

### 5.2. Evaluation of Toxicity

The eyelid is made up of haired skin, modified skin at the lid margin, and conjunctiva (a hairless

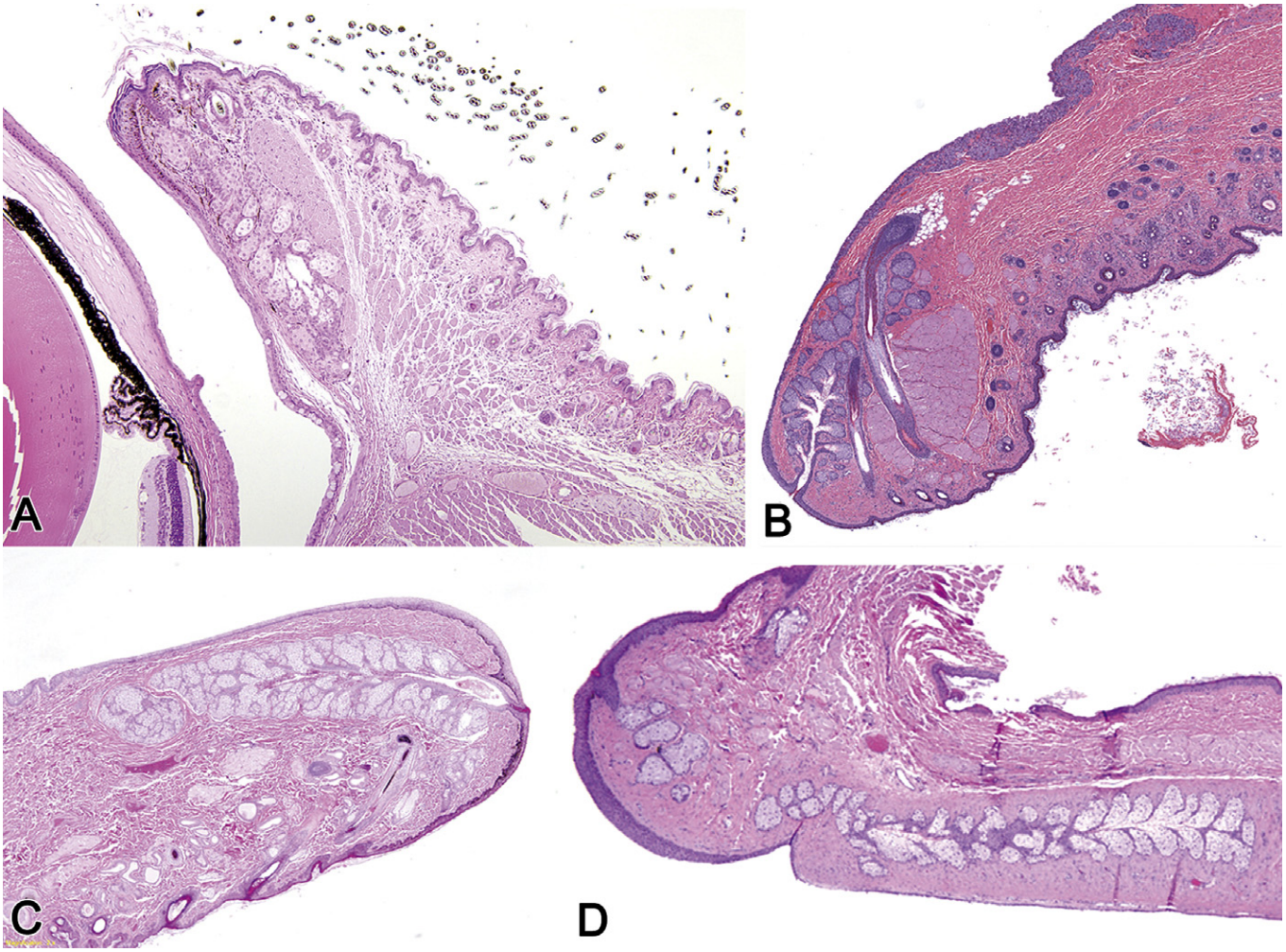


FIGURE 53.6 Normal eyelid architecture from various mammalian species used in ocular toxicity testing. (A) Mouse, (B) Rabbit, (C) Dog, (D) Non-human primate. Major features include haired skin on the external surface, non-haired sebaceous (meibomian) glands with ducts reaching to the inner surface or mucocutaneous junction at the palpebral tip. H&E, (A) 12.5×; (B, C, D) 40×.

mucosa) as well as skeletal muscle. The toxicities or changes relative to toxicologic studies are largely the same as those that develop in similar tissues elsewhere in the body. Because the tissues are exposed, they are prone to inflammatory conditions following contact with irritants, radiation, or microbes. When study protocols call for topical application of test materials to the ocular surface, there may be primary eyelid irritation followed by a variable degree of self-trauma. In some cases, a dose response may be apparent if higher doses lead to more eyelid self-trauma. Exposure to UV light can cause a variety of problems in some species. Solar elastosis, carcinoma *in situ*, or squamous cell carcinoma are among the common conditions that have been attributed to UV-induced damage to the cutaneous components of the eyelid. Exposure to ionizing radiation from cancer treatment can cause atrophy of the meibomian gland, vascular disruptions, and qualitative changes in the lid extracellular matrix. Extremely erosive chemicals applied to the lids can cause ulceration and promote secondary infections; animal-use protocols are designed to prevent continuation of experiments when this type of pathology is encountered. Muscle weakness affecting the orbicularis or levator muscles can cause problems in eyelid opening or closing. Inherent diseases of skeletal muscle (e.g., myasthenia gravis) or the nerve branches that supply them can be the cause.

## 5.3. Response to Injury

The response of eyelid tissue to injury is not complicated. The most common injury is inflammation or trauma. Tissue scarring from either of these problems can have a profound effect on the function of the lid by interfering with its motion or conformation. An inwardly turned lid (entropion), usually affecting the lower lid, can result in hairs contacting the cornea. This abnormal interaction causes pain and irritation, and may lead to erosion or ulceration of the cornea. In contrast, an outwardly turned lower lid (ectropion) can invite spillage of tears, which can result in dry eye (keratoconjunctivitis sicca [KCS]) and secondary infection. Weakening of the dorsal (superior) tarsal muscle associated with a defect in sympathic innervation, as in Horner's syndrome, causes ptosis (drooping of the upper eyelid).

Blepharospasm, the abnormal contraction or twitching of an eyelid, is a non-specific response to painful or irritating stimuli. This clinical abnormality can be triggered by many factors, including conjunctival or corneal irritation, or even injury or inflammation in the uvea. The identification of blepharospasm is important when clinically accessing the immediate response to topically administered drugs and ocular discomfort.

## 5.4. Mechanism of Toxicity

### *Ptosis and Eyelid Retraction*

Ptosis (drooping eyelids, especially affecting the dorsal lid) and eyelid retraction are relatively common reactions to systemic or locally administered drugs. Snake venoms, especially from elapids (e.g., cobras) and some vipers, succinylcholine, and botulinum toxin, can cause ptosis by blocking neurotransmission at the neuromuscular junctions. Other less common drugs associated with ptosis are tetraethylammonium, a ganglion blocker agent; guanethidine, a sympatholythic drug used to reduce lid retraction; penicillamine, a metal-chelator; the sedatives primidone, barbiturates, and alcohol; and the chemotherapic agent vincristine. No common mechanism of action has been defined to explain the presence of this response for these agents. On the other hand, stimulants such as phenylephrine, amphetamine, and cocaine are associated with upper eyelid retraction.

### *Blepharitis/Conjunctivitis*

Blepharitis (inflammation of the eyelid) and conjunctivitis (inflammation of the inner lid lining) are common reactions to numerous topical drugs. Drug preservatives such as thimerosal and benzalkonium chloride, as well as antiviral agents like vidarabine, trifluridine, and idoxuridine, are reported to cause ocular irritation. Most commonly used ophthalmic preparations present the potential for incidentally causing blepharitis and conjunctivitis.

Many inbred mouse strains, including BALB/cJ, BALB/cByJ, CBA/J, and 129P3/J, are reported to develop spontaneous ulcerative blepharitis. Although *Corynebacterium* sp. has been isolated from those lesions, the underlying abnormality and causative agent(s) are not totally clear. Mutations in the desmoglein 3 (*Dsg3*) gene were reported to be the main factor underlying ulcerative blepharitis in $Dsg3^{bal}$ and $Dsg^{3bal\text{-}Pas}$ mice (balding and balding Pasteur, respectively). These animals develop a pemphigus-like reaction with formation of suprabasilar vesicles affecting the mucocutaneous junctions. Such changes are identical to those observed in humans and animals with pemphigus vulgaris.

# 6. LACRIMAL SYSTEM

## 6.1. Structure, Function, and Cell Biology

The lacrimal system is comprised of a series of extraocular apocrine glands whose secretions contribute important elements to the tears that lubricate the surface of the eye. Primates (both human and non-human) only have one lacrimal gland, which is located dorsal and lateral to the globe. Dogs and cats have both an extraocular lacrimal gland and a gland of the third eyelid. Rodents and rabbits have lacrimal gland systems consisting of extraorbital (i.e., the exorbital lacrimal gland) and intraorbital (i.e., Harderian gland) components. The intraorbital component is located behind the globe, and generally in a medial (nasal) location. Rodents and primates lack a third eyelid (nictitating membrane), except for a vestigial remnant, but they have small lacrimal glands more or less in the conjunctival

sac or medial canthus where the root of the third eyelid would be. Rabbits have a third eyelid, but it has only minimal glandular tissue. Dogs and cats have a robust third eyelid and a large seromucinous gland of the third eyelid. All these glands are innervated by the facial nerve (cranial nerve VII).

Like most glands, the lacrimal glands are composed of secretory acini linked to the conjunctival surface by a series of small to large ducts. Both the acini and the ductules are surrounded by myoepithelial cells, which are cytokeratin-expressing, spindle-shaped epithelial cells that are contractile owing to their rich endowment of smooth muscle actin.

The lacrimal gland is a seromucinous gland. The contributions of the lacrimal glands are largely to the aqueous component of the tears. However, significant quantities of lipid are a part of product secreted by the Harderian gland, particularly in rabbits. The major lacrimal glands do not secrete at all times, and contribute little to routine tear formation. Instead, they form the majority of the excess tear formation ("crying") resulting from ocular discomfort. The continual formation of tears to keep the ocular surface moist is largely the function of the small ("minor") lacrimal glands of the conjunctival fornix. In all species, the glands secrete copious amounts of water containing enzymes and tissue cytokines as well as antimicrobial substances (peptides and proteins) to maintain the sterility of the anterior cornea. The exact proportions of these molecules differ considerably from species to species, but they include antimicrobial substances such as lysozyme, lactoferrin, and bactericidal permeability-increasing protein (BPI); immune active substances such as IgA; and small amounts of cytokines such as IL-1, IL-6, and IL-8. In addition, the Harderian gland, lacrimal gland, and conjunctival Goblet cells' secretion contains lipids as well as mucins and trefoil factor family (TFF) peptides. Mucins are present both in the epithelial glycocalyx and in the tear fluid. The hydrophilic characteristics of mucins play critical roles in stabilizing the connection between the surfaces of the corneal and conjunctival epithelium and the water component of the tear film, as well as in providing a continuous barrier across the ocular surface to prevent pathogen colonization and penetration. Mucins and TFF peptides have many other physiological functions in addition to their rheological properties, such as promotion of epithelial cell migration, reduction of apoptosis, induction of cell scattering, promotion of epithelial restitution, and enhancement of neuropeptide signaling.

## 6.2. Evaluation of Toxicity

The functional measurements for the integrity of the lacrimal system evaluate the quality of the tear film and the quantity of tear formation. This discussion is best left for Section 7, on the precorneal tear film (below), where all three layers of the tear film can be discussed in context. Conventional toxicologic pathology assessments of the lacrimal gland system are limited to histopathologic evaluation of the exorbital lacrimal and/or Harderian glands. However, these glands often are not included in the protocol-specified list of tissues to be taken for analysis in non-clinical toxicology studies.

### *Animal Models of Lacrimal Gland Dysfunction*

Animal models for diseases of the lacrimal glands have been created by surgical removal of the major lacrimal glands or by chemical ablation of the glands. These procedures create an ocular surface environment exposed to decreased tear protection, consequently predisposing affected individuals to secondary corneal disease (see precorneal tear film section below).

A common clinical condition in humans, and suspected in many animals, including dogs and non-human primates, is autoimmune adenitis affecting lacrimal and salivary glands. The classical multi-gland inflammatory disease in people is termed Sjögren's syndrome (SjS), and is characterized by a lymphoplasmacytic reaction against lacrimal and/or salivary glands. Throughout the past two decades, a variety of mouse models exhibiting various aspects of SjS have been advanced. Foremost among them are spontaneous models like NZB/NZW $F_1$-hybrids and the MRL/lpr, NOD/LtJ, NFS/sld, and IQI/Jic strains. However, important advances have also been provided by genetically engineered models like the C57BL/6.NOD-Aec1Aec2 congenic line; targeted null mutations ("knockout") of the Id3 or aromatase genes, and targeted

replacement ("knockin") of the Baff gene. These mice typically present with lymphocytic infiltration of the exocrine glands, increased expression of pro-inflammatory cytokines within tissues of the affected glands, and generation of autoantibodies to one or more molecules produced exclusively or mainly in these organs. Of those models, the more interesting are those derived from the non-obese (NOD) mice – NOD/Ltj and NOD.B10-H2$^b$ – which develop autoimmune dacryoadenitis/keratoconjunctivitis sicca characterized by diminished production of tears associated with mixed infiltrates of T and B lymphocytes in the exorbital lacrimal gland that greatly resemble SjS.

### 6.3. Response to Injury

All of the glands comprising the lacrimal system are apocrine glands, and they respond to injury much like other apocrine glands throughout the body. They are prone to ductular obstruction secondary to inflammation. This often leads to ascending inflammation affecting the gland acini, and can result eventually in atrophy. Lymphocytic clusters among acini are a fairly common background lesion in safety studies, especially in rodents. Viruses such as sialodacryoadenitis virus (SDAV), a coronavirus of rats, can directly infect the acinar epithelium in lacrimal glands as well as salivary glands, leading to necrosis, inflammation, and fibrosis or atrophy of the remaining parenchyma. Chronic infection with SDAV can cause corneal desiccation (keratoconjunctivitis sicca [KCS]), corneal ulceration, and uveitis leading to hyphema (blood accumulation in the anterior chamber), intraocular inflammation, formation of fibrovascular membranes over the iris (pre-iridal fibrovascular membrane), and eventually to obstruction of the aqueous outflow pathways with secondary (unilateral or bilateral) glaucoma.

Squamous metaplasia of the lacrimal gland ducts is occasionally seen. This change is usually idiopathic, but metaplasia associated with Vitamin A deficiency is a possible cause. Ionizing irradiation used for cancer therapy can affect the lacrimal glands leading to atrophy. The exact mechanism for this atrophy is unclear, but the likely explanation is that cumulative gene damage in irradiated stem cells leads to their apoptosis and a reduced capacity to regenerate the gland acini.

Like other apocrine glands, lacrimal glands are capable of neoplastic transformation. The spectrum of neoplasms seen in lacrimal glands is similar to that which develops in other apocrine glands: acinar, ductular, or solid adenomas or adenocarcinomas. When the myoepithelial component is involved, the architecture can form complex tumors with a spindle cell component (ranging from minimal to major); if there is osseous or cartilaginous metaplasia of the myoepithelial component, truly mixed tumors can arise in lacrimal glands. Occasionally the mesenchymal component will be the malignant cell population, so that osteosarcoma or chondrosarcoma arises as a primary tumor in a lacrimal gland, but generally this possibility is rare.

### 6.4. Mechanism of Toxicity

Apocrine glands are not often the target tissue of toxicants. Few compounds have been reported to be toxic to the lacrimal glands of animals. Among the drugs that do target these organs are phenazopyridine, sulfadiazine, and salicylazosulfapyridine. These drugs were reported to cause marked necrosis of the lacrimal gland, with evolution to fibrosis through an unknown mechanism. Dogs that presented with this toxic reaction later developed KCS.

## 7. PRECORNEAL TEAR FILM

### 7.1. Structure, Function, and Cell Biology

The normal functions of the cornea are, in part, dependent on the existence of a healthy precorneal tear film. This acellular fluid layer is adherent to the most superficial layer of the corneal epithelium. The tear film is essential for maintaining both the health of the cornea and the high-quality optics of the corneal surface. The proper function of this delicate film is challenged by gravity, evaporation, and rubbing or contact by foreign material.

The precorneal tear film is composed of three main layers. The inner mucinous layer is secreted largely by the conjunctival goblet cells with contributions from the lacrimal glands. The mucins are important because they adhere to

the cell membrane of the corneal epithelium to hold the aqueous component of the tear film in place by adsorption. The middle aqueous layer is secreted by the glands of the lacrimal system. Its main function is to keep the corneal surface moist. It also provides a mechanism for oxygenation and nutrient exchange with the avascular anterior corneal tissue. If the epithelial surface is unable to maintain an aqueous layer for whatever reason, the resultant disease – keratoconjunctivitis sicca – is a severe form of corneal degeneration leading to inflammation. The outer lipid layer is secreted principally by the sebaceous (meibomian) glands of the eyelid margins, although lipid tear elements also are contributed by the Harderian glands, particularly in rabbits. Unlike their counterparts in the skin, the large meibomian glands are unassociated with hairs. Tear film lipids form a monolayer on the tear surface, and function by enhancing the surface tension which supports the integrity of the tear film against collapse due to gravity and also slows the loss of the tear film by evaporation. Another important role of the lipid layer is to provide a glassy, smooth interface between the air and the transparent cornea.

The surface cell membrane of the corneal epithelium is characterized by a microvillus border. This surface is designed to maximize the adherence of tear film mucins to the cornea, but it is not able to provide the smooth surface that is necessary for refraction and light focusing. Instead the dried corneal epithelial surface scatters light, which greatly degrades the ability to form a focused image at the retina.

In order to maintain the tear film's integrity, mammals have developed structures and mechanisms that function to refresh the layering and distribution of the tear film rapidly and very frequently. This maintenance function is an important role of the constant, involuntary closure of the eyelids ("blinking") in primates and rodents, and/or the nictitating membrane in dogs, rabbits, and other species that have a third eyelid. Between blinks, gravity deforms the tear film by pulling it downward, with a meniscus forming at the lower lid. This sagging can create too much physical strain for the lipid layer to remain intact, so the three-layered tear film will break up until the next blink or excursion of the third eyelid. Paralysis of the blinking mechanism or exposure of the corneal surface beyond the reach of the closed eyelids degrades the tear film for extended periods of time and leads to keratoconjunctivitis sicca. Rabbits have a robust lipid layer which provides enhanced protection from the breakdown of the tear film between blinks. For this reason, rabbits are able to withstand a longer interval between blinks than most other mammals – a desirable evolutionary characteristic to reduce movements in an animal that is a highly attractive prey species in nature.

The tears are cleared from the ocular surface by a system of drainage ducts in the conjunctiva near the medial canthus. Two exit paths are available, one upper and one lower. This system is called the nasolacrimal drainage system, because the tear film material is deposited into the nasal cavity. The puncta (ductal openings) on the conjunctiva communicate with a canaliculus which comes together in a bladder-like sac called the nasolacrimal sac. This sac, in turn, connects to the nasal cavity through the nasolacrimal duct (Figure 53.7).

## 7.2. Evaluation of Toxicity

### *Schirmer's Tear Test*

The tear film is difficult to observe directly, other than by recording a bright and clear appearance to the corneal surface. There are many tools available to assess both the quality and quantity of the tear film, as a whole and by evaluation of its component parts.

The most commonly used evaluation of aqueous tear formation is Schirmer's tear test. A standardized strip of absorbent paper is placed in the fornix of the lower lid conjunctiva and allowed to absorb fluid for a set amount of time. The quantity of fluid absorbed into the paper is dependent on the ability of the various lacrimal glands to form aqueous tears. This test is best used only to measure the volume of the tear film; it cannot be used as a general test of tear film integrity. The Schirmer's tear test can be performed without anesthesia, and can be undertaken in a variety of animal models (e.g., non-human primates, dogs, and rabbits) using the same paper employed for the test in humans. The only adjustment needed in animals relative to the human assay is an altered duration of the test (5 minutes in non-human primates, 1 minute in dogs, and 1 minute in rabbits, relative to

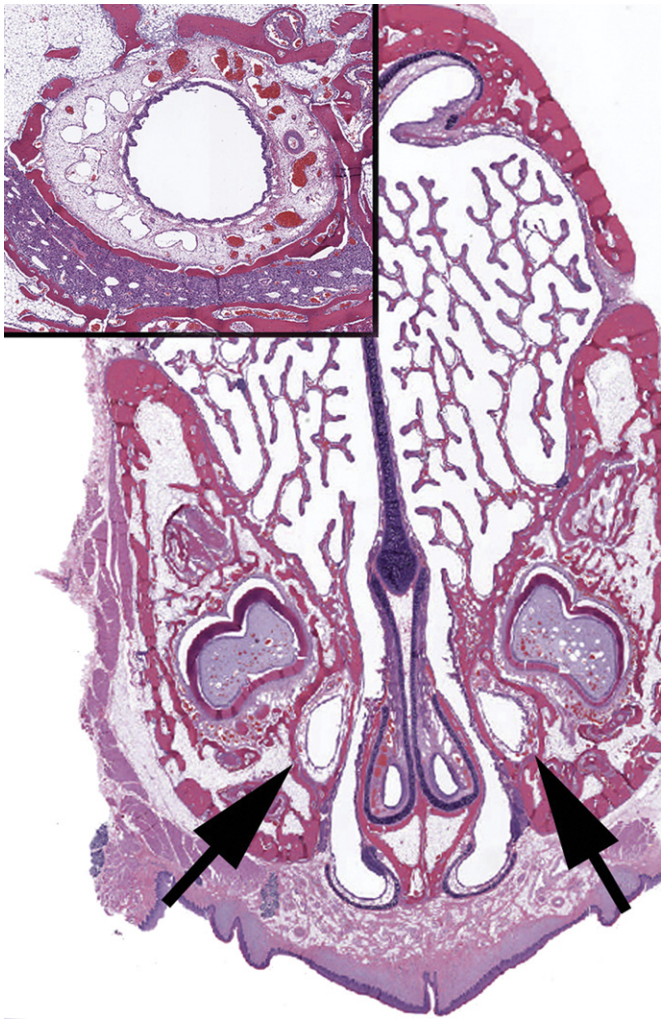

FIGURE 53.7 Normal architecture of the nasolacrimal duct. Decalcified section of the nasal cavity of a rabbit showing the position of the nasolacrimal duct (arrows) as it nears its orifice in the ventral wall of the rostral nasal passages. The ducts are on the lateral wall opposite the vomeronasal organs (at the base of the nasal septum). The inset is from the same animal but taken at a different (more caudal) plane of section. H&E, 12.5×, or inset, 200×.

5 minutes in humans). In rats and mice, due to the limited size of the globe, the Schirmer's tear test is usually performed using two-ply cotton threads stained with either fluorescein or phenol red instead of the filter paper. The test duration in rodents is generally 1 minute.

### *Tear Film Break-Up Time*

The tear film break-up time is a measure of the combined function of the mucin layer and the lipid layer in maintaining physical contiguity of the tear film. Dysfunction of either of these layers compromises the staying power of the tear film in the battle with gravity. Loss of mucin in the inner layer of the film reduces its adherence to the epithelial surface so that the middle aqueous layer flows downward rapidly, overwhelming the surface tension supplied by the hydrophobic interactions in the lipid layer. The loss of the outer lipid layer causes reduced surface tension, which allows the layers to separate under the influence of gravity.

The tear film break-up test is defined as the time interval following a blink to the occurrence of a break(s) in the tear film. After applying liquid fluorescein to the ocular surface using a micropipette or a fluorescein strip, the time from opening the eye to the appearance of the first spot on the corneal surface is measured in seconds. This test has been reported to be useful in dog and rabbit models of dry eye, but its applicability to small rodents is limited due to difficulties in visualizing the tear film break in the small corneas of these animals.

The quality of the lipid layer can also be assessed by physical observation of the tear film meniscus at the lower lid margin. A poor-quality lipid layer leads to a bulging meniscus at this point. The bulge represents a weak point in the lipid layer that is easily ruptured, thereby releasing aqueous tears from the corneal surface.

### *Anterior Segment Optical Coherence Tomography (OCT)*

Optical coherence tomography (OCT) is a new imaging modality that allows high-resolution, cross-sectional imaging of the eye. One variant of OCT (termed anterior segment OCT) has been used to measure corneal (full thickness) and corneal epithelium (partial thickness) dimensions as well as the depth of the precorneal tear film. This technique allows a rapid measurement of the film thickness without requiring direct contact or immersion, and it has higher spatial resolution than ultrasound.

## Other *In Vivo* Methods

Other *in vivo* tests may be useful in assessing the production and composition of tears. Chemical composition of the tear film is one common approach. Proteins like lactoferrin and epidermal growth factor (EGF), pro-inflammatory

cytokines, and mucins are among the molecules measured most often. Other common diagnostic techniques include application of stains (e.g., fluorescein and lisamine green) to detect discontinuities in the tear film, tear film osmolarity, and conjunctival imprints and biopsies. The conjunctival methods do not examine the tear film directly, but the structural analysis of the sampled epithelium provides indirect evidence regarding the adequacy of the tear film in maintaining corneal health.

If the lacrimal drainage system is obstructed or overwhelmed, the excess tears will spill over the eyelids and wash over the skin in a condition known as epiphora. The patency of the lacrimal drainage channels can be evaluated by instilling fluorescein dye into the conjunctival sac and observing whether or not fluorescein drains into the nasal cavity. An absence of such fluorescein drainage into the nasal passages generally results from obstruction of the nasolacrimal duct. Obstructions related to toxicant-induced lesions (e.g., epithelial necrosis, periductular inflammation) can often be managed by occasional flushing of the duct to clear the blockage.

### ANIMAL MODELS OF TEAR FILM DYSFUNCTION

"Dry eye" is a term used to characterize an eye in which the tear film is absent or inadequate to consistently cover the cornea and maintain corneal health. The debilitating degeneration and inflammation resulting from dry eye is called keratoconjunctivitis sicca (KCS).

In humans, the dry eye syndrome affects millions of people and represents one of the most common ocular diseases. It is a common spontaneous disease, especially in elderly populations, thereby creating a huge market for tear replacement drops and lubricating drops. The typical clinical presentation of KCS is marked superficial pain, typically in conjunction with a feeling that "something is in the eye" (a foreign body sensation). Left untreated, transient "dry eye" over time can become permanent KCS.

The exact pathology of KCS is somewhat species-dependent, but the most characteristic change seems to be epidermalization of the corneal surface. In this stage, the normal appearances of the corneal epithelium and superficial stroma are altered from their stereotypical arrangement to resemble the more irregular, disordered orientation of the epidermis and superficial dermis in the skin. There is thickening and squamous metaplasia of the epithelium, along with rete ridge formation. The superficial stroma loses its regular stratification and becomes endowed with newly formed capillaries (both blood vessels and lymphatic vessels). In dogs there is often migration of pigment-producing melanocytes into both the epithelium and the superficial stroma (Figure 53.8). At this stage, there is risk of secondary corneal infection and acute inflammation with eventual ulceration. Left untreated, advanced cases can proceed to rupture of the cornea.

Multiple animal models have been defined for dry eye. Mouse models that are characterized by lacrimal inflammation were described in Section 6.2, on animal models of lacrimal gland dysfunction (Sjögren's syndrome). A rat model of immune-mediated dacryoadenitis has been produced in Lewis rats by sensitization with a single intradermal injection of an extract of lacrimal gland in complete Freud's adjuvant

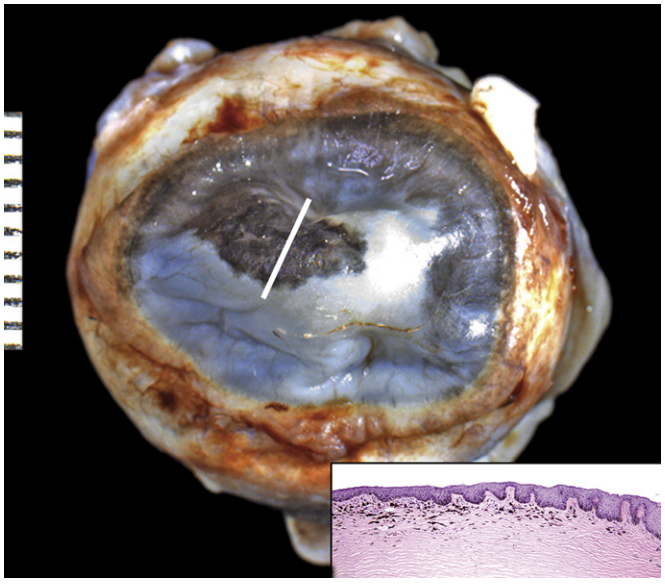

FIGURE 53.8 Pigmentary keratitis, dog. Gross image of a formalin-fixed dog cornea exhibiting marked opacity and dark pigmentation as reactive changes to a chronic inflammatory process. Inset: Histological section corresponding to the region of the cornea marked with a white line. Note the marked corneal hyperplasia (indicated by rete peg formation and hyperkeratosis) and pigmentation of the basal layers of the corneal epithelium and superficial corneal stroma. Scale, 1 interval = 1 mm. Inset: H&E, 100×.

(CFA) and simultaneous intravenous injection of dead *Bordetella pertussis* organisms. Evaporative techniques have been attempted in rabbits by using lid specula to prevent blinking, and in mice by exposing the corneal surface to continuous airflow under low ambient humidity in association with a transdermal injection of scopolamine (to block muscarinic receptors in the lacrimal glands).

Dogs present the only known spontaneous animal model for KCS. Brachycephalic dogs, whose eyes bulge forward from relatively shallow sockets and thus have an inefficient blinking motion, are particularly at risk. This condition affects 35% of the general dog population, with reported breed-specific incidences of 20.6% in the American Cocker Spaniel, 12.7% in the Lhasa Apso, and 11.5% in the Shih Tzu. Importantly, the relative incidence of spontaneous KCS in Beagles (the most common laboratory dog breed for toxicology studies) is much lower (1.2%). The pathogenesis of corneal disease in these breeds is not completely understood. The quantity of lacrimal gland secretions is reduced, as demonstrated by the decreased measurements on the Schirmer's tear test. Dacryoadenitis or atrophy of lacrimal glands is often seen in affected dogs. Surgical intervention or chemical ablation of the lacrimal glands can be performed to enhance the risk of dry eye. The main lacrimal gland, however, does not produce the aqueous secretion that is the principal component in the tear film which moistens the corneal surface. In dogs, cats, rabbits, and mice, removal of the main lacrimal glands produces a decrease in basal tear production measure by the Schirmer's tear test but by itself does not induce significant structural changes on the corneal surface, even after long-term follow-up. These major lacrimal glands function in humans mainly to produce excess secretions when tears are needed in bulk, as in crying to relieve emotion or to remove the foreign body sensation associated with stimulation of conjunctival nerve endings. Flooding of the tear film is not helpful in the routine maintenance of the three-layered tear film.

Specific functional disorders of the ocular-associated sebaceous glands, referred to as meibomian gland dysfunction (MGD), are increasingly recognized as a discrete disease entity. Alterations in the lipid phase of the tear film that point to MGD are reportedly more frequent than are isolated alterations in the aqueous phase in patients with dry eye disease. Several naturally occurring or induced animal models of MGD have been identified or developed. Rabbit and non-human primate models that feature hyperkeratinization of the meibomian gland and consequently impaired excretion of meibum have been produced by the topical application of epinephrine and systemic administration of isotretinoin, and have been reported in polychlorinated biphenyl (PCB) poisoning. In addition, cauterization of the orifices of meibomian glands in rabbits causes a decrease in the conjunctival goblet cell density, deposition of glycogen in the corneal epithelium, and stimulation of conjunctival inflammation, leading to a compromise in the formation of the lipid component of the tear film. Numerous mouse models exhibit impaired meibomian gland function mimicking MGD. These are either natural diseases of genetic origin (e.g., Rhino, Rough fur and Downless [locus] mutations) or have been generated by immunization (with human monoclonal anti-DNA antibody) or engineered transgenic overexpression (e.g., c-Myc, erbB2, Smad7, or parathormone-related protein [PTHrP]) or gene deletion (e.g., Acyl-CoA:cholesterol acyltransferase-1, Smad4, AIRE, or Blimp1). The most common phenotypes of mouse strains with MGD phenotypes are ductal hyperkeratinization, acinar cell loss, progressive glandular atrophy, and meibomian gland aplasia.

Drug candidates can be tested for the control of inflammation or infection once KCS has started. However, better animal models of KCS would help to improve understanding of the mechanisms that lead to pain and, eventually, ocular surface degeneration and inflammation in dry eye. They would also provide an important test system for the effectiveness of candidate tear replacement therapies or lacrimation-modifying drugs designed to prevent or control the processes responsible for the transformation of dry eye into full-blown KCS.

## 7.3. Response to Injury

The precorneal tear film is a thin tri-laminar fluid covering the surface of the corneal epithelium, and thus is not a tissue in itself. As such, the film can disintegrate or degrade, but it does

not respond to injury using the same pathological processes utilized by actual tissues. The response of the corneal tissue to degradation of the tear film will be covered in Section 8, on the cornea.

### 7.4. Mechanisms of Toxicity

Any toxicity that affects the tissues which secrete the three components of the tear film can be affected by toxicant exposure, and toxic effects in one or more of these tissues can impact the quality or quantity of the tear film. The types of toxicants and the lesions they produce which might affect the tear film are covered in Sections 5, 6, and 8, on the eyelids, lacrimal system, and conjunctiva, respectively.

## 8. CORNEA AND CONJUNCTIVA

### 8.1. Structure, Function, and Cell Biology

The cornea and the conjunctiva together form the ocular surface. The cornea is the central translucent zone through which light passes to reach the inside of the globe. The conjunctiva is the mucosal covering over the outer scleral margin (the "white"), both surfaces of the nictitans (third eyelid), and the inner surface of the eyelids.

#### *Cornea*

The cornea is a highly specialized, highly ordered tissue with many unique features (Figure 53.9). The mammalian cornea is covered on the surface by several layers of non-keratinizing, stratified squamous epithelium. This epithelium has a remarkably uniform thickness and structural consistency across the entire surface of the cornea. The lamination in this epithelium consists of a deep layer of basal cells resting on a basal lamina, an intermediate layer of wing cells, and a surface composed of one to several layers of squamous cells (with the number depending on the species: mice, rats, and rabbits, three to five layers; dogs, cats, and primates, five to seven layers). All the corneal layers are transparent to light in the visible spectrum. Behind the epithelial basal lamina in humans and non-human primates, but not in rodents, rabbits, or dogs, there is an acellular and homogeneous collagenous layer called Bowman's layer (or membrane) that consists of a random fibrillar network of collagen type I (and lesser amounts of type XII) fibrils. Although no Bowman's layer is visible by light microscopy in the mouse, by ultrastructural analysis a thin layer of randomly arranged collagen fibrils can be seen immediately underneath the corneal epithelium. The function of Bowman's membrane is not known. The bulk of the cornea is the stroma, which is located deep to Bowman's membrane (if one is present) or to the corneal epithelium (Figure 53.10). The transparent stroma, along with the opaque sclera, makes up the fibrous tunic of the globe. The junction of the fibrous zones in the cornea and sclera occurs at the limbus.

Since the mammalian globe does not contain any rigid matrix, such as bone or cartilage, structural rigidity to support the eye is achieved by building and sustaining an elevated IOP. The fibrous tunic facilitates this phenomenon while reducing the likelihood of spontaneous rupture. The physical properties of such a pressure-based system for achieving rigidity dictate that the globe should be perfectly spherical. However, the curvature of the cornea generally deviates from the spherical shape of the rest of the sclera. It is absolutely essential for retaining focus that the corneal curvature consistently varies in this fashion, as any imperfect areas will degrade the image on the retina. Too much curvature leads to myopia (near-sightedness), too little curvature leads to hyperopia (far-sighted), and irregular curvature or other imperfections leads to astigmatism.

Optical transparency of the cornea is dependent on a very precise spatial relationship between collagen fibers and non-collagenous matrix as well as the functional cells of the stroma. These cells are designated keratocytes (not to be confused with keratinocytes). The corneal stroma is avascular, containing neither blood nor lymphatic vessels. Several factors, mostly secreted by the corneal epithelium, help to maintain stromal avascularity. Among them, the most important are thrombospondins 1 and 2, endostatin, angiostatin, pigment epithelium-derived factor, and matrix metalloproteinases (MMPs). These molecules bind and inactivate pro-angiogenic molecules such as vascular endothelium growth factor (VEGF), fibroblast

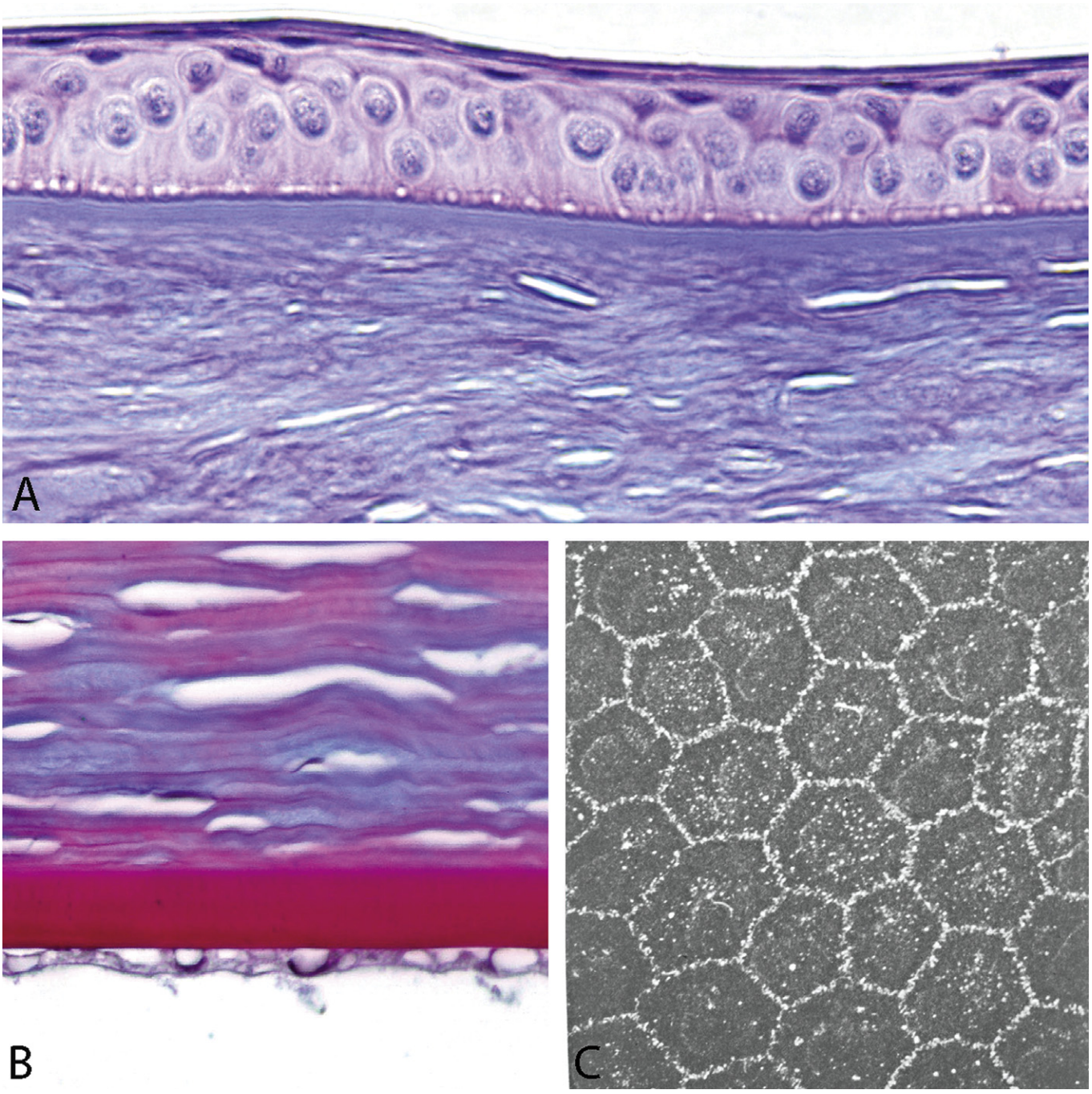


FIGURE 53.9 Normal architecture of the cornea. (A) Epithelium and superficial stroma from a non-human primate cornea. (B) Posterior corneal stroma bordered by Descemet's membrane (thick red band) and the corneal (posterior) endothelium from a non-human primate. (C) Scanning electron micrograph of the surface of the corneal endothelium from a dog. (A) H&E, 400×; (B) PAS, 600×; (C) 2500×.

growth factor (FGF), and platelet-derived growth factor (PDGF). The suppression of lymphatic vessels is achieved by the same soluble-binding molecules, but in this case they bind specifically to VEGF-C and VEGF-D. Exclusion of blood vessels in the corneal stroma is essential to sustaining tissue transparency, while preventing ingrowth of lymphatic vessels is important in maintaining corneal tissue as an immune-privileged site. The immune privilege

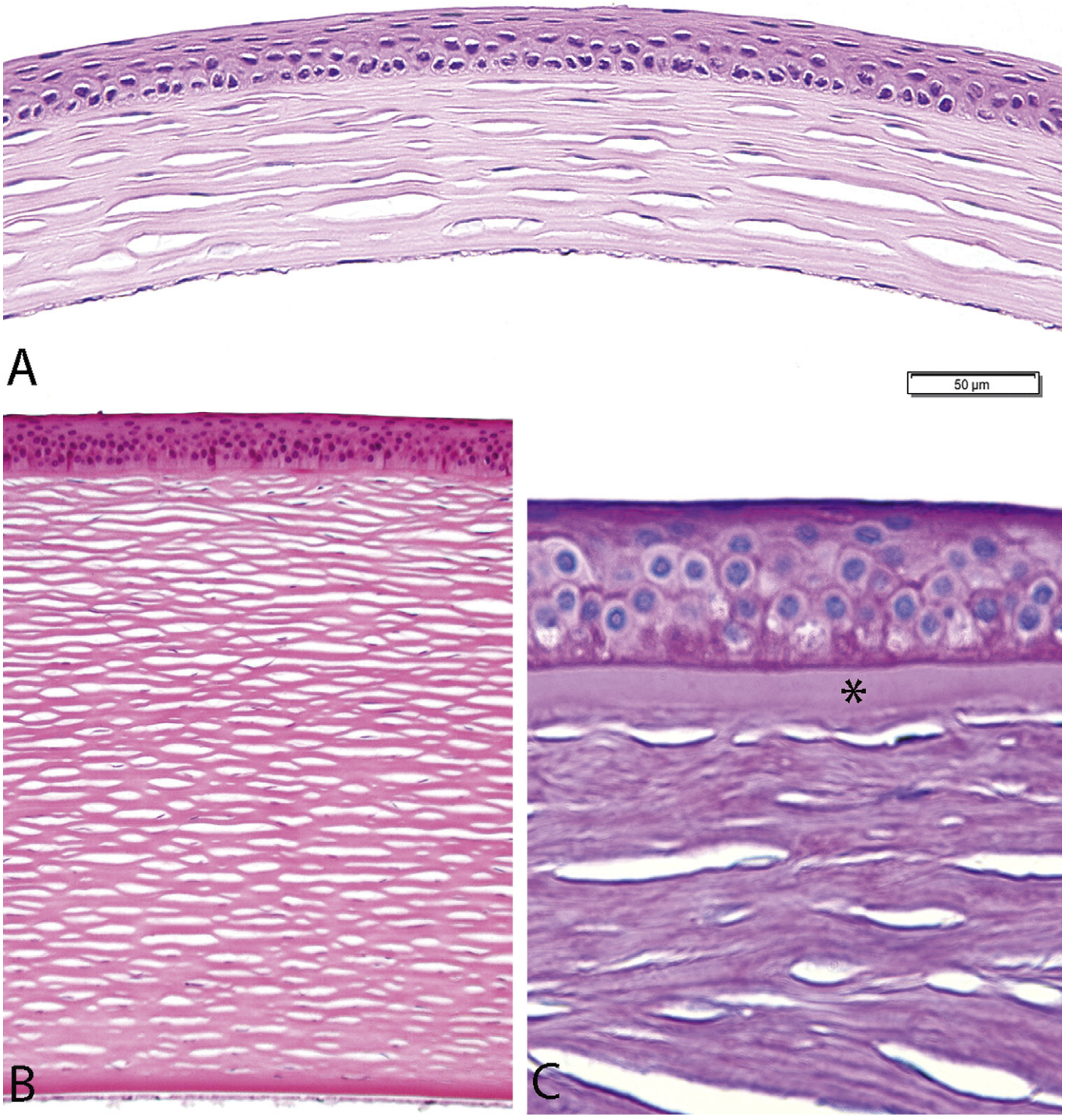


FIGURE 53.10 Histopathological representations of the cornea. Axial (central) cornea from an adult mouse (A) and an adult dog (B) show the relative thickness of the epithelium, stroma, Descemet's membrane, and corneal endothelium in these two species. (C) Epithelium and anterior stroma of the cornea from a non-human primate stained to show Bowman's membrane (*). In all three images, the clear spaces within the stroma are processing artifacts and not vascular channels. (A) H&E, 400×; (B) H&E, 400×; (C) PAS, 600×.

of the cornea permits corneal transplantation with less immunosuppressive therapy because the eye responds to the new tissue via the anterior chamber-associated immune deviations (ACAID) system to stimulate immune tolerance rather than to cause immune-mediated rejection (Figure 53.1). If the transplanted corneal tissue develops lymphatic vessels by virtue of inflammation, the long-term survival of the graft is greatly reduced.

The next layer of the cornea is Descemet's membrane, which rests under the stroma. This is a thick basement membrane with elastic properties that is composed mainly of laminin, fibronectin, and type IV collagen. The function of Descemet's membrane is unknown. It is secreted by the corneal endothelium (or posterior epithelium), the innermost layer of the cornea that borders the anterior chamber. The corneal endothelium is a monolayer of cuboidal epithelial cells, which has a similar microscopic anatomy and arrangement among mammalian species. The major difference among species is in the cellular density, which varies from 2211 cells/$mm^2$ in the rat to 4450 cells/$mm^2$ in non-human primates and humans. The endothelium is important in maintaining corneal transparency because it actively pumps water from the corneal stroma back into the anterior chamber against a steep pressure gradient. This linked leakage/pumping mechanism is an active process that provides for appropriate corneal nutrition from the aqueous humor in the anterior chamber while maintaining a normal degree of corneal hydration. The water content of the cornea is maintained at approximately 78%. A loss of endothelial function or breaks in its structural integrity leads to corneal edema, which is manifested as a translucent bluish quality to the corneal stroma during clinical evaluation or increased interfibrillar spacing within the stroma in histologic sections; the increase in fluid distorts the arrangement of the stromal fibers and disrupts the transparency of the cornea. The endothelium in most mammals is not renewable. There is attrition with age, and also when the cells are disrupted by intraocular surgery, lens luxation, or ocular trauma. If the endothelium is lost, it can only be restored, in humans, by transplantation (Figure 53.11).

### *Conjunctiva*

The conjunctiva has many essential functions. First, the conjunctival goblet cells contribute to secretion of the mucinous component of the tear film. Second, the conjunctiva forms a recess trough to hold the three layers of the tear film together and to aid in the redistribution of the tear film during blinking. Third, the conjunctiva provides a loose, flexible connection between the globe and the skin to anchor the globe within the socket while still facilitating its motion. Fourth, the conjunctiva physically protects the globe from invasion by harmful microbes by serving as a structural barrier to their entry. Fifth, the conjunctiva-associated lymphoid tissue (CALT) functions locally in immune surveillance and helps to modulate the immune response of the anterior segment and the ocular surface structures. Finally, by virtue of the movements of the nictitans, in species that have one, the conjunctiva helps to maintain tear film integrity.

The conjunctival epithelium in most areas is a thin, multilayered epithelium, which is not characteristically keratinized. The epithelium contains many goblet cells, although their distribution is not uniform. There is a specialized circumferential epithelial zone at the limbus (the border between the cornea and the sclera) that houses the stem cells of the cornea. The conjunctival stem cells of the limbus provide the epithelial cells that migrate toward the axial cornea to repopulate the epithelium under normal conditions and to repair corneal defects during pathological epithelium loss. Conjunctival tissue is not dependent on the limbal stem cells to repopulate in disease states. In rabbits, the palpebral (outer) surface of the nictitans is lined by an atypical conjunctiva comprised of non-keratinizing stratified squamous epithelium, and contains some delicate hair follicles in this area.

The CALT is thought to be involved in protecting the ocular surface by performing antigen uptake and processing to initiate local immune responses. In the dog and rabbit it occurs on the bulbar surface of the nictitans, while the same lymphoid tissue in rodents and non-human primates is localized to the palpebral conjunctiva. As with most related lymphoid tissues in the body, the amount of CALT varies depending on the age and extent

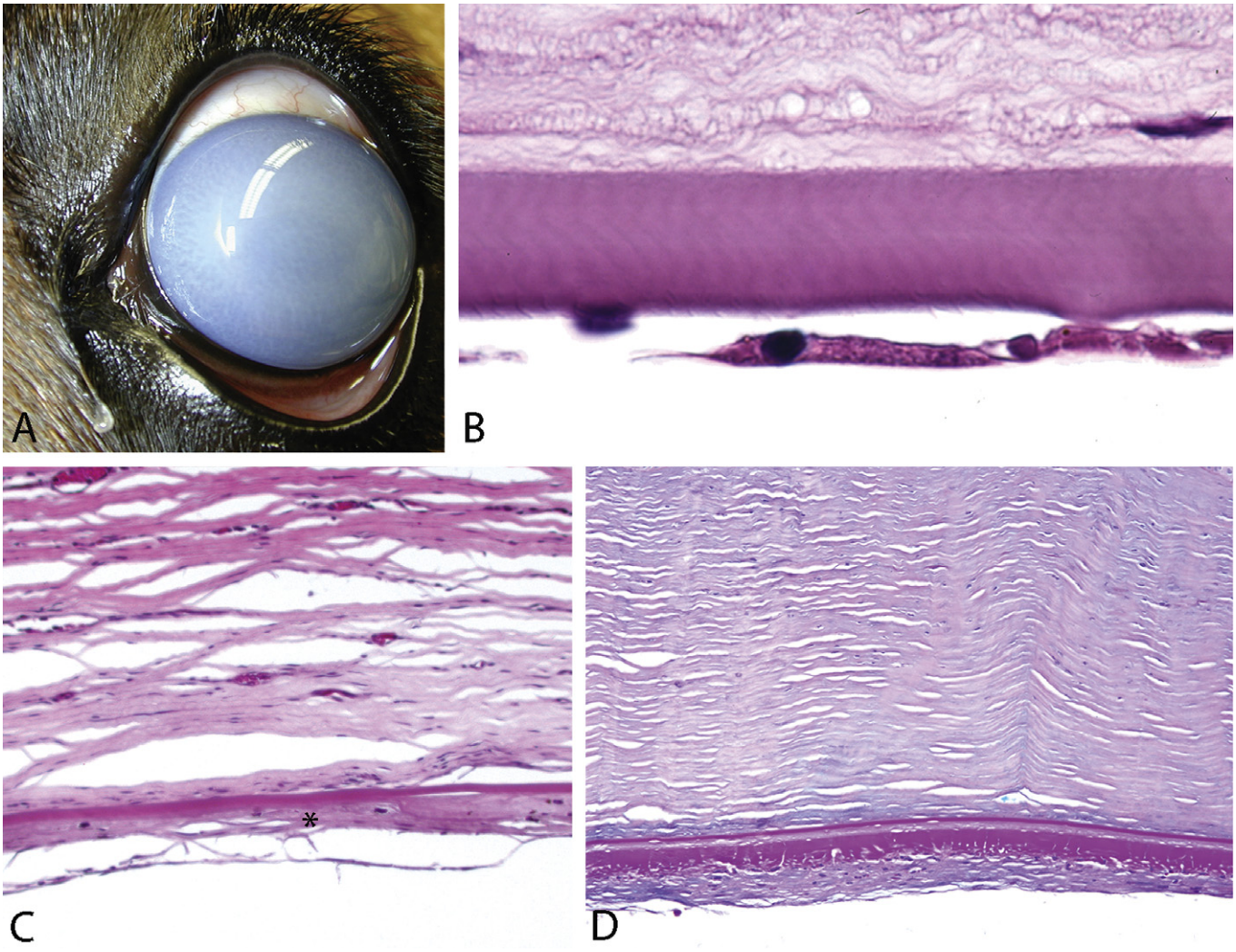


FIGURE 53.11 Corneal endothelial pathology. (A) Clinical image of a dog eye with a diffusely opaque and blue cornea secondary to edema caused by corneal endothelial loss. (B) Attenuated corneal endothelium in a dog with a hereditary endothelial dysplasia. Note the discontinuity and nuclear condensation in the endothelial cell layer beneath the thick eosinophilic band of Descemet's membrane. The stromal connective tissue exhibits an abnormal granular appearance, likely a reflection of fluid accumulation due to disruption of the endothelial barrier. (C) Replacement of the endothelium with a fibrous layer (retrocorneal membrane[*]) in a dog secondary to long-standing mechanical disruption of the endothelium. Using the eosinophilic band of Descemet's membrane as a reference, note the increased thickness of the retrocorneal membrane relative to the normal endothelial monolayer. (D) The retrocorneal membrane in a dog consists of disorganized deposits of basement membrane proteins. (B) H&E, 600×; (C) H&E, 200×; (D) PAS, 200×.

of immune stimulation (principally to antigens in the conjunctival sac, but to a lesser degree to those delivered systemically). Subtending the conjunctival epithelium is the substantia propria, a connective tissue layer containing many glands superficially atop a deeper layer of loose fibrous tissue. The superficial layer also harbors many blood and lymphatic vessels, while the deeper layer has more lymphatic than blood vessels. Derivations of the anterior ciliary arteries supply blood for the conjunctiva, and branches of the trigeminal nerve (cranial nerve V) innervate the tissue.

## 8.2. Evaluation of Toxicity

There are many tools available to evaluate corneal and conjunctival dysfunction. The most

basic is direct illuminated observation in the clinical setting. This non-invasive technique is suitable both for structural assessment and to confirm corneal transparency. Fluorescein dye applied to the corneal surface allows easy detection of such structural defects as ulceration, and aids in visualizing the extent of the cornea that is affected. Rose Bengal dye will accentuate areas of corneal and conjunctival necrosis. A very useful method of observation is the slit-lamp examination. A bright light is shined into the cornea not as a round beam but as a thin line. As the linear light beam traverses the cornea, or any other layer, imperfections that interfere with transparency will scatter the light; the redirected light will be visible from the side of the beam. In effect, the clinician sees a cross-section of the tissue, which emphasizes localized imperfections.

Corneal surface topography can be imaged by a variety of techniques. A map of corneal thickness can be made using pachymetry. The corneal endothelial cells can be studied in life by specular microscopy. The anatomic relationships between the cornea, limbus, iris, and iridocorneal angle can be imaged with high-resolution ultrasound or the even more modern technique of anterior segment OCT.

### *Animal Models of Corneal and Conjunctival Disease*

Animal models of various corneal and, to a lesser extent, conjunctival diseases are common. Those employed to study dry eye and KCS have been described above. The current section will examine those used for investigating other corneal diseases and evaluating the toxicity of xenobiotics toward the cornea and conjunctiva (e.g., the Draize test).

Many important causes of human corneal transplantation are incompletely understood because they do not have well-defined animal models. Examples include Fuch's endothelial dystrophy (degeneration of the posterior corneal epithelium and Descemet's membrane leading to corneal edema), keratoconus (corneal degeneration leading to thinning and conical deformation), and pseudophakic endothelial degeneration. In general, ocular toxicants do not cause lesions that mimic these conditions, so they would be expected to have limited utility as a means for evaluating toxic responses in the cornea and conjunctiva.

The avascular cornea has been used extensively to study the general phenomenon of neovascular proliferation, but the research has had more to do with the biology of blood vessels and their regulatory factors than the molecular regulation of the cornea itself. Irritating agents may incite an inflammatory response in the cornea and/or conjunctiva that can lead to secondary neovascular proliferation, so familiarity with the design of such investigations does have practical value for toxicologic pathologists.

Multiple animal models have been developed to study allergic conjunctivitis. Among them, mice and rabbits exposed to ovalbumin, ragweed, or other allergens are the most prominent in the literature. The allergic reaction is usually characterized by clinical symptoms such as conjunctival hyperemia and chemosis (conjunctival edema) associated with histological evidence of eosinophilic and lymphoplasmacytic infiltration in the substantia propria.

The literature also describes multiple animal models of bacterial keratitis, or corneal inflammation. Again, mice and rabbits are the most commonly used animals; infections with *Pseudomonas aeruginosa* and *Staphylococcus aureus*, the most common causes of bacterial keratitis in humans, are the most studied. Mice have also been used as models for both primary and recurrent herpes simplex type I keratitis. Common microscopic findings in such conditions include acute, necrotizing, and ulcerative corneal inflammation, typically in association with superficial microcolonies of bacteria. The main infiltrating leukocyte population is the neutrophil. Repair typically involves some degree of neovascular proliferation and formation of a localized, opaque scar consisting of disorderly meshes of collagen laid down by activated keratocytes.

### *Ocular Irritation Testing: The Draize Test, and Alternatives*

#### *IN VIVO* OCULAR IRRITATION TEST

The **Draize test** is an acute ocular toxicity test that was devised in 1944 by two toxicologists at the US Food and Drug Administration (FDA), John H. Draize and Jacob M. Spines. The test was first developed to provide a method for assessing the irritation potential of materials

that might accidentally come in contact with human eyes, such as household and office products, agricultural or environmental chemicals, and volatile organic compounds. Because of the widespread acceptance of this method, it was later adopted for testing eye-care products and drugs designed specifically for topical ophthalmic use prior to marketing.

The original Draize method involved the instillation of 100 μL of a test liquid (or 100 mg of a test solid) into the lower conjunctival cul-de-sac. Observations of various criteria (i.e., corneal opacity and area of corneal involvement, conjunctival hyperemia, chemosis, ocular discharges, and iris abnormalities) are taken at pre-defined intervals: 1, 24, 48, and 72 hours, and 1 week, after administration. The test is usually performed in rabbits due to their large eyes, well-described anatomy, ease of handling, relatively low cost, and ready availability. A complete description of the Draize test and its evolution over time is not within the scope of this chapter, but it suffices to say that multiple subjective parameters are analyzed so that a sum of ordinal-scale items regarding tissue reactions to the test article can be used to devise an index of likely ocular morbidity.

Numerous changes have been applied to the original Draize protocol during subsequent years. The volume and mass of the applied test substance have been reduced to 10 μL of fluid (or 10 mg of solid). A saline rinse has been incorporated after instillation of the test material. A slit-lamp examination has been added to allow better assessment of corneal lesions, and topical fluorescein is applied routinely to reveal any cornel ulceration. Optical or ultrasonic pachymetry is now implemented to measure the extent of corneal thickening. The protocol length has been extended to 21 days to allow evaluations for any recovery of the initial lesions. Although the Draize test is still the official model for eye irritation and toxicology studies worldwide, it has suffered major criticism in recent years due to the lack of objective quantification within its grading system, its unreliability in predicting chronic toxic reactions, and marked opposition by animal welfare groups.

### *IN VITRO* OCULAR TOXICITY TESTS

Several *in vitro* assays have been developed in order to circumvent the aforementioned limitations of the Draize test and to minimize the exposure of animals to potentially severe irritating materials. In spite of over 20 years of effort, however, no single *in vitro* assay has been validated as a full regulatory replacement for the Draize test. Instead, some of the techniques described here are widely used as primary screening methods for irritation potential.

1. **Isolated rabbit eye.** In this method, enucleated rabbit eyes (removed immediately after death) are placed in a temperature-controlled chamber and perfused with physiological saline. Test substances are applied topically to the cornea and conjunctiva, and the effects are observed over several days with a slit-lamp biomicroscope. Great advantages of this method over other *in vitro* tests include more ready identification of potential irritants, mimicry of the form in which the material would contact the eye *in vivo*, and marked versatility in the range of irritants that can be tested.
2. **Isolated chicken eye.** The isolated chicken eye test follows the same principles as the isolated rabbit eye test. A major advantage of the avian version is that numerous chicken eyes can be harvested daily from various animal agriculture facilities, thereby reducing the need to terminate laboratory animals merely to harvest donor eyes. Studies indicate that the toxicity results in isolated chicken eyes correlate well with those obtained with isolated rabbit eyes. Indeed, the chicken eye method was able to classify correctly all irritating compounds tested in rabbit eyes *in vivo* in another study.
3. **Isolated corneal preparations.** Since the cornea is the primary tissue of interest exposed to topical irritants, multiple *in vitro* methods using isolated corneal preparations have been developed. These methods are typically limited to assessments of corneal irritation. They cannot be utilized to assess the possibility for allergy, sensitization, or wound repair. **Isolated corneal opacity and permeability tests** are done using isolated bovine corneas collected from slaughter houses. The corneas are mounted in specially designed holders, incubated in Eagle's minimum essential medium at 32°C, and exposed on the external surface to the test article for 1 hour. Subsequently, changes in the opacity and

permeability of the corneal tissue are measured by an opacitometer and by spectrophotometry, respectively.
The **Eytex™ system** is a corneal opacification assay that uses a vegetable protein gel extracted from jack beans (*Canavalia ensiformis*). It predicts ocular irritation of materials based on alterations induced in its vegetable protein matrix. This method is quantitative and reproducible, and presents a high degree of correlation to the Draize test.
Other methods worth mentioning are the **corneal cup method** and the **corneal fluorescence probe method.** The former technique uses isolated fresh bovine corneas to form a "corneal cup" that is used to access the capacity of toxic substances to produce cellular damage by measuring the local production of leukocyte chemotactic factors. The latter procedure is based on the measurement of the degree of epithelium permeability measured using a fluorescent probe after application to fresh rabbit corneas.

4. **Alternatives to the use of eyes and ocular derivatives.** Substances that irritate ocular tissues also have the potential to cause irritation in other sensitive non-ocular tissue. The **chicken egg test (Huhner-Embryonen test)** uses embryonated hen's eggs to demonstrate chemical toxicity through embryo lethality, teratogenicity, and systemic toxicity. It is considered a borderline assay falling between an *in vivo* test and *in vitro* test. Chicken eggs also provide chorioallantoic membrane (CAM) for the **chorioallantoic membrane test.** In this method, the vascular CAM is exposed to the test article in multiple dilutions, and the tissue is scored for irritation effects such as hyperemia, hemorrhages, and coagulation activity.
Other tissues worth mentioning are the **vaginal mucous membrane** and mouse and rabbit **ileum.** For the first method, rat vaginal mucosa is exposed to a toxic substance, after which production of indicators driving inflammation and cellular toxicity (e.g., prostenoids) is measured. For the second technique, the effect of topical surfactants on the contractility of sections of rabbit terminal ileum is assessed as a surrogate for their likely effectiveness as ocular irritants.
5. **Cell culture.** In addition to isolated tissue, cultured cells also can be used as an alternative to the Draize test. The most common cultured ocular elements are conjunctival, corneal, and lens epithelial cells. Cell cultures have the advantage of being more readily available than isolated ocular tissues, thereby avoiding the need to specifically terminate test animals; furthermore, in some instances the cells to be treated may be of human origin, which mitigates the need for interspecies extrapolation. Several methods for measuring cytotoxicity in cell cultures are available (e.g., measurement of plasminogen activation and $^{51}$Cr-release method), and are applicable to multiple types of tissue. For a more complete description of cell culture methodologies, refer to the citations in the Suggested Reading list.

## 8.3. Response to Injury

### *Cornea*

The optical clarity of the cornea is dependent on the precise special distribution of keratocytes (i.e., stromal fibroblasts), collagen, and proteoglycans in the stroma. The corneal stroma shifts from transparent and colorless to become translucent blue when the tissue is disrupted even slightly by excess fluid (edema). The normal corneal stroma is maintained in a slightly dehydrated state by the intact epithelium, the exclusion of blood vessels from the stroma, and, importantly, by the energy-dependent pumping of fluid from the cornea into the anterior chamber across a pressure gradient created by the corneal endothelial cells. Due to the importance of maintaining normal levels of transparency and light refractivity, the cornea presents a very low threshold of tolerance for damage. This high vulnerability renders the measurement of corneal tissue responses to injury a complicated matter.

Several toxic effects might be associated with corneal edema. For example, permeability of the surface epithelium may be altered. This can occur as a result of physical or chemical damage to the epithelium, and is important when

irritants come in contact with the ocular surface. Second, the structural integrity of the stroma may be disrupted. This can be caused by damaging the balance of cytokines which regulate the balance in the arrangement and composition of the stromal elements. Deposition of lipids, mineral, and/or molecules which might enhance the colloidal pressure in the stroma can also cause the stroma to become opaque. Third, vascularization of the stroma and/or enhanced permeability of the limbal blood vessels may impact the ability of the cornea to bar the entry of excess fluid. Toxicant-induced changes in vascular permeability can lead to corneal edema even if new blood vessels do not proliferate into the corneal stroma. Finally, malfunction of the corneal endothelium will predispose to fluid accumulation within the corneal stroma due to the cessation of its active process of draining the corneal stroma of excess fluid.

The impact of KCS on the superficial tissues of the cornea has already been discussed above. Direct trauma with loss of epithelium can provide a portal for bacteria, and an edematous cornea secondary to damage at the corneal endothelium makes the risk of infection and progressive stromal damage all the more serious. Metabolic disorders, tumors, or hemorrhage can lead to deposition of lipid or the formation of lipid granulomas (often with high cholesterol content) in the corneal stroma. Similar deposits of iron (usually after hemorrhage) and calcium in the superficial stroma are present if the tear film is allowed to dry (Figure 53.12).

Corneal subepithelial and stromal mineralization is a prominent feature of spontaneous corneal pathology in some mouse strains. For instance, BALB/c, C3H, and DBA/2J mice frequently possess von Kossa-positive, extracellular, basophilic corneal deposits that are age-related in incidence and severity, and may be associated with focal corneal thinning and ulceration. Interestingly, these mouse strains are also prone to spontaneous cardiac calcinosis.

Many factors that affect the health of the corneal stroma induce the release of matrix metalloproteinases (MMPs) which can degrade the stromal collagen. In the worst cases, the collagenolysis is so fast and complete that the corneal stroma can be completely dissolved in a day or less. An example is the melting corneal ulcer, a devastating disease that is rare in humans but occurs frequently as a spontaneous condition in dogs, particularly the Shih Tzu breed. Affected dogs present with an acute episode of corneal opacity and edema that is cause by abrupt qualitative changes in the corneal stroma: loss of stromal lamellar architecture and severe liquefaction (collagenolysis) of the tissue, usually associated with marked neutrophilic infiltration. If left unchecked, extensive areas of the corneal stroma are affected and the lesion evolves to a descemetocele (prolapse of Descemet's membrane through an eroded corneal epithelium and stroma) and, eventually, corneal perforation.

The corneal epithelium does not have a native stem cell population, so there is a limited capacity of the epithelium to proliferate in response to injury. After ulceration, the existing epithelial cells disconnect from each other and migrate to cover the wound (restitution). However, newly differentiated corneal epithelial cells are recruited from a stem cell population that exists only in the conjunctiva at the limbus. If this population of cells is destroyed (e.g., by herpes virus, chemical burn, necrotizing inflammation, or some other disease process), the corneal epithelium is at a grave risk of permanent deficiency. Conjunctival epithelium will regenerate over the corneal surface, but this scar will not achieve the same optical clarity as normal cornea since it lacks the differentiation state needed to maintain the proper tissue organization to permit light passage at the proper angle. In addition, the scar will remain thin and at risk of renewed ulceration or even a full-thickness corneal rupture through this point of weakness. Limbal stem cell transplantation from the healthy eye to the diseased eye has made it possible for affected humans to regain the function of unilateral eye damage.

The corneal endothelium in most mammalian species does not proliferate in response to disease, and the endothelial cells do not renew themselves. In response to injury or age-related attrition, this cell population does extend so that fewer numbers of cells cover the inner surface of the cornea. There is a critical point at which endothelial cells are unable to adequately sustain their barrier function to fluid entry simply because there are too few of them. They are particularly sensitive to physical disruption from injections or surgical procedures.

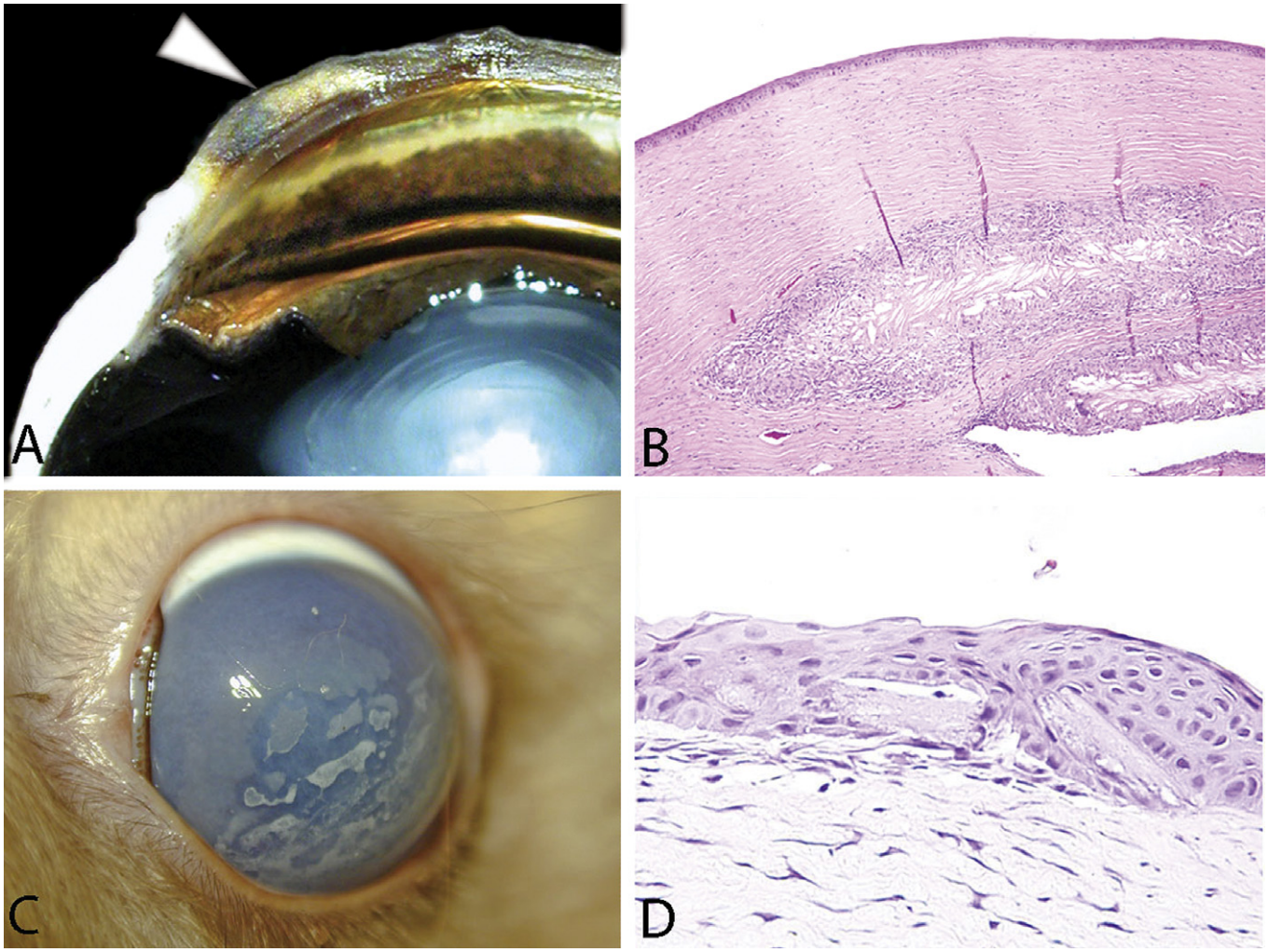


FIGURE 53.12 Corneal deposits. (A) Gross image of a dorso-ventral section of a dog globe showing yellow material, consistent with lipid, deposited in the corneal stroma (arrow). (B) Histologic section presenting a large cholesterol granuloma, comprised of numerous cholesterol clefts surrounded by a marked granulomatous reaction, embedded in the deep corneal stroma. (C) Gross image of a rabbit cornea showing white irregular plaques, composed of mineral and lipids deposited in the corneal stroma. (D) Multiple brick-shaped cholesterol crystals embedded in the corneal epithelium of the rabbit in Figure (C). (B) H&E, 100×; (D) H&E, 400×.

### *Conjunctiva*

The conjunctiva responds to injury like most mucous membranes of the body. The most common diseases of the conjunctiva are inflammatory. Most species have viral diseases that affect the conjunctival epithelium, causing epithelial necrosis and ulceration that often lead to secondary bacterial conjunctivitis with suppurative inflammation and tissue destruction. The conjunctiva also is a common site to manifest allergic diseases as a result of acute inflammation with edema and eosinophilia driven by type I mast cells.

A varied pattern of inflammatory reactions can be found on the conjunctiva, ranging from lymphoplasmacytic to granulomatous to perivascular lymphocytic with neutrophilic vasculitis. Infectious agents are hardly ever associated with this inflammatory infiltrate, suggesting that such infiltration results from an immune-mediated reaction of unknown etiology.

With chronicity, squamous metaplasia of the conjunctival epithelium can occur. If generalized, this change can reduce the numbers of mucus-producing goblet cells, leading to a vicious cycle of tear film dysfunction and dry

eye that can eventually progress to permanent KCS. The conjunctival surface is exposed to UV radiation and thus also can react with dysplastic changes, neoplastic transformation (typically squamous cell tumors), and – in dogs – with induction of vascular endothelial neoplasia. In general, these conjunctival changes are not reported to reflect prior exposure to toxicants.

## 8.4. Mechanisms of Toxicity

### *Corneal Epithelium*

The corneal epithelium, along with the conjunctival epithelium and the tear film, is the first tissue to be exposed when a substance is deposited on the surface of the eye. Substances given by other routes seldom achieve toxic levels in healthy corneal tissues because of their lack of blood supply. However, in principle substances delivered systemically can be concentrated in the lacrimal glands and thereby secreted in locally high bolus doses onto the ocular surface. The corneal epithelium is rich in smooth endoplasmic reticulum and functions to metabolize substances, which pass through the epithelium via the direct route. In this fashion, corneal epithelial cells might be able to activate or detoxify xenobiotics applied to their apical surfaces.

Irritating substances can cause necrosis of the corneal epithelium directly. Acid and alkali burns (described in more detail later) can cause neurotrophic keratitis, a form of corneal degeneration resulting from altered corneal sensory enervation. Surfactants can disrupt the tear film, sensitizing the corneal surface to infection or deep ulceration. Among them, benzalkonium chloride, which is used to increase the penetration of certain drugs to the eye, can cause conjunctival hyperemia, corneal opacification, corneal edema, and occasionally epithelial damage.

Some substances can cause thickening of the corneal epithelium. This increase may be reflective of different pathological processes. For example, long-term topical treatment with an immunosuppressive drug like tacrolimus or cyclosporine may induce superficial squamous cell carcinoma of the cornea in dogs. The degree of risk attributable to the drug treatment is unknown. Local immunosuppression can also enhance the likelihood of developing opportunistic ocular infections with protozoa such a *Toxoplasma* or an ameba. Eye drops containing irritating preservatives like benzalkonium chloride and, less often, chlorobutanol, thimesoral, sorbic acid, or polyquaterenuim ammonium chloride can be associated with a low-grade inflammation of the corneal and conjunctival surface when administered frequently over a long period. Accordingly, preservative-free formulations are favored in individuals who are sensitive or allergic to preservatives. However, preservative-free eye drops are considerably more expensive and usually come in disposable unit-dose tubes that need to be discarded after each use to avoid bacterial growth. It is been reported that local anesthetics such as lidocaine, propacaine, and butacaine can cause epithelial damage when applied topically on the ocular surface, and that they also retard epithelial healing in a dose-dependent manner. For more information on toxic drug reactions affecting the cornea, see Table 53.3.

In specific strains of mice in which open eyelids at birth are common (lids normally open at approximately postnatal days 12–14 in most mouse strains), severe bacterial keratitis, corneal scarring, and neovascularization of the corneal stroma are common. For example, open eyelids in neonates are associated with strains having a characteristic wavy hair coat and curly vibrissae in the waved-1 (T*gfa*$^{wa1}$) and Waved-2 (E*gfr*$^{wa2}$) mutations. The exposure of the eyes as soon as the mice are born makes them prone to trauma induced by bedding debris and contact with parents (especially hairs) and littermates (especially claws), and is accentuated by several factors that predispose to corneal desiccation (e.g., incompletely developed tear production systems, inability to blink effectively).

### *Corneal Stroma*

In response to injury, stromal keratocytes easily undergo metaplasia to develop functions resembling those of fibroblasts. When this activation happens, the keratocytes produce a matrix that is no longer transparent (i.e., a corneal scar). The transformation of this cell population is a risk of surgical treatments such as laser *in situ* keratomileusis (LASIK).

**TABLE 53.3** Topical and Systemic Medications Known to Cause Corneal Toxicity in Humans

| Compound | Lesions |
|---|---|
| Topical aminoglicosides *(tobramycin and gentamicin)* | Superficial punctuate lesion<br>Corneal ulceration and conjunctival pseudomembrane (rare)<br>Delayed corneal re-epithelization |
| Systemic biphosphonates | Conjunctivitis, (also uveitis, episcleritis and scleritis) |
| Topical chemotherapics *(mitomycin and 5-fluorouracil)*<br>Systemic chemotherapics *(imatinib)* | Corneal thinning and ulceration<br>Delayed corneal healing |
| Systemic COX-2 inhibitors | Conjunctivitis |
| Topical fluoroquinolones *(ciprofloxacin)* | Sterile corneal infiltrates<br>Corneal precipitates |
| Topical glaucoma medications *(latanaprost, travaprost, timolol, brinzolamide and pilocarpine)* | Keratoconjunctivitis<br>Keratitis<br>Corneal ulcerations<br>Corneal opacities |
| Topical iodine | Chemical keratitis<br>Corneal epithelium staining<br>Delayed wound healing |
| Topical NSAIDS | Keratomalacia<br>Delayed corneal healing<br>Prevent corneal reepithelization |
| Preservatives in eye drops | Direct damage to corneal epithelium |
| Systemic retinoids/isotretinoin *(isotretinoin)* | Keratitis<br>Corneal opacities<br>Corneal ulceration<br>Dry eye |
| Topical anesthetics *(tetracaine, proparacaine)* | Destruction of superficial cornea epithelium microvilli<br>Direct toxicity on stromal keratocytes<br>Delayed corneal reepithelization |
| Topical steroids | Delayed corneal healing<br>Prevent corneal re-epithelization<br>Posterior subcapsular cataract<br>Glaucoma |

The corneal stroma is at great risk from accidental exposure to caustic chemicals such as strong acids and bases, which can easily erode the corneal epithelium to expose the underlying stroma. The most common acids that may be involved in ophthalmic injuries are sulfuric and sulfurous acids, chromic acid, nitric acid, hydrochloric acid, sulfur dioxide, and silver nitrate; the

most common bases are calcium, magnesium, hydroxides of sodium, ammonium, and potassium. An acid burn to the cornea will coagulate the proteins from the epithelium and stroma. The precipitation of more superficial proteins either from the epithelium or stroma prevents acid substances, especially weak acids, from infiltrating more deeply into the stroma, which lessens the severity of the final lesions. This ameliorating effect does not occur with alkaline substances, as they will deeply penetrate the corneal tissue; thus they cause much more severe damage. The most severe base injuries to the eye are caused by alkalis with pH values greater than 12. On the corneal epithelium, alkalis cause saponification of fatty acids, cell membrane dissociation, and acute cell death leading to destruction and penetration of the epithelial layer. In the stroma, alkalis cause hydrolysis of proteoglycans and render the stromal matrix susceptible to enzymes such as collagenases from neutrophils and plasmin from damaged epithelial cells and fibroblasts, leading to lysis of the stroma. Interestingly, in contrast to acids and surfactants, alkalis tend to produce multifocal to focally extensive injuries presenting as a pattern of almost normal areas intermingled with deeply affected ones. Among these linear lesions, surfactants are also known to cause corneal irritation and tissue damage. Cationic surfactants generally tend to precipitate cellular proteins, with anionic agents causing cell lysis while non-ionic substances can cause either cell lysis or protein precipitation. The end result of chemical burns to the cornea is extensive scar formation and relatively widespread loss of transparency. The cumulative results of ocular irritation tests performed in rabbit corneas using many agents – acids, alkalis, surfactants and non-surfactants like acetone, cyclohexanol, parafluoroaniline and formaldehyde –suggest that the extent of the initial injury (i.e., the depth to which the corneal tissue is affected) is significantly correlated with the subsequent tissue response and is the principal factor determining the final outcome of the ocular irritation.

As mentioned before, neovascularization of the corneal stroma is regarded as a secondary phenomenon to corneal inflammation. It also can be seen as a background lesion in nude (*Fox*1$^{nu}$) and hairless (*hr*) strains of mice. Application of certain molecules with trophic properties for vascular growth, such as VEGF or pro-inflammatory cytokines, may also promote the formation of new capillaries. In general, this response requires the agent to be present for a prolonged period (e.g., by slow release from an adjuvant depot or implanted wafer). As such depots are not typical means of applying ocular formulations and ophthalmic drugs do not have pro-angiogenic actions, this corneal change is not a typical toxic response in the clinical setting.

Exposure to UV radiation is a significant risk factor for ocular disease in humans and animals. For example, experiments with UV radiation in 129S1/SvImj mice demonstrated that chronic exposure (over 50 weeks) induced loss of stromal keratocytes. This change led to stromal thinning, keratoconus, neovascularization, and stromal fibrosis of the cornea, and a high incidence of posterior cortical cataract. It is hypothesized that co-exposure to low doses of toxic agents and UV light might be able to induce corneal injury in an additive or even synergistic fashion.

### *Corneal Endothelium*

The corneal endothelium typically is exposed to high concentrations of a substance when the material is introduced into the anterior chamber by either injections or surgical procedures. Since the human endothelium is incapable of regeneration, any toxicity that compromises function or reduces the total number of corneal endothelial cells is serious. The endothelial cells are protected by the anterior chamber aqueous (flow of which quickly removes high local levels of injected agents) on one side and Descemet's membrane on the other. The endothelial cells do not tolerate any sort of contact. In dogs, lens luxation leading to contact with the endothelium will cause attenuation or spindle cell metaplasia of the axial endothelial cells. Similarly, intraocular surgeons go to great lengths to avoid touching the endothelium and to protect these cells using viscoelastic materials to coat their surfaces. In a commonly performed glaucoma surgery to create a surgical bleb as an alternative drainage portal, the surgeon will often use potent antimetabolite drugs such as mitomycin C to minimize scar formation and keep the drainage tract open. It is devastating to the endothelium if it is exposed to such drugs by inadvertent reflux from a depot deposited elsewhere in the

eye. Intracameral injection (i.e., directly into the anterior chamber) of the local anesthetic lidocaine in concentrations higher than 4% has been shown to be markedly toxic to endothelial cells in rabbits and humans. The preservative benzalkonium chloride, when inadvertently injected into the anterior chamber, causes severe toxic endothelial destruction in these same two species. Another important endothelial toxic reaction is observed with enzymatic detergents, which are used as sterilization agents on surgical instruments and supplies. These substances are associated with a dose-related corneal thickening and ultrastructural damage to the corneal endothelium in humans and rabbits.

Although rare, the corneal endothelium can respond to injury by proliferating rather than undergoing atrophy. In such instances, the corneal endothelium migrates over the iridocorneal angle and anterior aspect of the iris and sometimes produces a Descemet's membrane-like material. This phenomenon is known as endothelialization, and is associated with iridocorneal endothelial (ICE) syndrome and some forms of glaucoma in humans. In mice, ICE syndrome occurs in the DBA/2J and AKXD-28/Ty strains and can lead to progressive angle closure glaucoma.

Functional impairment of the corneal endothelial cells with minimal to no anatomical changes is a phenomenon that must be taken into account whenever a toxic substance is injected directly into the anterior chamber. This effect can sometimes explain variations in corneal thickness observed in toxicological studies. This phenomenon is usually attributed to inability of the endothelial cells to maintain their normal physiological processes. The usual outcome of such cell dysfunction is edema of the corneal stroma.

### *Conjunctiva*

Due to their close proximity, the cornea and conjunctiva are concomitantly exposed to the same toxic agents. The pathological responses of both tissues usually are also similar.

During chemical burns, the conjunctiva usually develops the earlier changes. In mild acid burns, the initial clinical alterations are turbidity and dulling of the conjunctival surface with tissue hyperemia and possibly petechial hemorrhages. With stronger acids, both conjunctiva and cornea become opaque immediately. There is loss of conjunctival epithelium followed in mild cases by rapid regeneration (5–10 days). In severe cases, the conjunctival substantia propria is more affected and the final result is granulation tissue formation and scaring. Acids and alkalis that cause conjunctival toxicity are the same previously described for corneal epithelium and stroma. Also, the same principles of toxicity associated with different acids and alkalis listed for the cornea apply to the conjunctiva.

One of the most popular routes for clinical administration of ocular therapeutics is via subconjunctival injections, so subconjunctival administration of drugs associated with biodegradable drug implants designed for sustainable drug delivery also is common practice in non-clinical toxicology studies. Poly [d,l-lactide-co-glycolide] (PLGA) or poly [d,l-lactide-co-caprolactone] (PLC) are among the most common biodegradable polymers used for this purpose; in particular, PLGA has been used extensively in studies to deliver a wide variety of drugs using various forms such as microparticles, emulsions, implants, and hydrogels. These polymers degrade through hydrolysis of their ester bonds into lactic acids, glycolic acids, and caproic acid, and eventually into water and carbon dioxide. In most instances these subconjunctival implants cause minimal to no reaction, and when they do develop, local conjunctival hyperemia and edema are the most common. In the rare instances where toxic reactions are observed, they are usually related to failed degradation of the polymer with secondary conjunctival fibrosis of the substantia propria to encapsulate the implants.

## 9. UVEA AND FILTRATION APPARATUS

### 9.1. Structure, Function, and Cell Biology

The uvea forms the continuous, heavily vascularized middle tunic of the globe. Its main function is to provide the globe's blood supply. The uvea is pigmented to help absorb reflected light and avoid glare when light is focused on the retina.

There are three designated regions of the uvea: the iris, ciliary body, and choroid. The iris and ciliary body together make up the anterior uvea, while the choroid is the main component of the posterior uvea. The long posterior ciliary arteries branch at the ocular equator and feed the anterior part of the choroid. The short posterior ciliary arteries divide to supply the posterior part of the choriocapillaris, and they also form an anastomotic circle (of Zinn) around the optic disc that contributes to the arterial network on the optic nerve. The anterior ciliary arteries send recurrent branches to the choriocapillaris, and also anteriorly to the major arterial circle at the iris base. Branches from this circle extend into the iris and toward the limbus. The veins draining the scleral venous sinus join the anterior ciliary veins and vortex tributaries.

The **iris** is cantilevered across the front of the globe, where it serves to separate the anterior chamber from the posterior chamber. The anterior surface of the iris has no epithelial lining, so fluid is free to diffuse from the iris stroma to the anterior chamber with no barrier. The posterior surface of the iris is lined by an epithelial complex, which is derived from the neural tube ectoderm. This epithelium is equipped with tight junctions that form a barrier to fluid passing from the iris stroma into the posterior chamber. Within this complex there is a simple posterior pigmented epithelium, which is in direct contact with the posterior chamber lumen, as well as a bifunctional anterior epithelium, in which the posterior aspect is pigmented but the anterior aspect is contractile in a manner resembling that of smooth muscle forming the iris dilator muscle (Figure 53.13). The dilator

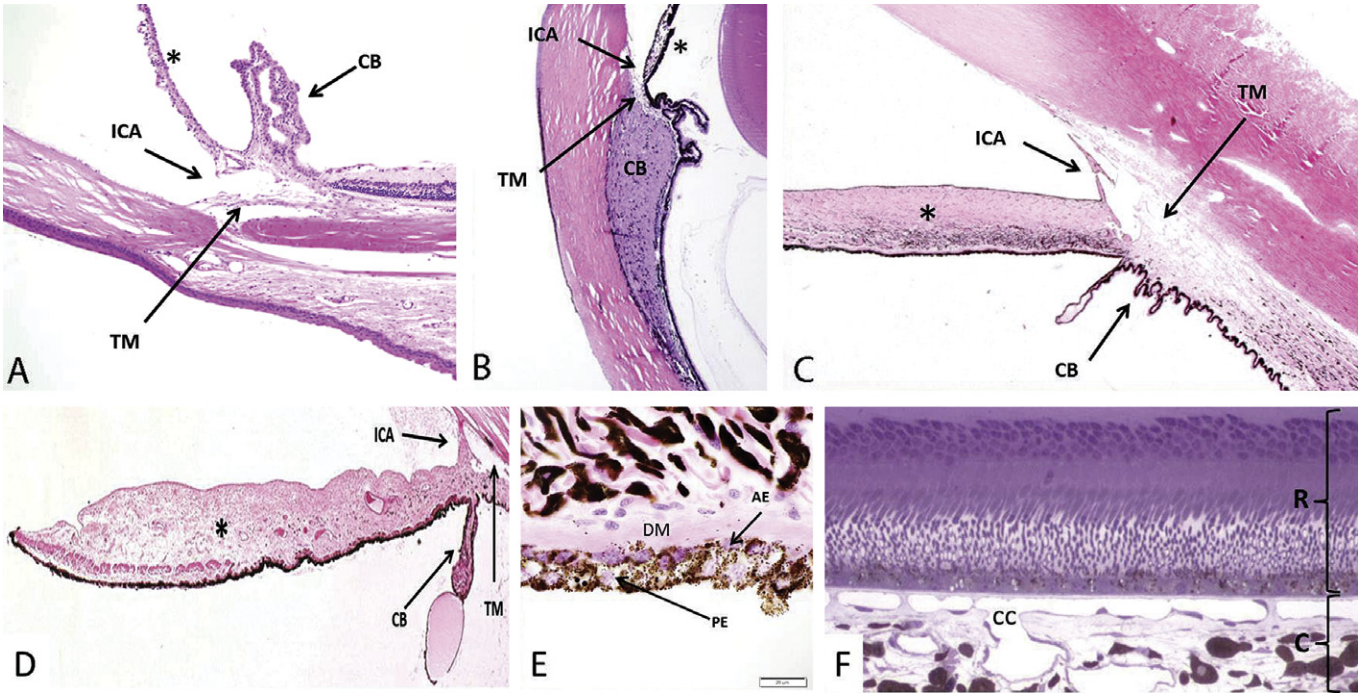


FIGURE 53.13 Normal architecture of the uvea. The iridocorneal angle (ICA), iris (*), trabecular meshwork (TM) and ciliary body (CB) from an albino mouse (A), non-human primate (B), dark-eyed dog (C), and blue-eyed dog (D). Note the marked lack of pigmentation of the iris stroma, characteristic of light-colored eyes, in the mouse (A) and blue-eyed dog (D). (E) Posterior iris epithelium showing the pigmented posterior epithelium (PE), the anterior epithelium (AE) with melanin surrounding its nuclei on the apical (near the posterior epithelium) aspect, and the smooth muscle appearance of its basal aspect, which contains large amounts of myofilaments and forms the dilator muscle of the iris (DM). (F) The outer retina (R) and inner choroid (C) from a non-human primate which was perfusion-fixed to allow better observation of the capillary network, the choriocapillaris (cc). (A, B, C, D) H&E, 12.5×; (E) H&E, 1000×; (F) Toluidine blue, 400×.

muscle is a contractile myoepithelial tissue, which is innervated by sympathetic nerves. The sphincter muscle, which closes the pupil, is formed of smooth muscle fibers encircling the pupillary margin. This muscle is also derived from the neural tube.

The **ciliary body** is subdivided into two parts, the anterior pars plicata and the posterior pars plana. The inner aspect of the ciliary body is lined by a double epithelium which is also derived from the neural tube. There is an inner non-pigmented epithelium and an outer pigmented epithelium. Both layers are bounded by a basal lamina on the basal aspect, which is away from the line of contact between the two layers. It is important to realize that the aqueous chambers of the eye are not in fact empty lumina, but rather represent liquid-filled extracellular spaces. The ciliary epithelium secretes the aqueous fluid against a pressure gradient. The epithelium also secretes hyaluronic acid, the major substance of the vitreous in the posterior chamber. The zonular ligaments that suspend the lens are also deposited by the ciliary epithelium and are anchored on the epithelial basement membrane. There are tight junctions between epithelial cells, which form a diffusion barrier between the ciliary stroma and the posterior chamber. The ciliary muscle is a smooth muscle, which functions in visual accommodation by controlling the suspension of the lens and thereby its curvature. The ciliary muscle is hypothesized to play a role in aqueous filtration in primates by regulating the tension of the trabecular meshwork at the level of Schlemm's canal. The ciliary muscle is robust in primates, and accommodation is, by far, more effective in these species than in most other mammals. Accommodation is almost vestigial in rodents and in dogs.

The ciliary epithelium plays an important role in the establishment and maintenance of the ACAID phenomenon. This system functions to lessen the destructive impact of inflammatory disease on the ocular tissues, which have little functional reserve. Immune cells reacting to antigens in the globe are programmed as they traverse the ciliary epithelium to home in on the spleen. In the spleen, they differentiate as T-regulatory ($T_{reg}$) cells or suppressor T cells. These cells favor immune tolerance rather than immune surveillance/immunoreactivity.

The **choroid** has as its most important function the delivery of oxygen and nutrients to the high-metabolizing cells of the retina. The cell population with the highest demand for energy in the body is the retinal photoreceptors. These cells require abundant oxygen during both the dark and light periods. The blood supply that most effectively nourishes the outer retina is the extensive choroid capillary bed known as the choriocapillaris (Figure 53.13). This extensive interconnected capillary network resides behind the RPE cells. The lumen of the choriocapillaris is separated from the basal cell membrane of the RPE layer by the fused basal lamina of the RPE and the vascular endothelial cells, as well as by a sandwiched layer of elastin; this five-layered barrier is called Bruch's membrane (Figure 53.14). The choriocapillaris has a higher perfusion turnover than any capillary vascular bed in the body.

The **filtration apparatus** is made up of several features that function to reabsorb aqueous humor back into the blood. As mentioned above, the aqueous is produced by the ciliary body epithelium, passes through the pupil into the anterior chamber, and is drained laterally though the iridocorneal angle and trabecular meshwork (Figure 53.13). The balance between secretion and drainage of the aqueous humor determines the IOP. Under normal conditions, this pressure is maintained at a relatively constant level of 15–20 mmHg in all mammalian species of interest for ocular toxicology research. Basic elements of this system are the trabecular meshwork, Schlemm's canal, the uveoscleral meshwork, and the aqueous veins. The angle formed between the base of the iris and the end of Descemet's membrane in the cornea is the iridocorneal angle. The space between these two structures, termed the ciliary cleft, is the channel through which the aqueous humor passes on its way to the trabecular meshwork. The trabecular meshwork begins posterior to the end of Descemet's membrane and extends posteriorly, and dissects between the ciliary body and sclera until a point midway along the ciliary body length. This meshwork is composed of a series of trabecular beams that run parallel to the long axis of the ciliary body. The trabecular beams are composed of a core of collagen fibers interspersed with small amounts of elastic tissue surrounded by a single

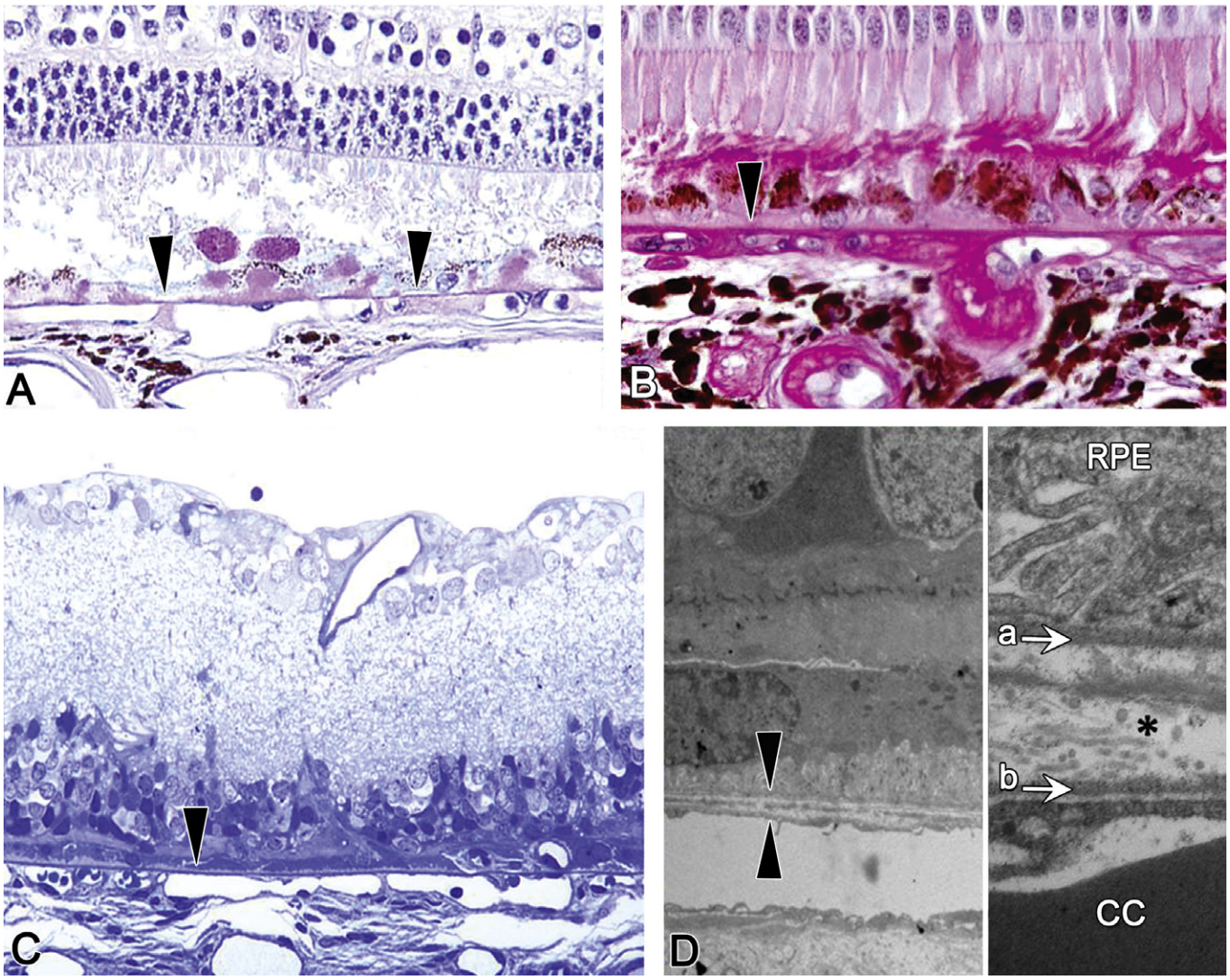


FIGURE 53.14 Normal architecture of Bruch's membrane. (A) Image of the outer retina from a dog demonstrating the location and uniform thickness of the normal Bruch's membrane (arrowheads). (B) Bruch's membrane (arrowhead) from a non-human primate with hypertension and diabetes, demonstrating irregular thickening. (C) Bruch's membrane from a rat with outer retinal atrophy, showing an intact Bruch's membrane (arrowhead) in spite of the marked outer retinal atrophy. (D) Transmission electron micrograph (TEM) from a rat showing the normal ultrastructural appearance of Bruch's membrane (between the two arrowheads). (E) At higher magnification, Bruch's membrane consists of an inner layer (a), formed by the basal lamina of retinal pigmented epithelial (RPE) cells, and an outer layer (b), formed by the basal lamina of the choriocapillaris (cc). Between these two basal laminae the membrane contains delicate layers of collagen and elastic tissue (*). (A) Periodic acid-Schiff (PAS), 200×; (B) PAS, 400×; (C) Toluidine blue plastic section, 200×; (D) TEM, 1025×; (E) TEM, 3100×.

layer of flattened endothelial cells that are laid over a basement membrane similar to Descemet's membrane. The aqueous flows through the spaces between the trabecular beams. Schlemm's canal is a circumferential, endothelial-lined channel that lies just exterior to the trabecular meshwork (Figure 53.15). This canal connects directly to the aqueous vein, where the aqueous exits the eye through the venous drainage of the conjunctiva and orbit. The juxtacanalicular tissue (JCT) is the area of the trabecular meshwork immediately adjacent to the Schlemm's canal. The JCT is the point of highest resistance to aqueous drainage in the trabecular meshwork, and it has recently sparked great interest due to the discovery that

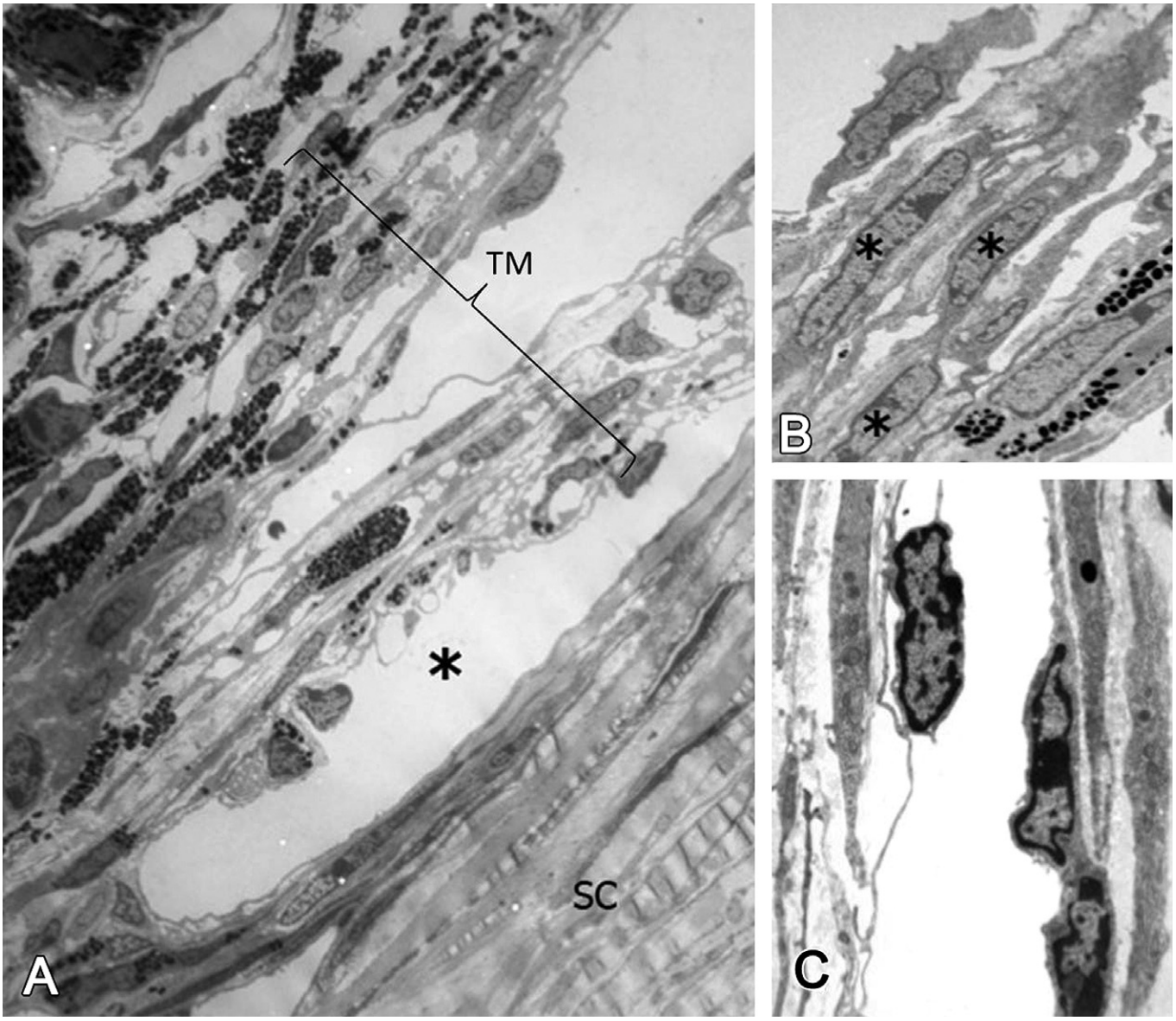


FIGURE 53.15 Normal architecture of the trabecular meshwork and Schlemm's canal. (A) In the mouse, the trabecular meshwork (TM), Schlemm's canal (*), and sclera (SC) may be shown to be closely related by transmission electron microscopy. (B) Trabecular beams composed of trabecular endothelial cells (*) surrounding a core of collagen fibers and small amounts of elastic fibers. (C) Detail of Schlemm's canal with vascular endothelial cells lining the lumen (central clear space). (A) 2250×; (B) 3300×; (C) 7100×.

it plays an essential role in the onset of multiple forms of glaucoma in humans.

There are two major pathways of aqueous drainage: the classic pathway and the alternative pathway. In primates, rodents, and rabbits, the central structure in the classic pathway is Schlemm's canal. Passing down this pathway, aqueous humor passes through the iridocorneal angle and trabecular meshwork to drain through Schlemm's canal. The process, which is not well understood, is energy dependent. The magnitude of absorption via the classic pathway is proportional to the IOP. In dogs, there is no circumferential Schlemm's canal, but instead the aqueous drainage plexus is intermittent. The alternative pathway is similar in rodents, rabbits, dogs, and primates. It is a passive system by which aqueous drains into a potential space posterior to the trabecular meshwork (i.e., into the anterior face of the ciliary muscle and

suprachoroidal space) just inside the sclera. Via this system, the aqueous can drain without barrier until it is reabsorbed into the blood in vessels within the sclera or choroid. This system clears about the same amount of fluid regardless of whether the IOP is high or low. The relative contributions of these two outflow pathways vary among species, with the alternative pathway accounting for 30–65% in primates, 13% in rabbits, 3% in cats, 15% in dogs, and 4–14% in humans during normal health.

The **albino rodent** is a popular and well-characterized animal test system for toxicologic studies. The natural uvea is highly melanized to reduce light dispersion in the eye, and the presence of pigment also dampens the damaging effects of light-mediated chemical reactions to tissues in the eye. There are several reasons why albino rodents might not be the best choice for test species if the eye is a particular target for toxicity testing. First, albino mice and rats are exquisitely sensitive to retinal phototoxicity from exposure to only slightly increased levels of ambient light. Accordingly, the background level of retinal damage in controls is likely to be high. Furthermore, phototoxic retinopathy can have a dose and sex distribution that mimics a dose effect, especially in females. The albino uvea is also hypoplastic and vascular perfusion is decreased, which may impact the delivery of systemic toxicants and/or enhance the toxicity to metabolically borderline cell populations resulting from vascular perfusion problems. In addition, melanin protects against the damaging effects of ultraviolet light in the eye and often binds test substances, so the toxicokinetics of the albino rodent are likely to be quite different from those in the pigmented eyes of other species. Taken together, these discrepancies can result in ocular toxicity data sets that can lead erroneously to interpretations that a test article's effects are different (either less or greater) from the impression that would have been gained by conducting the study in a more appropriate test species or rodent strain.

## 9.2. Evaluation of Toxicity

Many methods are available to test the structure and, to a lesser degree, the function of the anterior uvea. Gonioscopy is a morphological technique used in the clinic that employs a lens or prism placed on the corneal surface to directly observe the iridocorneal angle. Modern and sophisticated imaging techniques like ultrasound biomicroscopy and anterior segment OCT are used to evaluate the morphology of the anterior uvea. Development of anterior segment OCT offers the benefits of fine resolution and non-invasive examination to investigations of anterior segment anatomy to the depth of the iris plane. Fluorescence angiography is a technique often used while imaging the anterior uvea, and provides valuable information regarding vascular integrity of the iris. The reflex function of the iris dilator and sphincter muscles can be evaluated in the routine eye exam by testing the direct and consensual pupillary light reflexes. These reflex tests primarily assess the neural control of the pupillary light response.

In contrast to the anterior uvea, essentially no methods other than direct microscopic examination post-mortem are available for assessing the structure of the posterior uvea. No reliable techniques are available for evaluating posterior uvea function.

Cellular infiltration into the anterior uvea and aqueous humor is a common feature of spontaneous and experimental ocular diseases. The collection of aqueous humor can provide substantial diagnostic information when analyzing the responses of the intraocular tissues to specific agents, and during the characterization of animal models of intraocular inflammation. Specific procedures, including micro-enzyme linked immunosorbent assays (ELISA), polymerase chain reaction (PCR), flow cytometry, and cytokine analysis (e.g., Luminex® multiplex assays) may provide essential quantitative information for evaluating the extent and/or character of the immune response. The main advantage of these tools is their ability to measure a great number of molecules (up to 100 with Luminex assays) in a single small sample (25–50 μL) of aqueous humor.

As noted above, the IOP of mammals is maintained at a level approximately 20 mmHg higher than the turgor (fluid pressure) of surrounding tissues to sustain the shape and rigidity of the eye. Increased IOPs place the eye at risk of developing glaucoma (a spectrum of diseases characterized by persistent elevations of IOP).

In the clinic, the IOP is measured by tonometry. Applanation tonometry estimates the IOP from the force needed to applanate (flatten) a set area of cornea. This easily accessible technique is suitable for large-eyed laboratory animals (dogs, non-human primates) and humans. Accurate and non-invasive tonometric measurements had been unattainable in small-eyed rodents until the recent advent of rebound tonometry (in which a small magnetized probe is bounced against the cornea to create a current from which the IOP may be calculated) has permitted such assessments to become routine. The rate of aqueous drainage can be measured by fluorometric analysis.

The main findings in the uvea induced by toxicants are inflammation or vascular leakage with edema. Typical lesions include cellular infiltrates (often lymphocytes and plasma cells) and increased space between connective tissue elements.

### *Animal Models of Uveitis*

Uveitis (uveal inflammation) is often an idiopathic disease that can lead to blindness. It is commonly believed to have an autoimmune character, although there are many and varied clinical manifestations. Putative autoimmune uveitis in humans is thought to be driven chiefly by immunity to retinal antigens. Several distinct forms of human uveitis are strongly linked to specific HLA tissue types. Many forms of uveitis respond to treatments directed against T cell-associated inflammatory mechanisms (Type IV hypersensitivity responses).

The understanding of uveitis has advanced tremendously as a result of the development of animal models of the disease, referred to collectively as experimental autoimmune uveitis (EAU). Most models involve immunization of rodents with retinal antigens such as arrestin (S-antigen) or interphotoreceptor retinoid-binding protein (IRBP). In these models, elicitation of ocular pathology requires co-administration of adjuvants, the most common being bacterial fragments or pertissus toxin mixed in CFA. The goal in those models is to trigger pattern recognition receptors on innate immune cells, thereby promoting a pro-inflammatory environment in which there is an autoreactive component. In general, EAU models can be divided into those induced by immunization and those that develop "spontaneously" in genetically engineered animals.

Another widely used animal model of uveitis in which the target is assessing mostly the innate immune response is endotoxin-induced uveitis (EIU). This model can be performed in mice, rats, and rabbits to yield an acute anterior uveitis of short duration. Derivative fractions of melanin or tyrosinase may be used to induce a model of Vogt-Koyanagi Harada (VKH) uveitis. The most important animal models of uveitis are summarized in the Table 53.4.

## 9.3. Response to Injury

The uvea is the vascular tunic of the eye. Because of the need for transparency in the light-transmitting media of the globe, vascular proliferation is tightly regulated. There are many disease states where the release of vasoproliferative cytokines leads to the formation of neovascular proliferation associated with the uvea. These membranes are seldom actually within the uveal tissue, but rather extend out along the surfaces of the iris, ciliary body, and/or choroid. The aqueous, vitreous, or subretinal spaces also may harbor vascular proliferation. Such fibrovascular membranes can lead to synechiae (i.e., adherence of the iris to either the cornea [anterior synechia] or lens [posterior synechia]), iridocorneal angle closure, and/or hemorrhage. Retinal hypoxia as a result of restricted perfusion or retinal detachment is a common condition leading to the formation of these membranes, presumably because tissue hypoxia results in the local production of vascular-inducing growth factors. Intraocular inflammation, ocular trauma, and tumors in the eye are other possible causes. Neovascular glaucoma and choroidal neovascularization in the wet form of age-related macular degeneration (wet AMD) are two examples of diseases associated with the intraocular release of excessive amounts of vasoproliferative molecules, particularly VEGF.

The classical filtration system functions by the formation of a resistance to filtration across a sequence of trabecular columns. Proper functioning of the system to remove aqueous humor is highly dependent on the integrity of the matrix elements. Long-term or high-dose corticosteroid

TABLE 53.4 Relevant Animal Models of Uveitis

| Models | Animals | Characteristics |
|---|---|---|
| **Mice (induced):** | | |
| Classical EAU | B10.RIII, B10.A and C57BL/6 | Immunization of WT mice with IRBP in CFA or adoptive transfer of immune cells from immunized donors to naïve recipients |
| "Humanized" EAU | HLA-DR3 transgenic mice | Mice are immunized with retinal arrestin or adoptively transferred with cells from immunized donor |
| EAU<br>Syngeneic DCs | B10.RIII mice | Mice inoculated with splenic DCs pulsed with IRBP |
| MDP-induced uveitis | Not specific | Direct injection of MDP into mouse eye |
| Neo-self antigen | Not specific | Neo-antigen promoted transgenically by a retinal promoter or by retroviral transduction, then mice are immunized by antigen |
| **Mice (spontaneous):** | | |
| Deficient central tolerance | AIRE-deficient mice | Higher frequency and higher affinity of cells bearing TCRs specific for IRBP |
| Mice transgenic for human HLA | HLA-A29 mice | Mice transgenic for human HLA class I associated with uveitis. Develop a birdshot choroidopathy-like disease |
| **Rat:** | | |
| Immunization with retinal antigen | Lewis rat | Immunization with arrestin or adoptive transfer of immunized donors cells to naive recipient |
| **Non-human primate:** | | |
| Immunization with retinal antigen | Cynomolgus or rhesus | Immunization with retinal arrestin in CFA or Hunter's adjuvant |
| **Multiple animals:** | | |
| EIU | Mice, rats and rabbits | Induced by systemic injection of LPS in rats and mice and intraocular injection in rabbits |

Abbreviations: AIRE, autoimmune regulator; CFA, complete Freud's adjuvant; DC, dendritic cell; EAU, experimental autoimmune uveitis; EIU, endotoxin-induced uveitis; HLA, human leukocyte antigen; IRPB, interphotoreceptor retinoid-binding protein; LPS, lipopolysaccharide; MPD, muramyl dipeptide; TCR, T cell receptor.

use can induce increased IOP and disruption of this system.

Cynomolgus monkeys exhibit lymphocytic uveal inflammation as an idiopathic background change that should be distinguished from a toxic effect. This inflammatory infiltrate is seen in both naïve controls and animals exposed to test compounds. In reviewing hundreds of archived samples from naïve control cynomolgus monkeys, such mononuclear inflammatory infiltrates, compose mainly of lymphocytes with fewer plasma cells, were seen in the ciliary body and choroid of approximately 27% of the animals. This inflammatory infiltrate is most often seen in

the *pars plana* of the ciliary body and is usually focal, minimal to mild, and unilateral. Nonhuman primates also can present with focal to multifocal areas of hyperplasia and dysplasia of the ciliary epithelium.

### 9.4. Mechanisms of Toxicity

The Toxic Anterior Segment Syndrome (TASS) is a sterile uveitis syndrome seen after intraocular surgery. Uveitic symptoms develop more rapidly after surgery than in the presence of septic endophthalmitis. "Cell and flare" (the combined presence of leukocytes as tiny white specks [clinically termed "cell"] and protein as a gray-white haze [clinically termed "flare]) as well as fibrin exudate predominate in TASS, and corneal edema secondary to corneal endothelial compromise might also be seen. TASS is thought to be caused by exposure to irritating irrigating solutions or other fluids or additives placed in the eye during intraocular surgery. Substances such as anesthetics, viscoelastics, and antibiotics have been found to be related to TASS. Chemicals used to clean or sterilize surgical instruments used in eye procedures can also be the cause.

Uveitis induced by minute amounts of endotoxin is a constant worry for the producers of sterile biologic products intended for use within the eye. Profound neutrophilic exudates, vascular leakage, and microthrombosis of ocular microvessels are the morphologic hallmarks of endotoxin-induced uveitis. The presumed mechanism is the vigorous immune response raised against the bacterial toxin.

The choriocapillaris and adjacent uveal tissues are exposed to focused light in a local environment where lipid membranes are constantly being degraded by phagocytosis. These tissues are susceptible to toxicity by anything that enhances oxidative stress, such as increased fat in the diet, chronic zinc deficiency, or hemochromatosis. To our knowledge, the cells within the posterior uvea are not directly targeted by toxicants.

## 10. THE LENS

### 10.1. Structure, Function, and Cell Biology

The lens is suspended in the aqueous humor of the posterior chamber and held in place by modified elastin fibers called the zonular ligament. The fibers in this suspensory ligament encircle the equator of the lens and are anchored to the ciliary body. The posterior chamber is the space between the anterior face of the vitreous humor (near the posterior lens capsule) and the posterior border of the iris. Aqueous fluid produced by the ciliary body fills the posterior chamber and flows into the anterior chamber through the pupillary space. The vitreous cavity holds the vitreous humor.

The lens contains only one cell type, and has no blood supply. The lens epithelium arises from an invagination of the surface ectoderm after an embryonic induction event when the optic vesicle contacts the surface ectoderm. The infolding epithelium hypertrophies to form the thickened lens placode. The invagination separates from the skin to become the lens vesicle, and becomes solid when the lens epithelial cells (LECs) on the posterior pole elongate to form the first lens nucleus. The LECs on the anterior pole stay active for the life of the animal and continuously form new lens fibers, which are pushed deeper into the nucleus by newly developing fibers in a process that continues until death. This means that the lens continues to enlarge slowly and becomes more dense and rigid with age. During development and until shortly after birth, the lens is nourished by a network of capillaries just outside the posterior lens capsule called the tunica vascularis lentis (Figure 53.2). These vessels atrophy and disappear, along with the last vestiges of the primary vitreous and pupillary membranes, shortly after birth. From that time on, the lens receives nutrition from the oxygen-poor aqueous humor and anterior vitreous.

The fully developed lens is formed from a monolayer of cuboidal epithelial cells on the anterior pole. These cells proliferate slowly in the mid-periphery, and that causes a gradual movement towards the equator. At the equator, each LEC begins to elongate and also rotate such that it becomes oriented parallel with the lens fibers at the equator. As this happens to consecutive LEC generations, the nucleus of each elongated cell is pushed farther into the cortex; this process forms a graceful arch called the nuclear bow (Figure 53.16). Fully differentiated lens fibers stretch from the posterior pole to near the anterior pole. Eventually, the LEC

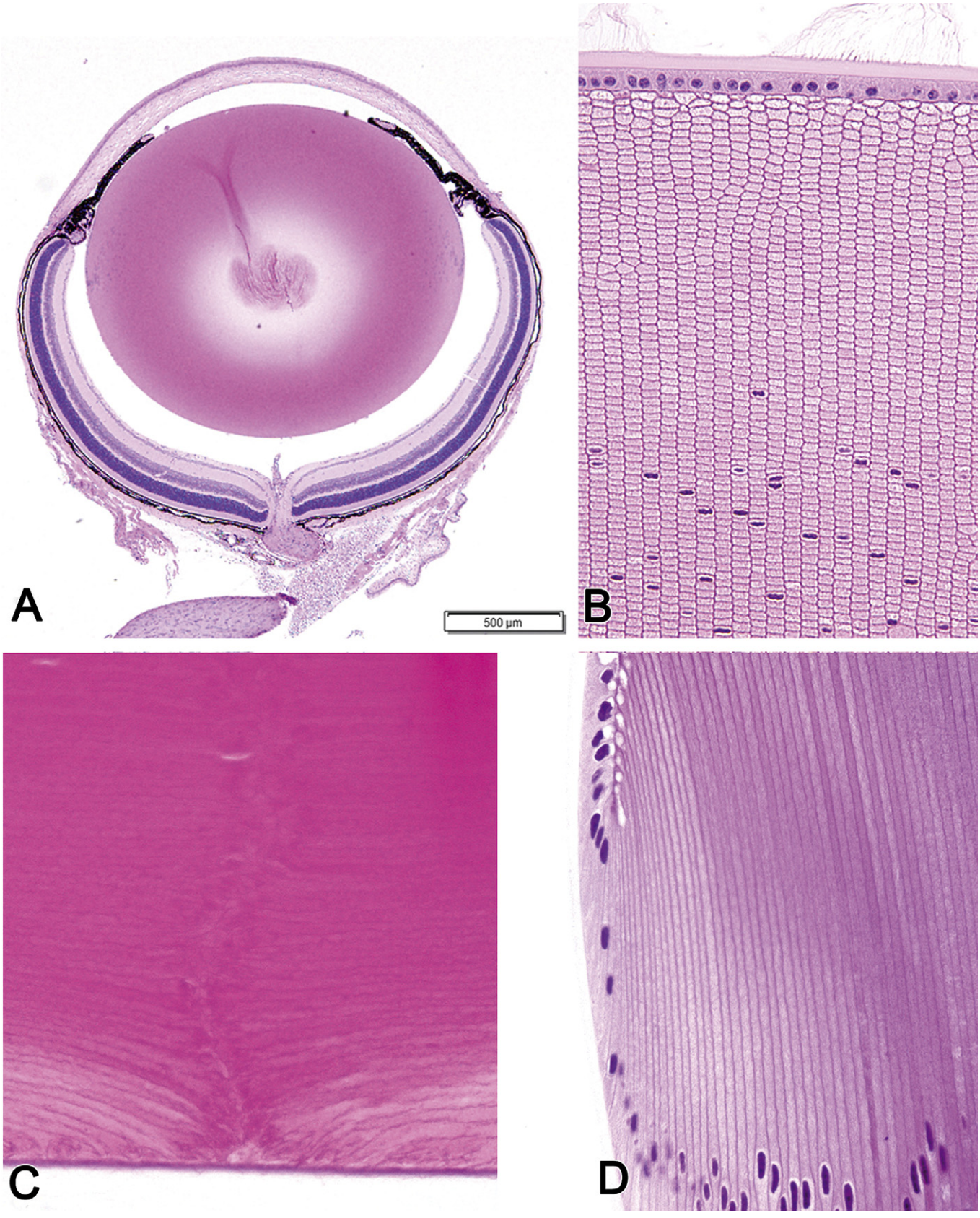
A
500 µm
B
C
D

nucleus disappears. The lens fibers can be distinguished by light microscopy as hexagonal-shaped columns at the cortex of the lens but not within the nucleus. Davidson's fixative is excellent for preserving the cell membranes of lens fibers (Figure 53.16).

The lens fibers have extensive interdigitations of the plasma membranes. Furthermore, they are able to communicate chemically via an extensive network of gap junctions that connect adjacent fibers.

The LECs secrete a basement membrane, termed the lens capsule, which has remarkable elastic qualities. The elasticity of the lens fibers is the source of power that drives visual accommodation in the mammalian eye.

The lens functions to refract light so as to help focus an image on the plane of the retina. Transparency of the lens throughout life is dependent on relatively ordered packaging of lens proteins and the relative dehydration of the lens. The lens is suspended across the entrance to the posterior chamber by a network of zonular fibers or ligaments. These ligaments attach on one end to the equatorial zone of the lens capsule, and on the other end to the ciliary body epithelial cells which secreted them. Ultrastructurally, at the region where the zonular ligament fibers contact the lens, the lens capsule presents a lamellar appearance that denotes the area where the zonules merge with the capsule. The zonules are made of bands of fibrils 10–12 nm in diameter with a periodicity of 11–18 nm in humans. The exact composition of the zonules is not known, but fibrilin constitutes a large portion.

## 10.2. Evaluation of Toxicity

The functional health of the lens is evaluated by ophthalmic examination with an indirect or direct ophthalmoscope and a slit lamp. The ophthalmologist using these tools is looking for any opacity in the lens that might impact light transmission, and/or problems with the suspension or position of the lens that might alter the plane at which transmitted light will be focused. It is not standard practice to evaluate the refractive state of the lens, but this can be done by streak retinoscopy, which estimates the refractive status of the curved cornea and lens together.

Cataract is a common toxic endpoint affecting the eye, so lens clarity should always be monitored in toxicity studies as an indicator of ocular health.

### *Rodent Models of Cataract*

Approximately 50 million blind people are estimated to be alive in the word today, and half of these cases are thought to be due to cataracts. Therefore, cataract (an opacity of variable size and density in the crystalline lens and/or its capsule) represents the major form of lenticular pathology. The heritability of age-related cataracts is approximately 50%, so there is a marked need to understand the mechanisms responsible for the initiation and progression of this disease.

With these facts in mind, the mouse has served as an excellent model for cataract investigations, and our knowledge about the genetics of cataract has been enhanced from the analysis of spontaneous and induced mutations in mice. Due to its location in the eye, mutations affecting the lens can be easily phenotyped by visual examination ante-mortem (Figure 53.17). The number of specific cataract mutations in mice has increased greatly in recent years, and comprises more than 100 to date.

Most of the genetic mouse models of cataract are models of congenital cataracts, but a few models develop cataracts in old age. The most common mutations in mouse congenital cataracts are in genes coding for γ-crystallins (*Cryg* gene). Some postnatal progressive cataracts have mutations in the β-crystallin (*Cryb* gene) encoding genes. Mutations of the α-crystallin (*Cryaa* and *Cryab* genes) also induce cataractous changes but with diverse phenotypes, with only the homozygous animals developing lesions.

FIGURE 53.16 Normal architecture of the lens. (A) Low-magnification image of an adult mouse eye showing the relative size of the lens compared to other components of the globe. (B) The anterior pole of a mouse lens fixed with Davidson's fixative showing individual profiles of well differentiated lens fibers. (C) The posterior pole of the lens from an adult dog showing the posterior suture (curved seam in the middle where fibers meet). (D) The equator of a rabbit lens showing the nuclear bow. (A) H&E, 40×; (B) H&E, 400×; (C). H&E, 600×; (D) H&E, 600×.

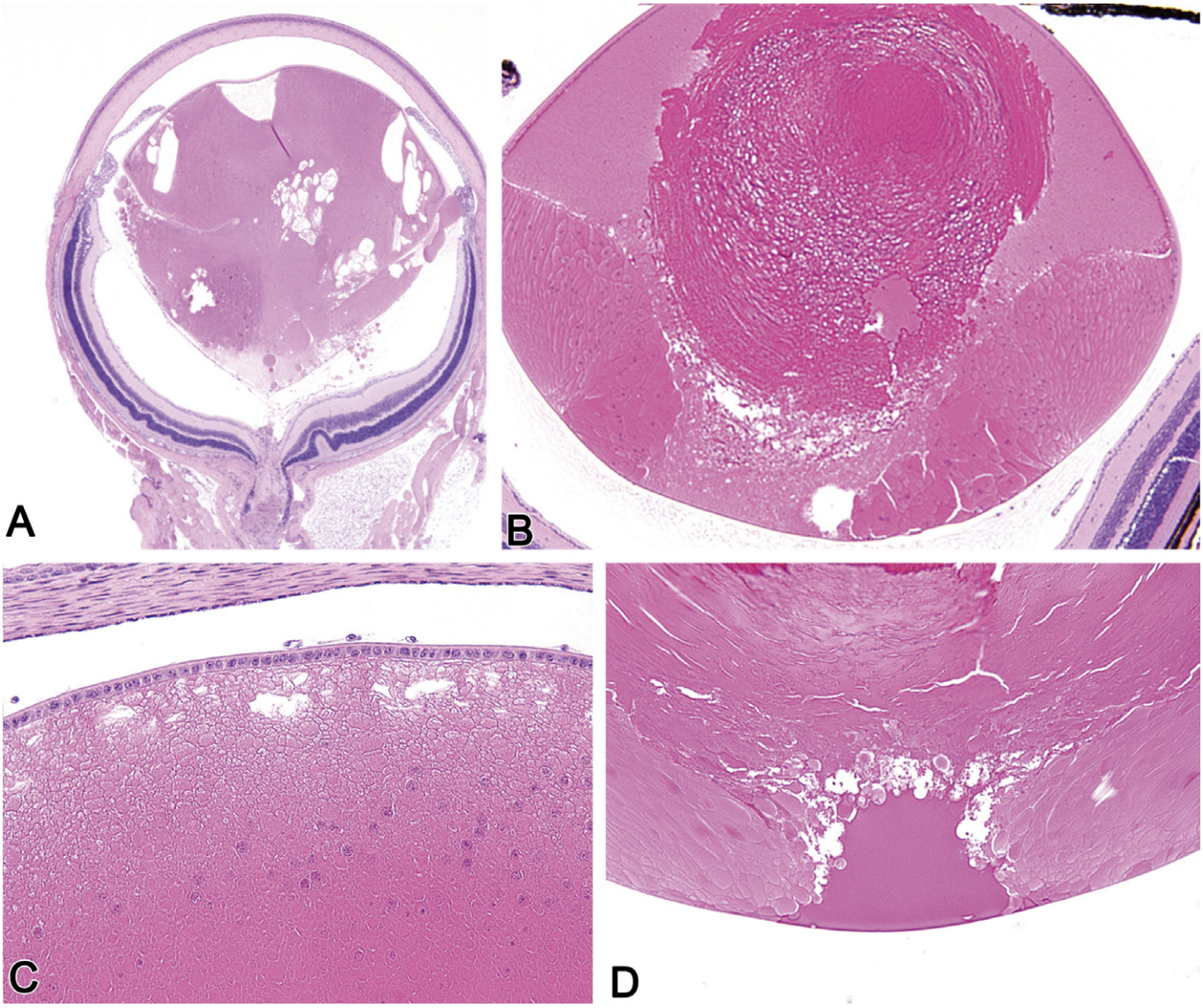


FIGURE 53.17 Congenital cataract. (A) Sub-gross view of a mouse globe with a cataract distorting the posterior pole of the lens. (B) Lens from a mouse with fairly normal equatorial regions but abnormal nucleus that protrudes caudally to disrupt the posterior pole of the lens. (C) Cortical cataract in a young mouse (indicated by the persistence of an intact *tunica vascularis lentis* on the surface of the lens). (D) Cortical cataract at the posterior suture. (A) H&E, 12.5×; (B) H&E, 100×; (C, D) H&E, 200×.

Mutations in genes coding for membrane proteins like major intrinsic protein (MIP) or connexins can also induce congenital cataracts. Mutations in genes coding for transcription factors such as FoxE3, Maf, Sox1, and Six5 also cause cataracts, among other ocular abnormalities. The cataractous changes in congenital cataract are predominantly observed in the lens nucleus, with near normal appearance of the cortical and equatorial lens associated with reduplication of the lens capsule. Regardless of the genetic event, the morphologic appearance of congenital cataracts is quite similar.

Spontaneous mouse models of hereditary age-related cataracts have not yet been characterized genetically. The most prominent models in this category are the senescence-accelerated mouse (SAM) and the Emory mouse. Mouse models of metabolic cataracts also exist. The most prominent are related to abnormalities of sugar metabolism (*Glk1*-deficient and SDH-deficient mice), protein-bound carbohydrate

**TABLE 53.5** Biologic Features of Compounds Causing Cataract in Rats

| Compound | Species | Biologic feature |
|---|---|---|
| Chloroquine, chlorphentermine and iprindole | Rat | Intralysosomal drug–lipid complexes |
| Diquat* | Rat and dog | Formation of free radicals and loss of lenticular ascorbic acid. |
| Methionine sulfoximine | Rat | Interference with protein synthesis |
| Morphine, morphine-like compounds | Rat, mouse and guinea pig | Cataracts prevented by simultaneous administration of nalorphine |
| Myleran | Rat | Prevents lenticular epithelial cell division |
| Naphthalene | Rat | More consistent, earlier, and severe cataracts in pigmented rats; changes due to a toxic metabolite, 1,2-dihydroxynaphthalene, which is metabolized to 1,2-naphthaquinone and hydrogen peroxide, diminishing the lenticular oxygen and ascorbic acid supply |
| $N^2$-Phenyl-β-hydrazinopionnitriles | Rat | Decreased lenticular ATP concentrations |
| Selenium | Rat, guinea pig, and rabbit | Decreased lenticular concentrations of sulfhydryl groups and glutathione, increased lenticular concentrations of insoluble protein, increased amount of lenticular water, interference with glutathione metabolism |
| Streptozotocin | Rat and primate | Cataract due to hyperglycemia of diabetes resulting in lenticular osmotic changes from increased concentrations of sorbitol, glucose, and fructose |
| Triparanol | Rat, human and dog | Inhibition of cholesterol biosynthesis with reduction of lenticular sulfhydryl content, accumulation of sudanophilic material causing uptake of water and sodium leading to swelling and disruption |
| Galactose | Rat | Lenticular accumulation of dulcitol resulting in an osmotic accumulation of water in the lens, decrease in lenticular glutathione concentrations, failure of cationic pump, decreased glycolysis, decreased concentrations of ATP |

** Diquat = 9,10-dihydro-8a, 10a-diazoniaphen-anthrene dibromide.*

metabolism (*Ggtal*-knockout mice), or cholesterol metabolism (Nsdhl-mutant mice). Cortical cataract with formation of Morgagnian globules and bladder cells, posterior migration of the lens epithelial cell over the inner aspect of the posterior lens capsule, and liquefaction and mineralization of the lens fibers are the most common histological findings. Again, regardless of the cause, the morphologic appearance of these adult-onset cataracts is comparable.

Toxicant-induced rat models have been developed. An interesting and rapidly developing cataract model is the selenite-overdosed model. Here, cataracts are produced in suckling rats by a single subcutaneous administration of elevated doses of the trace mineral selenite between postnatal days 10 and 14. Lesions appear in 4–6 days and are characterized by altered lens epithelial metabolism, lens fiber mineralization, and proteolysis of the lens fibers. Cataracts also have been induced in suckling Sprague-Dawley rats by a single intraperitoneal injection of N-methyl-N-nitrosourea (MNU) given 100 mg/kg at birth (postnatal day 0) or at postnatal days 5, 10, 15, or 20. Rats of both sexes are susceptible.

## 10.3. Response to Injury

Transparency and refraction are the functions of the lens, and toxicity is manifest by changes in these features. The most readily apparent is a change in transparency, and this is the definition of cataract. A list of cataract-causing substances and their mechanisms of action is provided in Table 53.5. Not all cataractous changes can be detected microscopically. A good example is changes in the lens nucleus (or core), which occur where lens fibers are no longer distinguishable as individual units. In addition, cataracts may be manifested histologically by changes that are the same as those which occur with certain artifacts. The most reliable histologic evidence of genuine cataracts includes swelling of lens fibers, formation of bladder cells and Morgagnian globules, and posterior migration of the lens epithelial cells adjacent to the posterior lens capsule (Figure 53.17). Posterior migration of the lens epithelial is the initial morphologic finding in many early cataracts. It is particularly important that this initial change be recognized when screening for morphological phenotypes, especially in developmental cataracts. Bladder cells are formed when abnormal cellular metabolism in lens epithelium causes cytoplasmic accumulation of coarse granular material that causes the cells to swollen. When bladder cells lose their nuclei and become even more swollen, they receive the name Morgagnian globules. Mineralization is often seen with chronic cataract. Complete liquefaction of the lens fibers is another feature of chronic cataract, and is usually present in cases of hypermature lesions. The contents of the liquefied lens fibers have the potential of leaking from the capsule, and thus might incite an intraocular immune-mediated response culminating in uveitis. Lens epithelial cells can undergo spindle cell metaplasia and deposit collagen within the lens. These deposits are called subcapsular cataracts because the metaplastic LECs cling to the capsule. The metaplastic cells atrophy over time, and often only the collagen is left behind.

Numerous toxic pathways can manifest as cataract (Figure 53.18). For example, if the chemical environment in the lens differs from the normal state, the lens epithelial cells can undergo an epithelial-to-mesenchymal transformation, or alter the differentiation path by which lens epithelium transforms to lens fibers. If the external pressure of the zonular ligament is altered, this mechanical change also can cause cataract. The proliferating and differentiating lens epithelium is very sensitive to ultraviolet (UV) light, and also to a large number of toxic substances and disease states. A classic example is cataract formation associated with diabetes in dogs. In this species, the insulin imbalance induces metabolic shifts in the metabolism in lens fibers, causing increased production and cytoplasmic accumulation of sorbitol, which in turn induces cellular edema and lens fiber degeneration secondary to increased cytoplasmic osmolality.

The posterior lens capsule is thinner than the anterior capsule, and is usually the location where lens capsule rupture may occur in association with cataract. Lens capsule rupture can also occur as a post-traumatic event. In any rupture, the lens protein and fibers are exposed and extruded into the intraocular spaces. Some mouse mutation models are associated with spontaneous rupture of the lens capsule. These include lens rupture

(*lr*), lens opacity 10 (*Lop10*), and lens opacity 12 (*Lop 12*) animals. Unlike traumatic lens capsule rupture in most species, where a granulomatous inflammatory reaction occurs, these genetically mediated ruptures seldom mount an inflammatory response; the reason for this phenomenon is not known. The most reliable histologic changes associated with lens capsule rupture are coiling of the free edges of the ruptured capsule away from the site of the break, and infiltration of inflammatory cells between the exposed lens fibers.

### 10.4. Mechanism of Toxicity

Cataract, defined as any opacity or loss of transparency on the lens, is the most common and significant abnormality of the lens. Changes in the lens proteins during toxic cataract formation are similar to the changes that occur during aging. The appearance of cataract varies among species, as does the sensitivity to toxic cataract development.

These differences are thought to be related to different lenticular metabolism profiles among species. For example, glutathione (GSH) is an important lens antioxidant. Chronic corticosteroid exposure can lower GSH levels in the lens, and therefore increase the risk of cataract associated with oxidative stress. Substances that affect cell mitosis, such as radiation or radiomimetic drugs, interfere with the organized stepwise differentiation of the lens cortex and can lead to cortical cataract, usually at the nuclear bow. Diabetic dogs and rats, but not mice, rabbits, or non-human primates, are at high risk of osmotic cataract formation. It is thought that the different risks among species are due to the fact that dogs and rats have relatively high levels of aldose reductase (AR) in the lens. This enzyme reduces various sugars (for example, glucose to sorbitol). Because sorbitol does not readily diffuse out of cells and its further oxidation (to fructose via the action of sorbital dehydrogenase) is slow, the accumulation of sorbitol in the hyperglycemic state would increase the intracellular osmotic pressure within the lens, leading to water retentiont and eventual rupture of the lens fiber cells. Therefore, rats and dogs that have high levels of AR in their lenses are prone to develop diabetic cataract, whereas mice that have low lens AR activity are not. Rats and dogs also develop galactose-induced cataracts readily. This is because the polyol of galactose reduction, galactol, is not further converted to other metabolites, resulting in faster build-up of this polyol and faster development of the osmotic cataract.

Many photosensitizing agents are thought to cause cataracts. Among them, UV light is the most cited; however, most researchers believe that UV light exposure alone is not enough to produce the lesion but that other photosensitizing agents must also be present to play a simultaneous role. Recently, in a study assessing the effects of UV light exposure in 129S1/SvImJ mice, cataract was diagnosed in both older unexposed and UV-exposed mice, demonstrating for the first time the formation of spontaneous cataract in 129 strain mice.

## 11. THE VITREOUS BODY

### 11.1. Structure, Function, and Cell Biology

The vitreous body fills the vitreous cavity, which is the space that spans the distance from the posterior pole of the lens to the inner aspect of the retina. The vitreous is transparent and contains only a very few cells (hyalocytes), which are more easily recognized in younger mammals. It has been suggested that hyalocytes have a monocytic/macrophagic origin based on their antigenic expression (CD11a+, CD45+, and CD64+), although they are not merely visitors from the systemic circulation but rather true vitreal resident cells. It also has been suggested, based on their expression of TGF-β, that they play a role in controlling cell proliferation in intraocular diseases.

The vitreous body consists of collagen bundles supported by hyaluronic acid produced by the non-pigmented ciliary body epithelial cells. The anterior face of the vitreous closest to the lens has a more robust collagen structure. The vitreous harbors matrix attachment points to the retinal inner limiting membrane, which is a basement membrane for the retina. The vitreous helps maintain the retina in place by eliminating shock waves in the space between the lens and the retina.

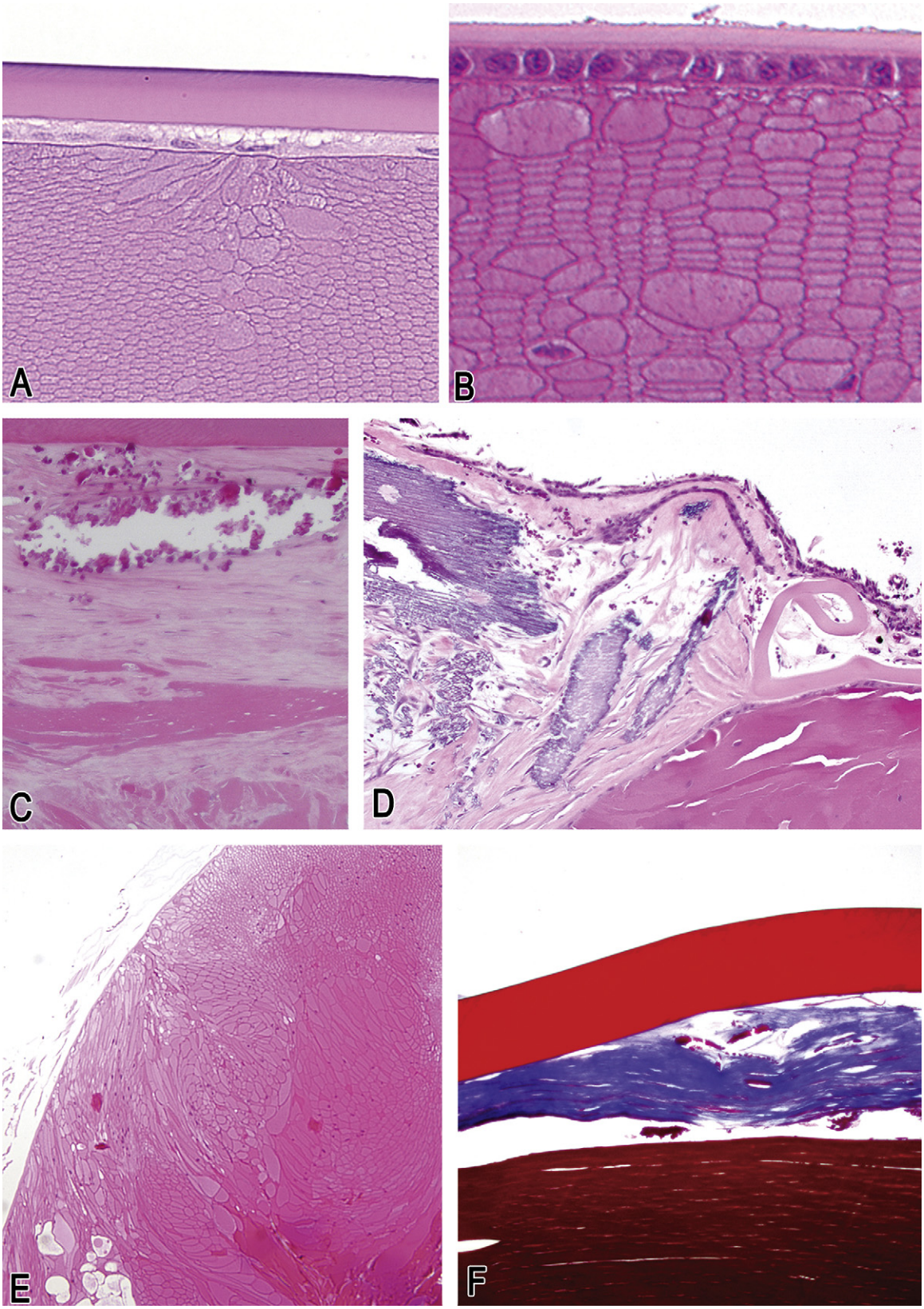
A
B
C
D
E
F

## 11.2. Evaluation of Toxicity

Since the vitreous is transparent, it offers little evidence of structure in the normal state. Abnormalities, however, can often be recognized within it using slit-lamp examination, or by ophthalmoscopy. Ultrasound or OCT can be powerful tools to evaluate the vitreous profile, especially in its relation to the retina. The increase in the usage of intravitreal injections as an ocular treatment modality, specifically targeting the retina, has made necessary an improved understanding of the reactions of the vitreal tissue after having been exposed to different drugs. In order to achieve this knowledge, flow cytometry and ELISA-based techniques are commonly used to characterize cellular infiltrates and to quantify the concentrations of cytokines, growth factors, and other bioactive molecules that have been released into the vitreous.

## 11.3. Response to Injury

Degeneration of the vitreous body does not lead to a specific morphologic change within the gel-like matrix. However, degradation of the vitreous may be recognized indirectly as a primary cause leading to secondary retinal detachment. Liquefaction of the gel-like vitreous causes the retina to be buffeted by energy waves in the fluid media; in the absence of structural protection, the resulting trauma to the neural retina leads it to separate from the underlying RPE. The formation of collagen traction bands in the vitreous is a less common means that might promote physical pulling of the retina away from the RPE, and such bands can also lead to tears in the retina. With age, the vitreous separates from the retina spontaneously. As this happens, there is an increased risk of traction on the retina with detachment, tears, or both.

Substances injected into the vitreous are free to diffuse into the retina because the blood–retinal barrier exists in the retinal vascular endothelial cells and the apices of the RPE cells. As mentioned before, this intravitreal route has become a popular method of drug delivery to the posterior segment of the eye, and particularly the retina. Injection sites are usually in the pars plana, and are directed into the vitreous body rather than the retina proper. Histologic evaluation of injection sites in animal models at necropsy shows small defects in the ciliary epithelium as well as the ciliary stroma and sclera associated with mild fibrosis and minimal infiltration with macrophages and lymphocytes, but in general such injections are fairly well tolerated. Spindle cells and/or glial cells can extend into the vitreous, and this might change the risk of traction bands in the vitreous – especially over the life of a patient who receives intermittent intravitreal injections for an extended period.

It is tempting to think of the vitreous body as a structural lumen, but it is actually a cell-poor, transparent, extracellular space filled with a gel-like matrix. As such, it responds to injury in the same way as other connective tissue compartments do. If there is a stimulus for fibrovascular proliferation, then new blood vessels and spindle cells will move into the vitreous, and collagen fibrils will be deposited there. Proliferative vitreoretinopathy after retinal detachment, retinopathy, or premature birth are good examples. The fetal vitreous vasculature normally regresses shortly after birth. In cases where regression is impaired, remnants of embryonic vessels accompanied by fibrous connective tissue can be seen in the vitreous and posterior aspect of the lens for extended periods after birth. This condition is referred to as persistent hyperplastic primary vitreous (PHPV), and is a common congenital abnormality in human eyes. PHPV also is associated with several different mutant mouse models,

FIGURE 53.18 Pathology of the lens. (A, B) Lens fiber swelling in the anterior cortex of a mouse eye, indicative of cortical cataract; Davidson's fixative. (C, D) Collagen deposition, spindle cell metaplasia of lens epithelial cells, and lens fiber mineralization as part of a subcapsular cataract. The lens capsule is ruptured and coiling in (D). (E). Morgagnian globules (round and swollen lens fibers) and extensive disorganization of the lens fibers in a mature cortical cataract. (F). Collagen (blue) subtending the lens capsule (thick upper red band) secondary to spindle cell metaplasia of lens epithelial cells in the formation of a subcapsular cataract. (A) H&E, 200×. (B) H&E, 400×. (C) H&E, 600×. (D) H&E, 400×. (E) H&E, 100×. (F) Masson's trichrome, 600×.

including the *p53*-null and Norie's disease homolog (*Ndph*) strains, and can be induced in animals with double-null mutations for members of the retinoic acid receptor family.

Asteroid hyalosis is a degenerative condition of the eye involving small white opacities in the vitreous. It is known to occur in humans, dogs, cats, and chinchillas. Clinically, these opacities are quite refractile, giving the appearance of stars (or asteroids) shining in the night sky. Histologically, they present as round, amphophilic, laminated to radiating structures of variable size within the vitreous. Asteroid hyalosis has been associated with diabetes mellitus, hypertension, hypercholesterolemia, and, in dogs and cats, intraocular tumors. In dogs, asteroid hyalosis is considered to be an age-related change.

Vitreal inflammation is usually a secondary change rather than a primary response to vitreal disease. Vitreitis is more likely to develop as a sequel to corneal ulceration, endophthalmitis, scleral perforations, or systemic infections.

### 11.4. Mechanisms of Toxicity

The most common toxic reactions of the vitreous body are the same types of reactions that occur in spontaneous connective tissue diseases elsewhere in the body: cellular and matrix proliferation. Rabbits are notorious for the formation of spindle cells and collagen membranes in the vitreous, favoring the production of traction bands and subsequent retinal detachment.

An important aspect of intravitreal injections is recognizing the potential of the test articles to cause vitreal degeneration and inflammation. Special attention must be paid when analyzing intravitreal injection sites of biodegradable drug implants designed for sustainable drug delivery, since the nature and size of the implants can sometimes induce vitreal inflammation. In general, such reactions are of minimal degree and limited to lymphocytes. Another important issue is to analyze the rate of dissolution of these drug depots. Large amounts of opaque and dense substances can stay in the vitreous for extended periods of time, thereby causing temporary visual impairment. With this in mind, another important aspect of safety studies for assessing intravitreal products is to take into account the animal model that has been used in the study. For example, rabbits are notorious for having a denser vitreous, and thus are more inclined to retain substances locally for longer periods. This fact can also influence the rate of diffusion of the drug through the posterior globe.

## 12. RETINA AND RETINAL PIGMENT EPITHELIUM (RPE)

### 12.1. Structure, Function, and Cell Biology

The retina is a highly differentiated and complex multilayered neural tissue derived from an outward extension of the rostral neural tube. Transduction of light energy to neural impulses in the retinal photoreceptors is the initiating event in all vertebrate vision systems. The retina can be roughly divided into an inner neural retina and an outer retinal pigment epithelium (RPE). These two layers are separated by a potential space, but they are not physically attached to one another. The outer neural retina, particularly the photoreceptor cells, consumes oxygen and nutrients at a higher rate than any other tissue in the body. For this reason, the choroidal blood supply of the outer retina is designed to deliver oxygenated blood quickly and with swift turnover. The endogenous retinal blood supply is less demanding. Mice, rats, dogs, and non-human primates all have an extensive intrinsic retinal vascular bed (i.e., a holangiotic pattern) in addition to the choroidal system. In contrast, rabbits have a limited intrinsic retinal vascular system (i.e., a merangiotic pattern), which leaves most of the retina without an endogenous blood supply (Figure 53.19).

#### *Neural Retina*

The neural retina is a 10-layered neural tissue responsible for phototransduction and the signal processing across a three-neuron network that ultimately ends in the transmission of nerve impulses to the brain by the retinal ganglion cells. The layers of the neural retina are listed below in order, from the inner to the outer layer of the retina (Figure 53.20).

1. *Inner limiting membrane*: a basement membrane, synthesized by the basal foot processes of the Müller cells (which serve as

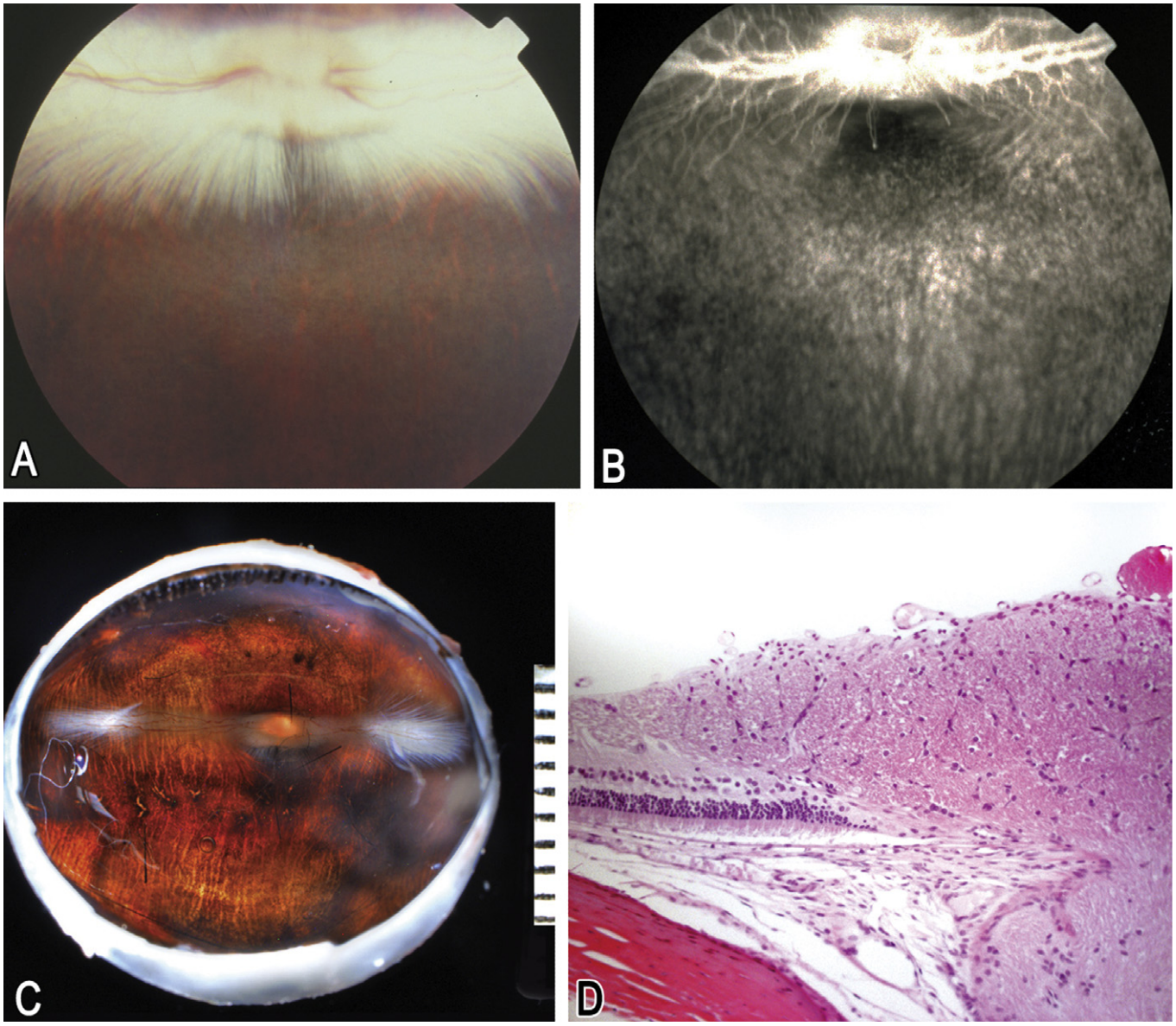


FIGURE 53.19 Blood vessels of the rabbit medullary ray. (A) Fundus image showing the medullary ray posterior and superior in the globe. The vascularization of the rabbit retina begins at the optic nerve head (ONH) and projects outward in specific tracts in a merangiotic (localized) pattern that tracks the medullary rays; other mammals of interest for ocular toxicology studies (e.g., rodents, dogs, non-human primates) have a uniform dispersion of blood vessels from the ONH, which is termed a holangiotic pattern. (B) Fluorescein angiography of the rabbit fundus demonstrating the localization of retinal blood vessels (bright branching lines). (C) Gross image of the rabbit fundus demonstrating the medullary ray in the horizontal plane with the optic nerve in the center. (D) Section through the medullary ray showing myelinated axons in the nerve fiber layer. (D) H&E, 200×.

retinal glia), that separates the retina and the vitreous body.

2. *Nerve fiber layer*: axons from the retinal ganglion cells traveling horizontally towards the optic nerve at the inner surface of the retina.
3. *Retinal ganglion cell layer*: neurons which collect signals from interneurons of the inner nuclear layer and transmit nerve impulses to the optic nerve and from thence to the brain.

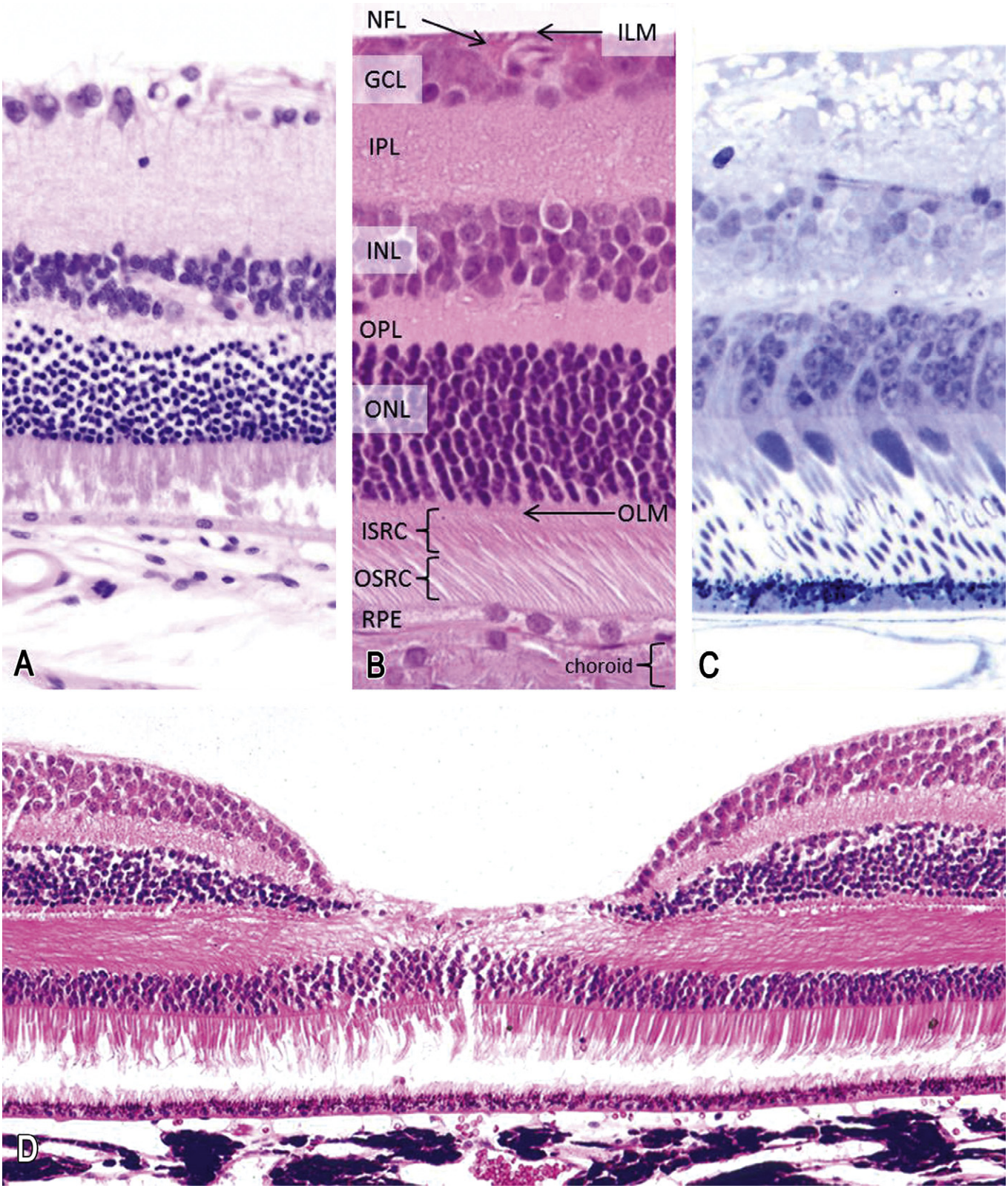
NFL
ILM
GCL
IPL
INL
OPL
ONL
OLM
ISRC
OSRC
RPE
choroid
A
B
C
D

4. *Inner plexiform layer*: houses the synapses between retinal ganglion cells and the interneurons of the inner nuclear layer.
5. *Inner nuclear layer*: houses the interneurons (horizontal cells, bipolar cells, and amacrine cells) and Müller cells.
6. *Outer plexiform layer*: houses the synapses between the photoreceptor cells and the interneurons of the inner nuclear layer. These include rod spherules and cone pedicles.
7. *Outer nuclear layer*: cell bodies and nuclei of the rod and cone photoreceptors.
8. *Outer limiting membrane*: this line reflects the presence of an anastomosing network of tight junctions formed between photoreceptor cells and Müller cells.
9. *Inner segments of the rods and cones*: houses an area rich in rough endoplasmic reticulum for high-efficiency protein synthesis, and an outer layer rich in mitochondria for energy production.
10. Outer segments of the rods and cones: supports phototransduction.

Retinal ganglion cells transmit nerve impulses to the brain carrying information that is the result of the interaction of the nerve networks of the photoreceptor cells in the outer retina and the integrating interneurons of the inner nuclear layer. Ganglion cell axons pass through the optic disc into the optic nerve. Damage to the nerve axons at any point can interrupt the axon, thus leaving the cell body separated from its brain connections. Brain-derived neurotrophic growth substances travel from the brain to the ganglion cell body, and are essential for maintaining the integrity of the ganglion cells. Damage to the axons of the ganglion cells in the nerve fiber layer, optic disc, lamina cribrosa (the point where the fibers pass from the optic disc into the optic nerve), or anywhere in the optic nerve (including the chiasm and optic tracts) will cause a dropout of ganglion cells.

The inner nuclear layer contains multiple categories of interneurons. Horizontal cells reside in the outer aspect, bipolar cells in the center, and amacrine cells toward the inside. Horizontal cells have connections laterally to modulate the boundaries of the image (which increases resolution), whereas bipolar cells function vertically to modulate the brightness and color information. The inner nuclear layer also houses the nuclei of the Müller cells, which function as the glia of the retina. The Müller cell processes extend from the innermost retina to the outer limiting membrane, and are intimately entangled with the processes of all the retinal neurons. In particular, their processes are distributed around vessels, and nutrients are distributed within the retina via the cytoplasm of the Müller cells. One of the earliest changes in the stressed retina is an alteration in phenotype of the Müller cells. In the healthy retina, Müller cells express glial fibrillary acidic protein (GFAP) only in the inner aspect near the inner limiting membrane, but after a severe stressor (e.g., detachment, hypoxia or phototoxicity) they express GFAP throughout the retina.

The outer nuclear layer (ONL) houses the nuclei of the rods and cones. Rod nuclei make up the bulk of cells within the inner aspect of the ONL, while cone nuclei are nestled mainly against the outer limiting membrane. Degeneration of the rods usually results in an in-place degeneration of their cell bodies, but cone degeneration sometimes leads to a displacement of the cell into the outer retina, which eventually settles against the RPE. The outer segments of the photoreceptor cells are said to be the most metabolically active tissue in the body. Maintenance of the depolarized state in the photoreceptor cells is a process that still occurs when

FIGURE 53.20 Normal architecture of the retina. (A) Normal retina from an albino mouse. (B) Area centralis from a normal cat retina, with the retinal layers labeled from outside (bottom) to inside (upper). (C) Plastic section of the retina from a non-human primate. (D) Image of the fovea from a non-human primate retina. This site contains a heightened number of cone photoreceptors, and thus is critical for proper perception of color and visual acuity in bright light. (A, B) H&E, 400×; (C) Toluidine blue, 400×; (D) H&E, 200×. Abbreviations (listed from top): ILM, inner limiting membrane; NFL, nerve fiber layer; GCL, ganglion cell layer; IPL, inner plexiform layer; INL, inner nuclear layer; OPL, outer plexiform layer; ONL, outer nuclear layer; OLM, outer limiting membrane; ISRC, inner segments of rods and cones; OSRC, outer segments of rods and cones.

the cells are not functioning, and thus requires a continuous energy supply. There is also a continuous production of cell membranes for the discs and opsin proteins, as well as a host of other enzymes and transport proteins which are consumed and recycled by RPE phagocytosis. The whole process takes place in the presence of focused light, so high oxidative stress is constantly an issue for these tissues (Figure 53.21).

### *Retinal Pigment Epithelium (RPE)*

The RPE is derived from neural tube ectoderm, and therefore is analogous to ependymal cells in form and function. As the optic vesicle folds on itself to form the optic cup, the RPE remains as a single cell layer in direct contact with the outer cells of the neural retina that eventually become the photoreceptor cells (Figure 53.3). The photoreceptor cells and the adjacent RPE function as a unit, and together they are responsible for phototransduction, the transformation of light energy into the electric signals that are the basis of vision.

The RPE cells are smooth and hexagonal in shape when viewed from the inner surface. In histologic sections, the RPE cells consist of an outer non-pigmented basal region with an oval nucleus, and an inner, pigmented portion which extends as a series of straight villous processes between the photoreceptor outer segments. The basal surface of the RPE cells is characterized by extensive infolding. The basal lamina of the RPE cell forms the innermost layer of the five-layered Bruch's membrane which separates the retina from its rich vascular supply in the choriocapillaris. There is an anastomosing network of tight junctions near the apex of the RPE cell layer that forms the outer blood–retinal barrier (Figure 53.14), which is similar in structure and function to the blood–brain barrier (see *Nervous System*, *Chapter 52*).

The melanin pigment in the RPE protects the outer retina from excessive light reflection and glare, and thus from unrestrained oxidative damage. The RPE actively transports nutrients such as amino acids, omega-3 fatty acids, and glucose to the outer retina across the tight junctions. In addition, the spent 11-*trans* form of retinol is taken up by the RPE after phototransduction and transformed back into functional 11-*cis* retinal so that it can be transported back to the photoreceptors. Interphotoreceptor-binding protein is secreted by the RPE and handles the transport of retinol between the photoreceptors and the RPE. The RPE also removes water from the retina and pumps it back to the choroid. The RPE engages in phagocytosis to remove the senescent outer discs of the rods and cones every morning, triggered by first light; the outer segments turn over entirely every 11 days by this mechanism. The RPE is important in maintaining immune privilege within the eye. The subretinal space is occupied by a specialized extracellular material referred to as interphotoreceptor matrix (IPM). The IPM is mainly composed of proteoglycans, and mediates key interactions between the photoreceptors and RPE, including adhesion, phagocytosis, outer segment stability, nutrient exchange, development, and Vitamin A trafficking in the visual cycle. The IPM also helps prevent vascular proliferation in the surrounding tissues.

### *Retinal Vascular Supply*

The main blood supply that brings oxygen to the metabolically active outer retina is the choriocapillaris. Mice, rats, dogs, and non-human primates all possess an extensive (holangiotic) intrinsic retinal vascular bed in addition to the choroidal system (Figure 53.22), while rabbits have a limited (merangiotic) intrinsic retinal vascular system (Figure 53.19). In the holangiotic arrangement, blood vessels traveling within the inner retina form a capillary network extending into the retina to the level of the outer plexiform layer, but not further into the inner retina than that. In non-human primates, the retinal vessels come from the central retinal artery, which, in turn is embedded directly in the optic nerve. Also in primates, there is a vessel-free zone within the center of the fovea such that there is no obstruction to vision. In mice, rats, and dogs, the retinal vessels penetrate from the ciliary arteries and never enter the optic nerve. In rabbits, retinal blood vessels are only seen in a horizontal line extending from the optic disc (medullary ray). Many of these vessels are not embedded in the retina but instead are within the vitreous, more specifically in a space between the vitreous and retina that is better visualized ultrastructurally. The rest of the retina is avascular. Many mammals have no

endogenous retinal vessels (i.e., a parangiotic or anangiotic pattern). Among these species, the guinea pig is commonly used in laboratory experiments to evaluate basic visual system biology.

## 12.2. Evaluation of Toxicity

There are many different ways to evaluate retinal function and retinal morphology that are applicable to toxicologic studies. Like the skin, the retina is accessible for direct observation by fundoscopy. Ophthalmoscopic examination is a common component of toxicity testing protocols. Direct ophthalmoscopy is easy to learn, and most veterinarians employed to evaluate or care for animals in a testing facility would be expected to be comfortable with this procedure. During a study, any variance from the normal retinal architecture would trigger concern regarding the potential for toxicity. There are inherent problems with direct ophthalmoscopic examinations. The view of the fundus is greatly magnified (approximately 15-fold), and appears as an upright, or uninverted, image. Accordingly, competence in direct opthalmoscopy requires training and experience to be able to evaluate the fundus in a systematic manner and interpret the meaning of any variations from the norm. The indirect ophthalmoscopic examination is preferable for complete examination because of the ability to evaluate the entire fundus at only a modest degree of magnification (typically two- to five-fold), although the image is reversed. However, the indirect ophthalmoscope is not an instrument that is familiar to most non-specialist veterinarians. To maximize the benefit of fundoscopy, fundus photography can be important, both for documenting changes and for permitting a more detailed *post hoc* analysis. This allows comparison over time for a given individual and among animals, and it also can be very helpful in site selection for more detailed histopathology examination (Figure 53.22). Again, few individuals are skilled in fundus photography, so such a focused procedure is likely to be chosen only when the eye is a likely target organ. Fluorescein angiography (FA) is a technique that allows assessment of the retinal and choroidal vasculature via fundoscopy and fundus photography. Fluorescein dye is delivered via intravascular injection into a peripheral vein, and the dye is traced through the eye by examination with blue light having a wavelength of 490 nm. Such functional attributes as vascular obstruction, leakage, hemorrhage, and venous clearance can be assessed. FA has proven to be the most important endpoint measurement in assessing the efficacy of treatments to control neovascular proliferation, an important aspect in the treatment of AMD (Figure 53.23).

A second important endpoint to evaluate the loss of retinal function is electroretinography (ERG). This technique measures the integrity of the retinal neural pathways that generate electrical responses when the retina is exposed to light in a carefully controlled setting. The ERG represents the summation of the activity among the various neurons in the retina, including the photoreceptors (rods and cones), interneurons (bipolar and amacrine cells), and retinal ganglion cells. Since the ERG and histopathology measure different aspects of the retina, the two tests are recommended in combination if retinal toxicity is a suspected target.

Multiple ERG variants may be employed, the use of which may elicit greater responses from certain components within the system. For example, one option is to use a flash of light as the ERG stimulus. Using such flashes will primarily test the rods in the dark-adapted eye but probe the cones in a light-adapted eye. A full scope of protocols for inclusion in a flash ERG incorporates the following steps:

1. Combined rod and cone response recorded by a bright light stimulus in a dark-adapted eye;
2. Rod response recorded by using a dim light stimulus in a dark-adapted eye;
3. Inner nuclear layer (interneuron) responses recorded be evaluating oscillatory potentials;
4. Cone response recorded with a dim light stimulus in the light-adapted eye; and
5. Cone response recorded with photopic flicker.

Pattern ERG (PERG) uses a particular light pattern as a stimulus to probe inner retinal function. Multifocal ERG (mERG) allows retinal function to be evaluated regionally rather than globally.

The recently developed OCT technique creates images of the retina in a histology-like "virtual" section in the living animal by examining optical scattering of ultrashort laser bursts of near infrared light, which is able to penetrate the tissues. The

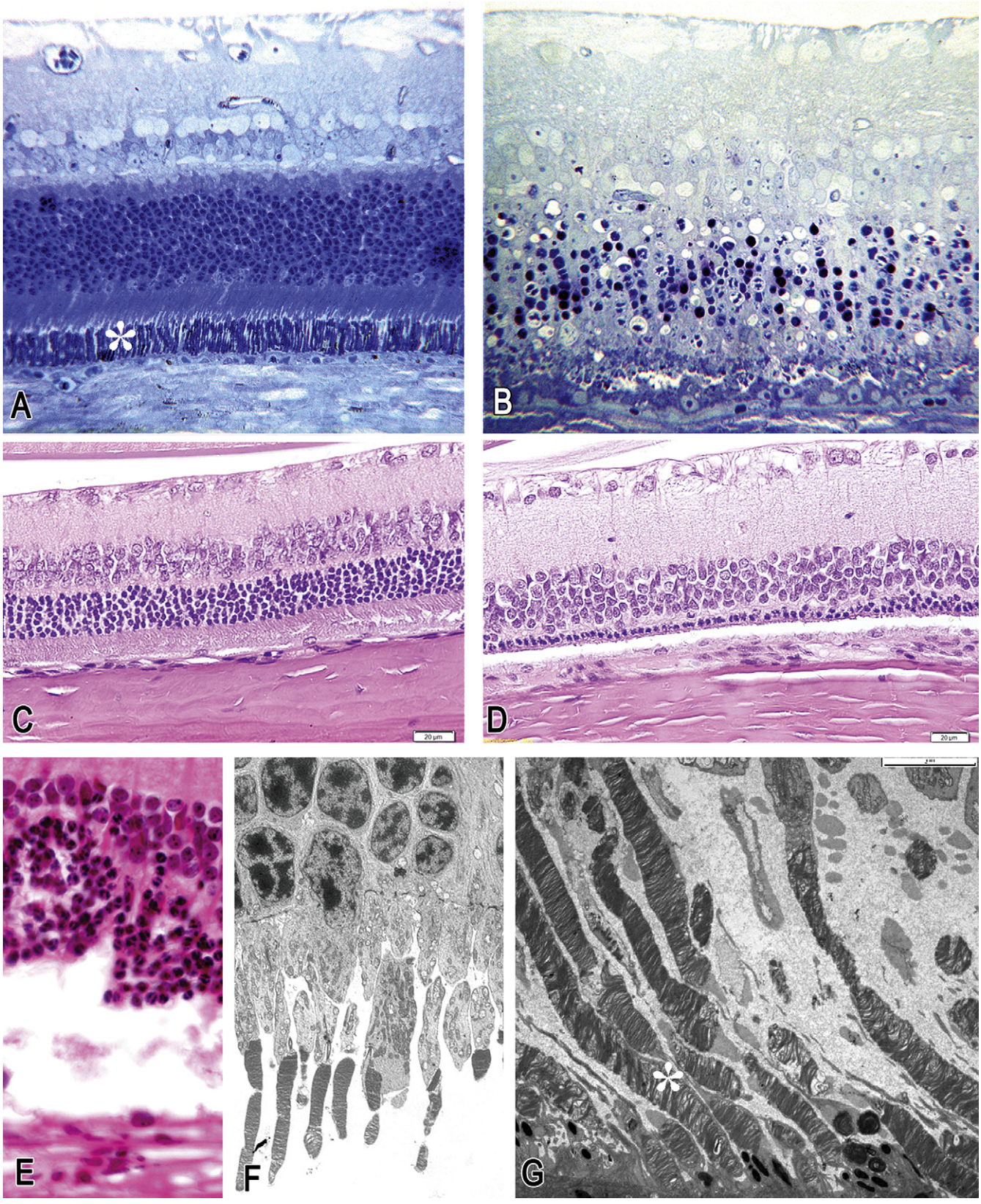
A
B
C
20 µm
D
20 µm
E
F
G

scattered light is processed by computed tomography to display retinal micromorphology in cross-section. This is a rapidly developing imaging modality, and higher-resolution images of impressive quality are achievable with modern instruments. Spectral domain ocular coherence tomography (sdOCT) is able to image individual photoreceptor inner and outer processes and distinguish, in high detail, the interrelationships of the retinal layers and the vitreous body (Figure 53.24). The latest models can image features as deep as the choroid. Since OCT is largely an imaging tool, its use in a toxicologic study will be defined by what information it can provide that is not available by conventional histopathology. Monitoring retinal morphology in the live animal might be important in evaluating time points of progression or recovery from toxicity. Subretinal drug injection for gene transfer is in use today, and being studied intensely. OCT has much to offer in such studies.

Retinal histopathology remains the gold standard in evaluation of toxicity in the retina. The eye, and the retina in particular, present several challenges in the production of high-quality sections for histologic evaluation. The globe needs to be fixed intact unless there is an overriding reason to sample only selected parts of the eye. Opening the unfixed globe generally leads to retinal wrinkling and a loss of orientation among macroscopic features within the eye. Davidson's fixative has proven to be a superb choice to achieve excellent histological preparations of the retina, especially when electron microscopy and immunohistochemistry are not considerations in the study protocol. Rodent, dog, and rabbit eyes should be sectioned in the vertical plane so that the retina is sampled above and below the optic nerve. The goal is to have the optic nerve and the pupil in the section together. In contrast, primate eyes should be sectioned in the horizontal plane so that the optic nerve, fovea, and pupil are included in the same section. Large eyes should be trimmed prior to embedding to achieve these orientations, while mouse and rat eyes should be processed for embedding without trimming. Some method to identify the dorsal (superior) aspect of the globe is important so that the appropriate plane for trimming/embedding can be defined. When the retina is processed into paraffin after formalin fixation, artifacts characterized by little spatial defects within and adjacent to the retina may interfere with interpretation. With Davidson's fixative, which includes ethyl alcohol, these artifacts are avoided. Alternative fixative protocols for special procedures (e.g., electron microscopy) would use mixtures of paraformaldehyde and glutaraldehyde. Such concoctions are a suitable fixative for any experimental technique except immunohistochemistry, but they are essential for electron microscopy. To achieve the best ocular fixation for electron microscopy, intravascular perfusion fixation should be considered as the method of choice for initial fixation. This approach has the added advantage of opening up the vasculature. If immunohistochemistry is a priority, PLP fixative (4% paraformaldehyde, 0.2% periodate, and 1.2% lysine in 0.1-M phosphate buffer) has been recommended. However, cryostat sectioning of flash-frozen fresh tissue is the gold standard for ocular IHC.

### *Animal Models of Retinal Disease*

There are many forms of genetically determined retinal disease in humans. These diseases are broadly characterized by death and gradual loss of photoreceptors. Photoreceptor degeneration has been recognized for a long time,

FIGURE 53.21 Retinal photoreceptors. (A) Plastic section of normal feline retina showing the intact photoreceptor outer segments (*). (B) Plastic section of a feline retina treated with a retinotoxic dose of a fluoroquinolone antibiotic, which manifests as vacuolation, necrosis, and atrophy of the photoreceptors. (C) Normal retina from an albino rat. (D) Photoreceptor atrophy at a toxic response of a test substance resulting in thinning of the outer nuclear layer and almost complete absence of the inner and outer layers of the photoreceptor processes. (E) Jumbling of the outer nuclear layer in another high-dose rat with a retinotoxic dose effect. (F) Transmission electron micrograph (TEM) showing swollen and distorted inner segments in a dog retina. (G) TEM focused on the outer segments from an non-human primate retina showing disarray in the expected stacking of the outer segment discs (*) as a response to test material. (A, B) Toluidine blue, 200×; (C, D) H&E, 100×; (E) H&E, 400×; (F) TEM, 710×; (G) TEM, 2025×.

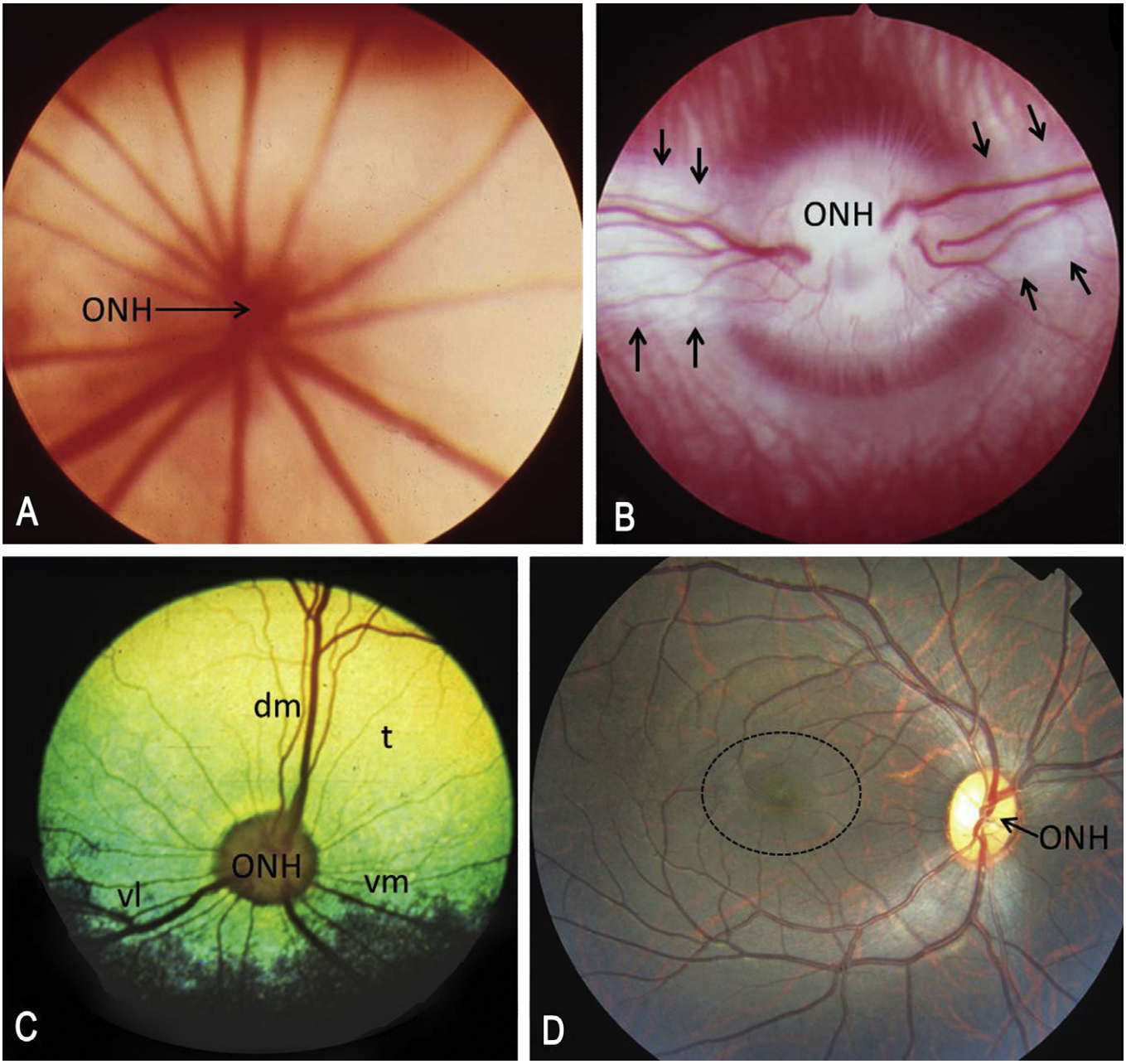


FIGURE 53.22 Gross anatomy of the optic fundus. (A) Albino mouse, holangiotic fundus with blood vessels radiating outward from the optic nerve head (ONH). (B) Albino rabbit, merangiotic retina, with retinal vessels emanating from the ONH in discrete zones along the horizontal plane; these zones, or medullary rays (between arrows), represent a thick white band of myelinated nerve fibers that are characteristic of the rabbit. (C) Cat. Holangiotic retina, with retinal vessels departing the ONH in all directions but especially in the dorsomedial (dm), ventrolateral (vl), and ventromedial (vm) directions. The cat has a prominent, highly reflective yellow-green tapetal area (t) dorsally (D) Non-human primate. Holangiotic fundus, with retinal vessels exiting the ONH in all directions but arcing around the relatively avascular – and thus vulnerable – macula (dotted circle). This fundus image is almost indistinguishable from a human fundus.

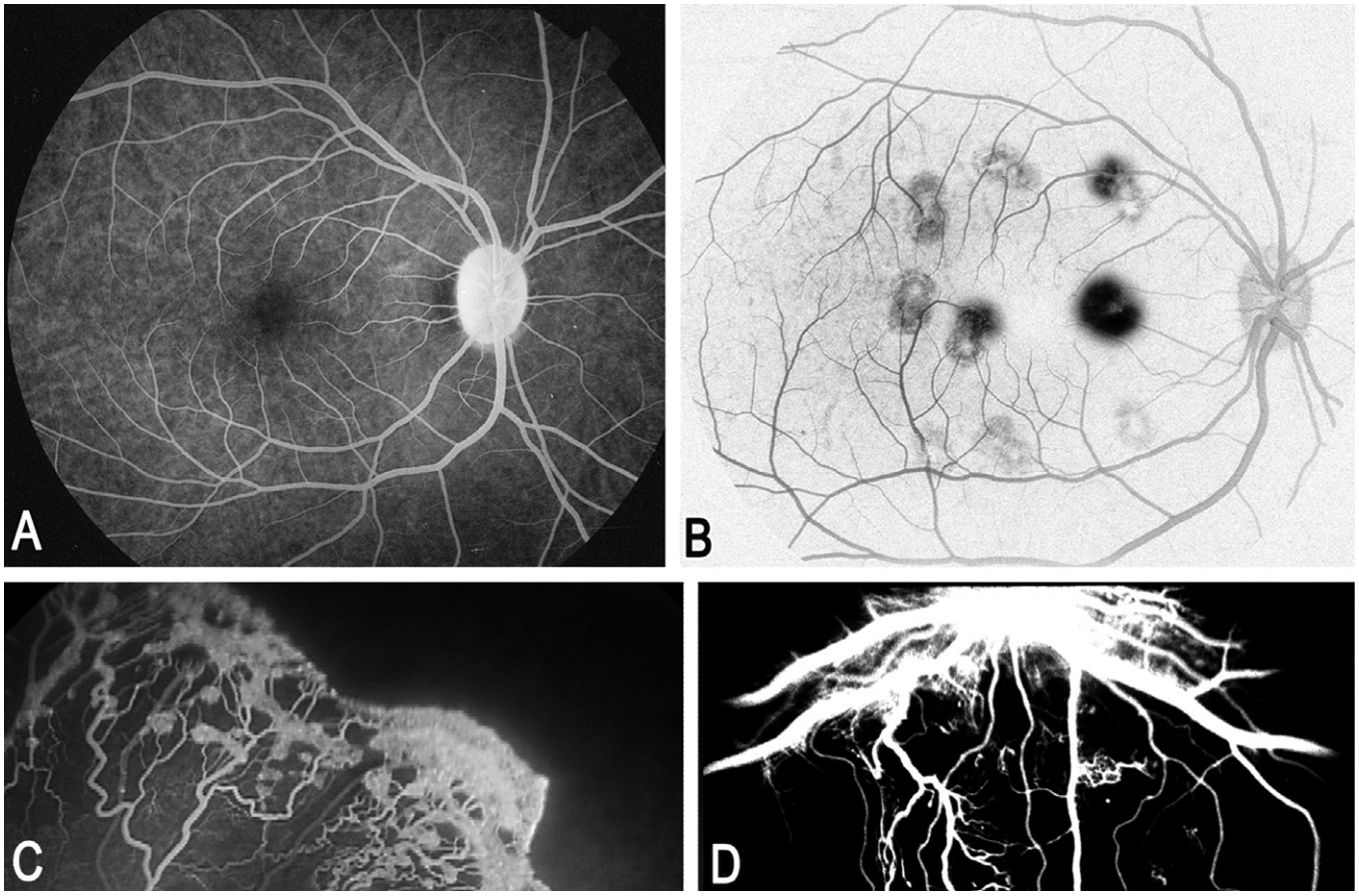


FIGURE 53.23 Fluorescein angiography of retinal vasculature. (A) Positive image of fluorescein angiography from a normal non-human primate. (B) Negative image of fluorescein angiography from a non-human primate in which laser burns (dark spots) were used to destroy Bruch's membrane, causing vascular proliferation and leakage as a model of age-related macular degeneration (AMD). (C) Fluorescein angiography of the retina of a human infant with vascular proliferation associated with retinopathy of prematurity, demonstrating proliferation of tortuous, newly form vessels. (D) Fluorescein angiography of dog retina in a model of diabetic retinopathy, showing markedly thickened central vessels and proliferation of tortuous neovascular profiles.

and this change is a common background lesion in many common laboratory rodent strains. There are large numbers of mouse models that present with primary photoreceptor degeneration, some of which are described in Table 53.6.

#### AGE-RELATED MACULAR DEGENERATION (AMD)

AMD is the leading cause of blindness in the industrialized world among individuals older than 65 years. Age, genetic predisposition, and environmental factors contribute to the disease. Risk factors include a family history of AMD, tobacco smoking, female sex, Caucasian race, and high-fat diet. AMD affects the macula in humans, a cone-dense retinal region that mediates high-acuity vision. It is a degenerative condition that begins at Bruch's membrane and progresses to involve the RPE and outer retina. Histologically, the "dry form" is characterized by the accumulation of cellular debris (termed drusen), composed mainly of lipids, carbohydrates, and inflammatory proteins, within the Bruch's membrane. These deposits impair choriod–RPE transport and promote subsequent RPE and photoreceptor degeneration. The "wet form" of AMD is mainly characterized by formation of a subretinal neovascular membrane. Growth of this tissue is driven by the increased production of angiogenic factors, most notably

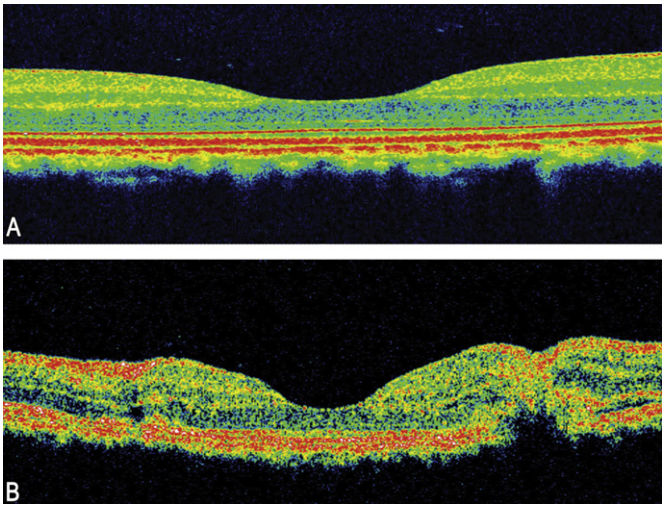


FIGURE 53.24 Ocular coherence tomography (OCT). (A) Spectral domain OCT image of the macula from a normal non-human primate. The inner surface of the retina is located at the top of the image. The depressed central region represents the *fovea centralis*. (B) Spectral OCT showing an experimentally induced laser burn leading to retinal distortion (characterized by disruption of the normal retinal layering) in a non-human primate.

VEGF. Rodents and non-human primates are the primary models in which neovascularization is induced and in which anti-angiogenic factors are tested.

Multiple models of AMD exist, but since none is able to completely mimic the full disease, the various models focus on particular aspects. For example, the ABCR$^{-/-}$ mouse, the ELOVL4 transgenic mouse, and the cathepsin D transgenic mouse are all examples of models that focus on altered RPE physiology. These mice develop impaired RPE metabolism culminating in cytoplasmic accumulation of lipofuscin and N-retinylidene-N-retinylethanolamine (A2E), which in turn leads to RPE and photoreceptor degeneration. One characteristic of the Cfh$^{-/-}$, C3ar$^{-/-}$, and C5ar$^{-/-}$ mouse models is the systemic deposition of the complement proteins C3a and C5a, which are components of drusen in humans and also stimulate choroidal neovascularization. These models exhibit loss of photoreceptors and reduced rod function. Ccl2$^{-/-}$ and Ccr2$^{-/-}$ mice have decreased CCR2-mediated recruitment of macrophages from the circulation into tissues through complement stimulation, and were instrumental in demonstrating the relationship of AMD and complement deposition. These animals develop AMD-like pathology, when older than 16 months, characterized by drusen-like formations, RPE loss, choroidal neovascularization, and photoreceptor atrophy. It is accepted that oxidative stress along with inflammation also plays a role in the development of AMD. Sod$^{-/-}$, Sod2$^{-/-}$, and ceruloplasmin/hephaestin double knockout mice present with AMD-like lesions ranging from sub-RPE deposits of debris to photoreceptor atrophy. Epidemiological associations between AMD and cardiovascular factors have prompted speculation regarding the role of lipids on AMD development, with conflicting results. The majority of models that explore this potential relationship have shown relatively modest sub-RPE deposits and Bruch's membrane thickening. Examples include APOE 3-Leiden transgenic, ApoE-null, and targeted APOE replacement strains of mice.

Macular degeneration associated with drusen accumulation occurs spontaneously in rhesus and cynomolgus macaques, with differences in the pattern of inheritance and onset of lesions between the two species. The rhesus disease closely resembles human AMD, while the cynomolgus condition more closely approximates early-onset maculopathies. In the cynomolgus monkeys, symptoms appear at 2 years of age (early onset) and progress slowly. Lesions in this species are characterized by fine yellow-white dots on fundoscopy, and RPE lipofuscin accumulation and complement (C5)-rich drusen between the RPE and choriocapillaris. The rhesus monkeys, which originated from Cayo

**TABLE 53.6** Selected Mouse Models of Retinal Degeneration

| Mutation | Disease associated | Characteristics |
|---|---|---|
| Retinal degeneration-1<br>*Pde6b$^{rd1}$* | Retinitis pigmentosa | Early onset. Affects the ONL* with sparing of few cones. Mutation common in several laboratory strains. |
| Retinal degeneration-2<br>*Prph2$^{Rd2}$* | Retinitis pigmentosa | Slowly progressive. Complete atrophy of outer retina by 9 months. |
| Retinal degeneration-3<br>*rd-3* | Usher syndrome deafness | Early onset. Autosomal recessive mutation in the RBF/DnJ strain. |
| Retinal degeneration-4<br>*rd-4* | — | DBA/2J male mice. Total ONL atrophy by 6 weeks. |
| Retinal degeneration-5<br>*tub* | Alstrom or Bardet-Biedl syndromes | C57BL/6J-tub. Combine retinal degeneration and progressive hearing loss. |
| Retinal degeneration-6<br>*Rd-6* | — | Autosomal recessive. Distinctive white dots on retina associated with subretinal macrophages. Atrophy by 1–2 months. |
| Retinal degeneration-7<br>*Nr2e3$^{rd7}$* | — | Retinal waves, whorls, and rosettes. Later onset photoreceptor degeneration. |
| Cone photoreceptor function loss 1<br>*cpfl1* | Congenital achromatopsia | No cone-mediated but normal rod-mediated photo responses from 3 weeks to 15 months. |
| Neuronal ceroid lipofuscinosis<br>*nclf* | — | Mixed genetic background,C57BL/6J; C57BL/10J and C3HeB/FeJLe. Develop progressive ataxia, myelination defects, neurodegeneration, neuromuscular defects and retinal degeneration at 6 months. |
| Purkinje cell degeneration<br>*pcd* | — | Slower retinal degeneration. C57BR/cdJ strain. Complete photoreceptor degeneration at 1 year. |

* *ONL, outer nuclear layer.*

Santiago Island in Puerto Rico, exhibit incidences of macular drusen of 50% at 9 years of age (adult onset) and 100% at 25 years. Histologically and ultrastructurally, the rhesus lesions present as large drusen on Bruch's membrane and RPE.

The control and treatment of neovascular processes in the eye is in the forefront of ocular drug development. AMD along with retinopathy in premature infants and diabetic retinopathy are among the main reasons for this emphasis. However, in order to test the efficacy of those drugs, reliable models of neovascularization need to be established. The laser-burn model of choroidal neovascularization (CNV) is widely used. It consists of creating a laser-induced rupture on Bruch's membrane that allows choroidal fibrovascular proliferation to reach the subretinal space, similar to the wet form of AMD. Rodents (mice and rats) and non-human primates (cynomolgus and squirrel monkey [*Saimiri sciureus*]) are often used. This model has proven to predict drug effectiveness in several generations of successful therapies in affected humans. The model makes no attempt to define any of the underlying mechanisms that lead to wet AMD, but rather establishes a setting in which the ability of the test substance to decrease neovascularization may be determined.

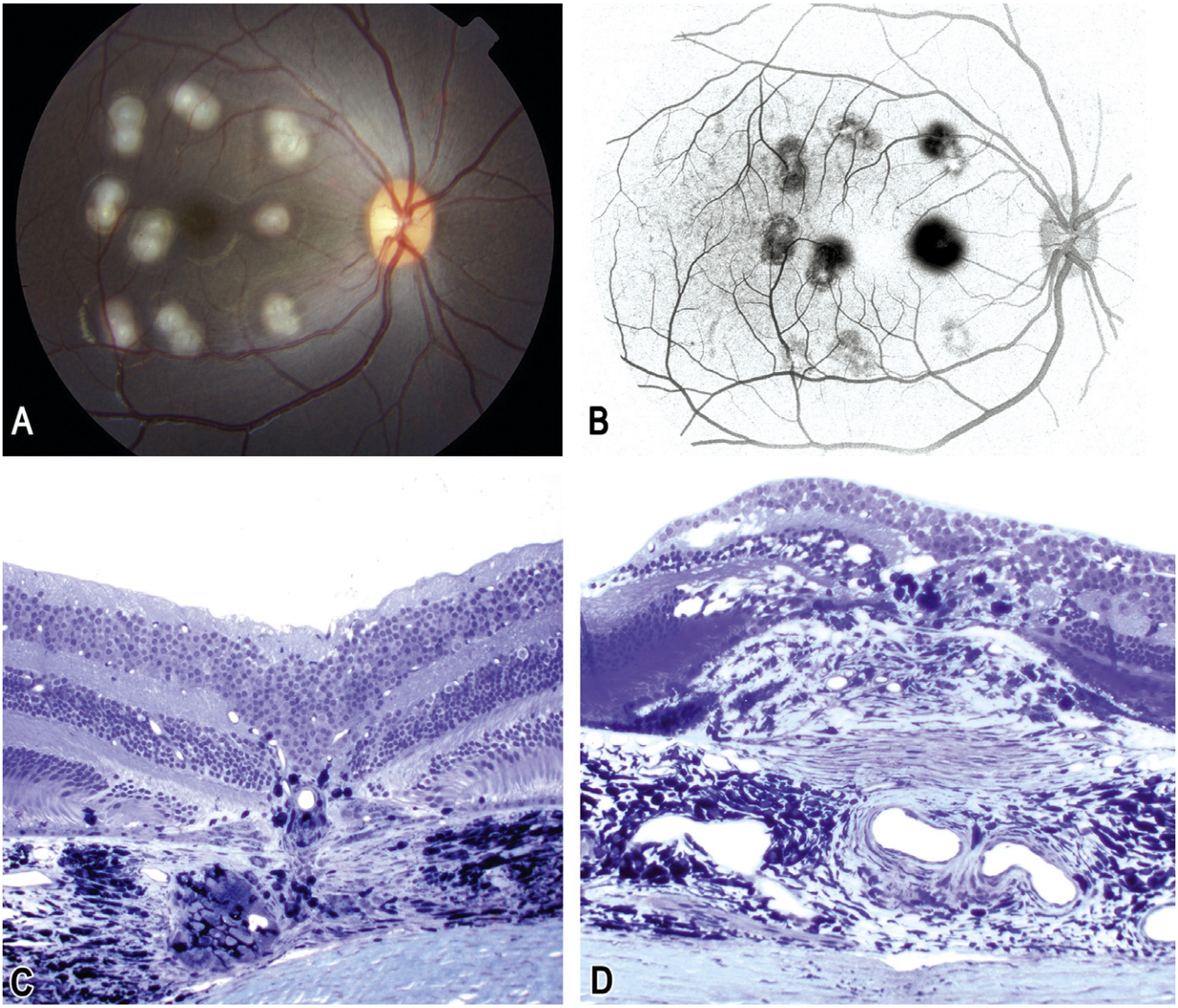


FIGURE 53.25 Laser-induced model of age-related macular degeneration (AMD) in the non-human primate retina. (A) Fundus photo showing the characteristic nine laser burns (white spots) oriented around the macula (central dark spot). The large orange spot from which the retinal vessels are radiating represents the *fovea centralis*. (B) Negative image of a fluorescein angiogram showing vascular leakage as gray/black areas associated with the laser burns. (C) Histopathologic image of a laser burn showing a minimal proliferative response extending from the choroid into the outer retina, a desirable effect from an efficacious test article. (D) Histopathologic image of a laser burn from an untreated control showing a profound choroidal proliferative response beneath and extending into the retina. (C) Toluidine blue, 100×; (D) Toluidine blue, 200×.

In non-human primates, the laser burns are clustered near the macula. The most effective endpoint for evaluating the laser-burn model has been fluorescein angiography. The histopathological assessment of this model is problematic because the site selected needs to be precise and the laser burn needs to be sectioned in the center. The rodent model has the benefit that large portions of the eye can be serially step-sectioned to ensure that the laser-induced lesions winds up in the section to be analyzed (Figure 53.25).

### RETINAL NEOVASCULARIZATION

The pathogenesis of retinal neovascularization (RNV) is better understood than that of choroidal neovascularization. Studies indicate that ischemia is the main cause of RNV. Usually there is a loss of regional retinal perfusion, and the resulting hypoxic tissue stimulates the release of signaling molecules that promote an excess neovascularization. Resulting lesions include edema, hemorrhage, and retinal detachment.

A number of conditions produce this effect, including diabetes, premature delivery, and occlusion of either the central vein or a branch retinal vein. Based on their hypoxic mechanism, these diseases are collectively referred to as ischemic retinopathies. All these conditions can be recapitulated using animal models. Examples include oxygen-induced models (reported in mouse, rat, cat, dog, and zebrafish), vascular occlusion models (rat, pig), transgenic mouse models of neovascularization, and intraocular injection of proangiogenic molecules (mouse, rabbit). A detailed description of all the available models can be found in the Suggested Reading list.

## 12.3. Response of the Retina to Injury

Retinal toxicity primarily affects the photoreceptors, retinal ganglion cells, and RPE. The RPE is closely integrated with the photoreceptors, such that a toxic effect on the RPE will often affect the photoreceptors and vice versa.

Shortening of the photoreceptor outer segments along with loss of nuclei from the outer nuclear layer is often seen following exposure to ocular toxicants. Cone nuclei often prolapse into the subretinal space rather than undergo apoptosis. Ganglion cell dropout is the most likely change to the retinal ganglion cells. Swelling, vacuolation, necrosis, and apoptosis might also be seen in various retinal neurons (Figure 53.26).

Hypertrophy of RPE cells and the accumulation of lipid vacuoles or lipofuscin are common changes seen following toxicant exposure. However, atrophy or metaplasia of the RPE can also be a toxic effect. Retinal anatomy differs among mammalian species used for toxicity testing, and this needs to be understood when choosing an animal species for such testing.

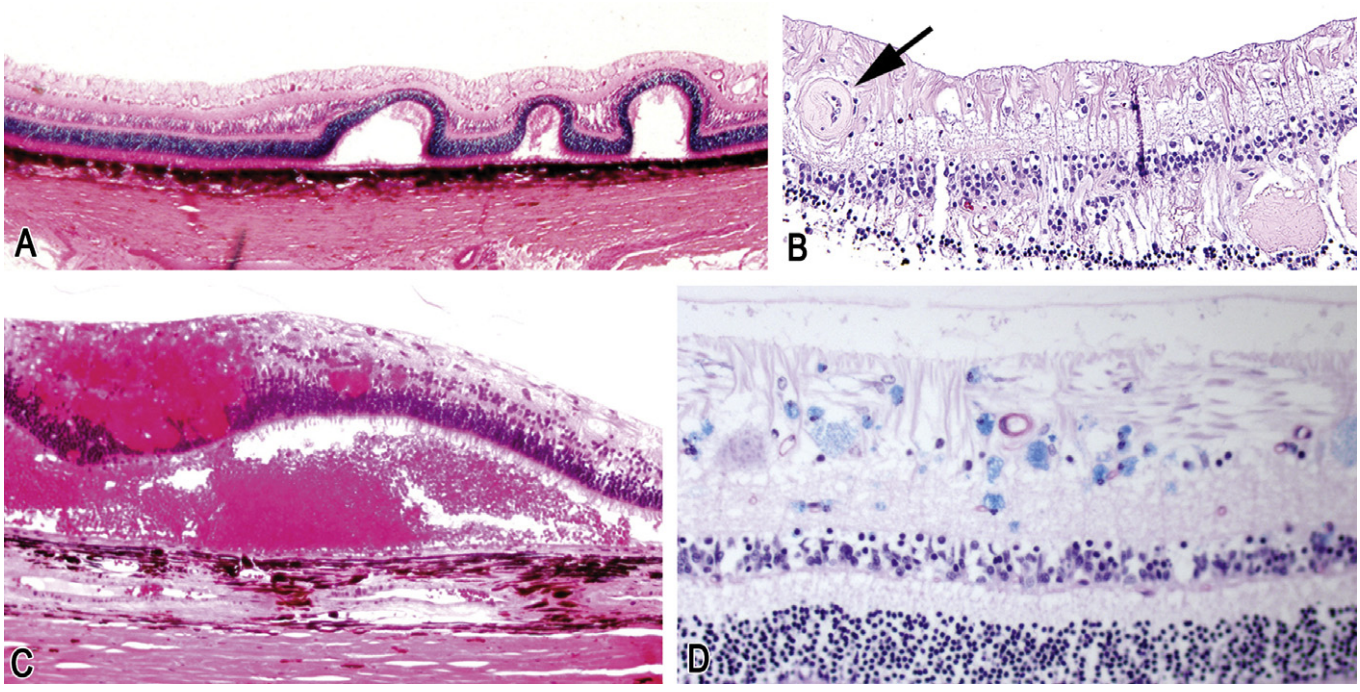


FIGURE 53.26 Pathology of the retina. (A) Canine retina with retinal folds after an invasive procedure. (B) Canine retina with hypertensive vasculopathy (thickened vessel wall [arrow]). (C) Canine retina with extensive retinal and subretinal hemorrhage following radiation therapy (radiation retinopathy). (D) Canine retina with blue product accumulated in the cytoplasm of neurons from a dog with an undetermined lysosomal storage disease. (A) H&E, 100×; (B, C) H&E, 200×; (D) Luxol fast blue/PAS, 400×.

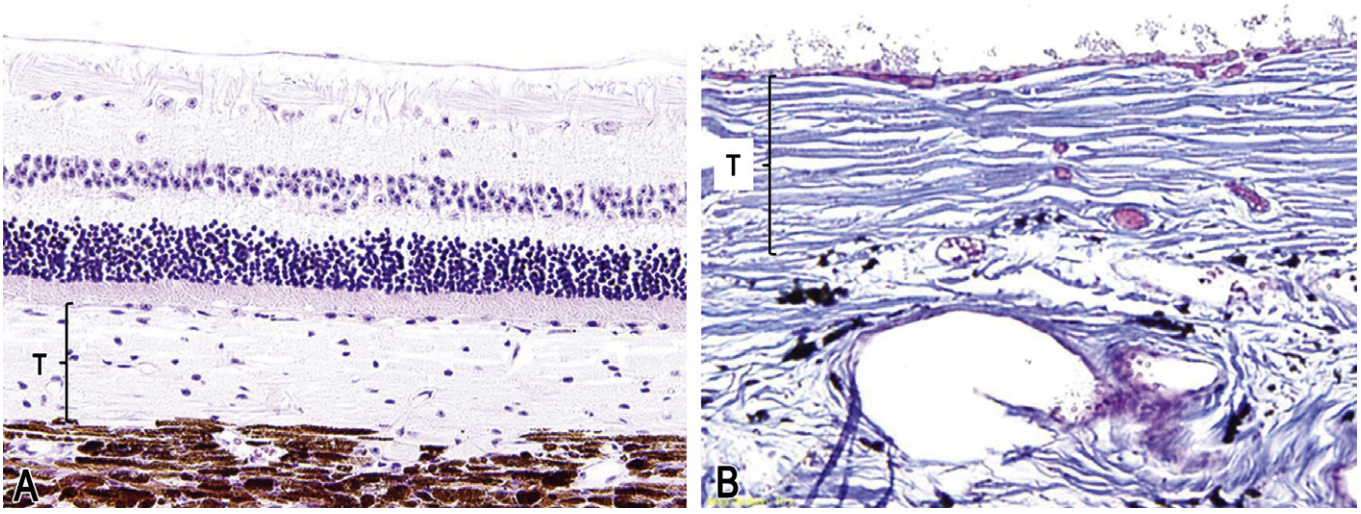


FIGURE 53.27 Normal architecture of the tapetum. (A) Cellular tapetum (T) typical of a carnivore, such as a dog or cat. (B) Fibrous tapetum (T) from a goat, made up of collagen. (A) H&E, 100×; (B) Masson's trichrome, 200×.

These differences include the type of blood supply, the presence of a fovea, and the presence of a tapetum lucidum. Toxic effects of the tapetal cells are not usually detected histologically; rather, they are observed as hyper-reflectivity of the fundus on the fundoscopic exam. It is important to identify this phenomenon and to differentiate it histologically from retinal lesions, since a toxic effect on just the tapetal cells would have limited significance in humans (Figure 53.27).

Many compounds bind chemically to melanin and therefore accumulate in pigmented cells and tissues, particularly the RPE of the eye. Melanin binding does not predict ocular toxicity. Some drugs can be detoxified by melanin binding (e.g., fenthion and vigabatrin), while others may accumulate locally, causing an enhancement of the toxic effect (e.g., chloroquine and phenothiazines).

The pathologist needs to be aware of normal physiologic and background changes in RPE cells when assessing the significance of alterations recorded. Common physiologic changes that may be misinterpreted as evidence of toxicity include age-related cytoplasmic accumulation of lipofuscin, variations on cytoplasmic pigmentation, and focal areas of RPE hypertrophy, especially in Dutch belted rabbits (Figure 53.28).

A common mistake in designing ocular toxicity studies is to automatically choose rodents as the test species. Many rodent strains are affected by hereditary retinal degeneration, such as Royal College of Surgeons (RCS) rats or retinal degeneration (*rd*) mice. These animals are docile and make good experimental animals, but they lose essentially all of their photoreceptors as a normal background condition. Albino rodents are prone to photoreceptor loss in association with phototoxicity when exposed to high levels of blue light. Study protocols usually take this rodent idiosyncrasy into account. Nonetheless, in 2-year rodent bioassays, phototoxic changes are seen fairly frequently as a background change, especially in females. The authors have seen 2-year studies where phototoxic retinopathy in albino rodents has presented with a pattern suggesting a dependence on toxicant dose and sex. We think that this phenomenon is associated with slightly stronger light levels combined with an otherwise trivial compound-related effect on one of the pathways associated with phototoxicity, such as oxidative stress or apoptosis, rather than overt ocular toxicity by the test agent alone. In rats, a clue that the change is phototoxicity rather than retinal toxicity is an unusual vascular proliferation seen in the RPE layer of the retina (Figure 53.4).

Dutch belted rabbits have a common background change in RPE cells which must not be confused with evidence of chemical toxicity. Affected RPE cells are usually located near the

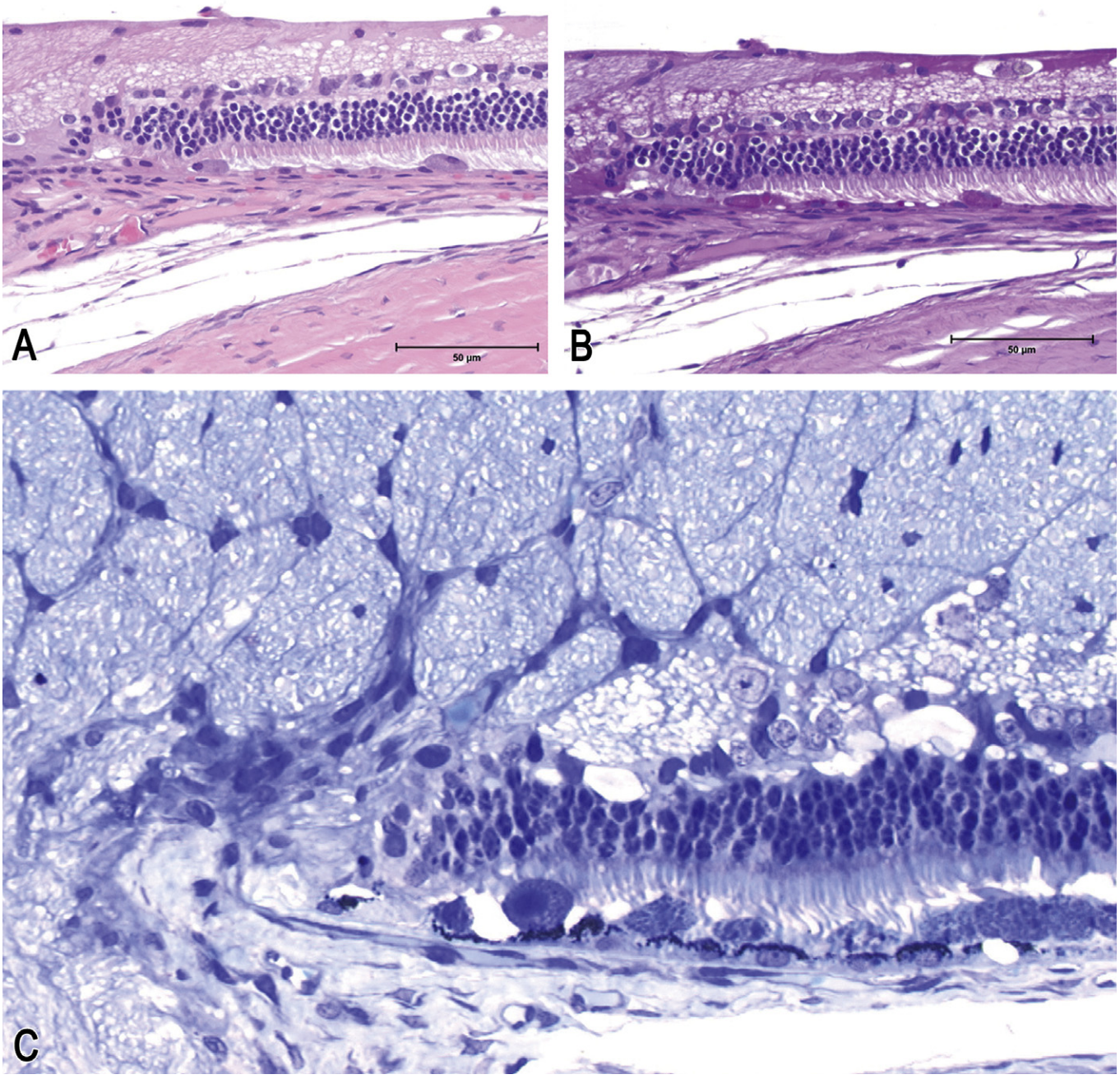


FIGURE 53.28 Spontaneous background change in the retinal pigmented epithelium (RPE) in Dutch-belted rabbits. (A, B) Retina near the optic nerve with swollen RPE cells weakly staining positive with PAS stain. (C) Plastic section from another rabbit showing the same RPE features. (A) H&E, 100×; (B) PAS, 100×; C. Toluidine blue, 400×.

optic nerve and are characterized by a swollen and granular cytoplasm. Focally, this change might be associated with secondary atrophy of the outer retina (Figure 53.28).

Rarely, rhesus or cynomolgus macaques develop a bilaterally symmetrical optic nerve atrophy characterized by an absence of retinal ganglion cells from the macula, and therefore an absence of axons in the temporal portion of the optic nerve. Affected animals might have minimal to severe involvement, the extent depending on the degree of ganglion cell loss.

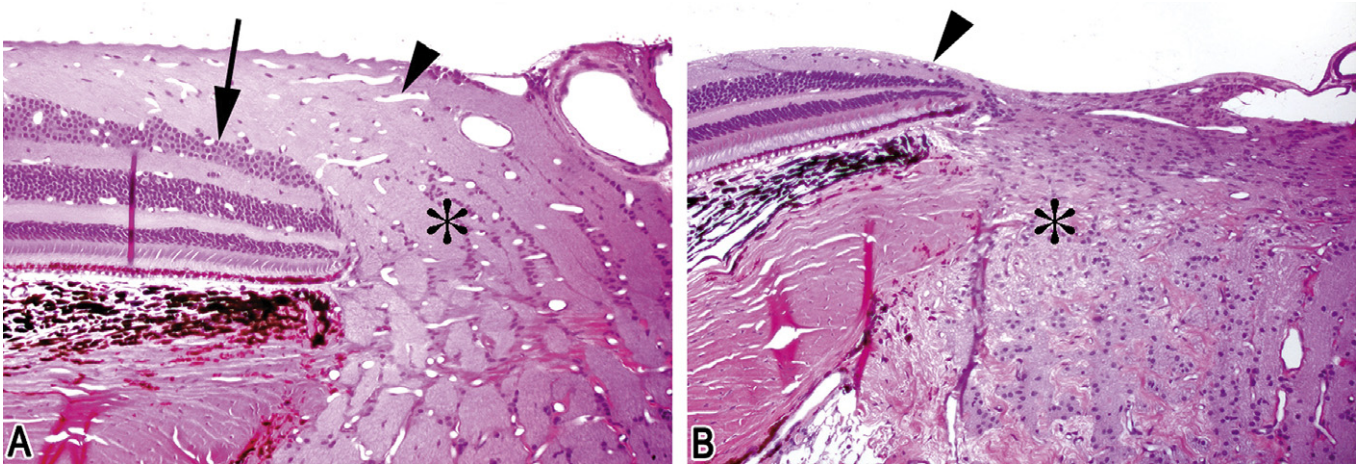


FIGURE 53.29 Bilateral optic atrophy of macaques. (A) Image of the temporal aspect of the normal optic nerve head from a control macaque showing a thick nerve fiber layer (arrowhead), abundant ganglion cells (arrow), and normal appearance of the temporal aspect of the optic nerve within the lamina cribrosa (*). (B) Image of the same area from an affected macaque. The nerve fiber layer is thin (arrowhead), the ganglion cells are reduced in number, and the temporal aspect of the optic nerve is atrophic (*). (A, B) H&E, 200×.

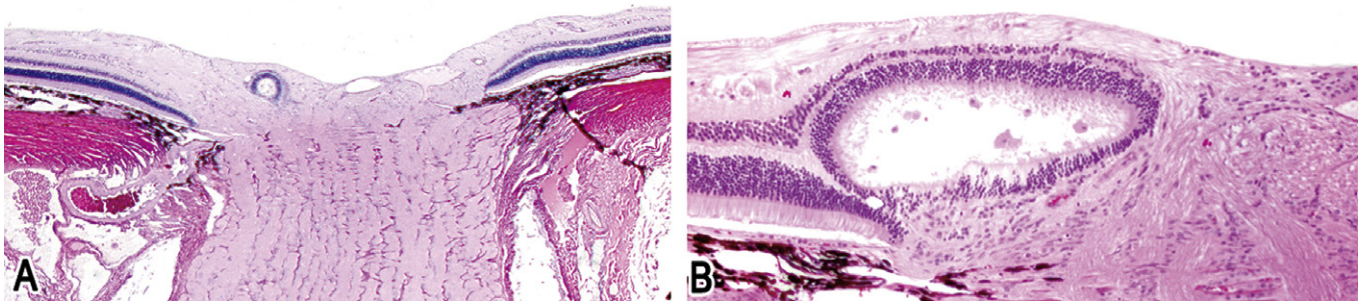


FIGURE 53.30 Retinal rosette (a background lesion) in a research Beagle dog. (A, B) Incidental retinal rosette in the optic nerve head as a background lesion in some lines of experimental Beagle dogs. (A) H&E, 100×; (B) H&E, 200×.

Only the most severely affected animals have been able to be detected ante-mortem by fundoscopic examination (Figure 53.29).

Beagle dogs sometimes develop focal retinal dysplasia as a background lesion. Affected dogs have a focal fold or rosette of retinal tissue, often in or near the optic disc (Figure 53.30). The change is usually quite small, and does not appear to be associated with any functional abnormalities.

Not all functional impairments of the neural retina or RPE will result in morphological alterations. This discrepancy underscores the importance of combined histologic and electrophysiological endpoints when evaluating the impact of xenobiotic treatment on the eye, especially when seeking to detect very early stages of toxicity.

## 12.4. Mechanism of Toxicity

Toxic effects to the retina ore often best appreciated with transmission electron microscopy (TEM; Table 53.7), although microscopic changes of retinal toxicity also may be appreciated (Table 53.8). The following substances that affect the retina may be considered as prototypes of the kinds of changes that may be seen when evaluating the retina for toxicity using various morphological techniques.

**TABLE 53.7** Ultrastructural Alterations Produced by Some Compounds Retinotoxic to Rats

| Compound | Utrastructural alterations |
|---|---|
| Vitamin A | Increased lipid droplets and mitochondrial destruction in RPE, mitochondrial destruction in PRC inner segments |
| Trimethyltin | Membrane-bound vacuoles and polymorphic dense bodies in PRC inner segments, PRC necrosis, dense-cored vesicles and tubules in ganglion cells, intracytoplasmic dense bodies in INL |
| Amphiphilic cationic drugs | Accumulation of crystalloid or lamellated inclusions in the cytoplasm of RPE or neuroretina; chloroquine only: multilamellated bodies in PRC inner segments |
| Fenthione | Loss of PRC outer segments, hypertrophy of RPE, pigment granules in subretinal space and penetrating OLM |
| Perhexiline maleate | Lamellar and reticular cytoplasmic inclusions in all retinal cell types, crystalloid inclusions in RPE |
| L-ornithine hydrochloride | Marked expansion of cytoplasmic matrix and destruction of organelles in RPE → RPE degeneration/hyperplasia → secondary disruption of PRC outer segments |
| 2-Aminoxy propionic acid | Disorientation, vacuolation and disruption of PRC outer segments → secondary increase in lysosomal bodies and phagosomes in RPE |
| Zinc chelators | Non-membrane-bound, electron opaque, scalloped inclusions in basal cytoplasm of RPE |
| Doxorubicin | Neurofilament accumulation in cell body and proximal axon of ganglion cells |
| Guanidinoethane sulfonate and β-alanine | Disorganization of PRC outer segment membrane discs |
| D, L α-Amino-adipic acids | Decreased electron density, cytoplasmic vacuolation and necrosis of Müller cells |
| Lead | PRC necrosis with electron-dense, shrunken inner and outer segments; necrosis in INL |
| AY9944 | Niemann-Pick disease-like inclusions in various retinal cell types, especially ganglion cells |
| Glutamate | Swelling of nucleus, cytoplasm and dendritic processes of ganglion cells; swelling and pyknosis in inner aspect of INL |
| Hexachlorophene | Vacuolation and tubulovesicular degeneration of PRC outer segment membrane discs |

Abbreviations: Ay9944, trans-1,4-bis (2-chlorobenzylaminomethyl) cyclohexane dihydrochloride; INL, inner nuclear layer; OLM, outer limiting membrane; PRC, photoreceptor cell; RPE, retinal pigment epithelium.
*Table reproduced from* Handbook of Toxicologic Pathology, *2nd Ed. W. M. Haschek, C. G. Rousseaux and M. A. Wallig, eds. (2002) Academic Press, Vol 2, Table VIII, p. 564, with permission.*

**Aminophenoxyalkanes** are schistosomicidal drugs that induce retinal toxicity in several animal species, including rat, rabbit, cat, dog, and non-human primate. Toxicity appears to affect the RPE, independent of pigmentation. The RPE cells show rapid necrosis that is associated with disruption of photoreceptor outer segments. Remaining RPE cells accumulate disc material and become hyperplastic.

TABLE 53.8 Microscopic Alterations Produced by Some Compounds Retinotoxic to Rodents

| Compound | Species | Microscopic alterations |
|---|---|---|
| Urethane | Rat | Loss of PRC outer segments, decreased melanin granules in RPC, debris in subretinal space → loss of ONL, thinning of INL and focal proliferation of RPE |
| Trimethyltin | Rat | Pyknotic nuclei in ONL and INL, swollen dark staining PRC inner segments |
| Vigabatrin | Rat | Disruption of ONL with outward displacement of PRC nuclei |
| P-1727 | Rat | Loss of rods and cones, disorganization of ONL and INL |
| *N*-Methyl-*N*-nitrosourea | Hamster | Arcades within the ONL, degeneration of RPE → retinal atrophy |
| | Mouse | Retinal thinning and rosette formation in off-spring following maternal administration |
| Cycasin | Mouse Rat | Necrosis of the neuroblastic layer of the retina in neonates → retinal rosette formation |
| Carbon disulfide | Rat | Acute degeneration of retinal ganglion cells |
| Fenthione | Rat | Thinning of central retina, swelling and disorganization of RPE, melanin pigment about vessels |
| L-Ornithine hydrochloride | Rat | Degeneration and focal denuding of RPE → secondary disruption of PRC outer segments |
| 2-Aminoxy propionic acids | Rat | Fragmentation of PRC outer segments with outward migration and arcade formation by nuclei of ONL |
| Kainic acid | Rat | Pyknotic cells in inner aspect of INL and edema in the IPL → thinning and increased mitosis in INL |
| Glutamate | Mouse Rat | Necrosis and loss of cells in the ganglion cell layer and INL, vacuolation in plexiform layers |
| Doxorubicin | Rat | Decreased chromatin staining in ganglion cells, swollen axons in NFL → massive loss of ganglion cells |
| L-Cysteine | Rat | Marked reduction in thickness of the NFL, ganglion cell layer, IPL and ONL |
| Cytosine arabinoside | Rat | Retinal dysplasia characterized by rosette formation and retinal disorganization and thinning |

Abbreviations: INL, inner nuclear layer; IPL, inner plexiform layer P-1727, *dl*-(*p*-trifluoromethylphenyl) isopropylamine hydrochloride; NFL, nerve fiber layer; ONL, outer nuclear layer; PRC, photoreceptor cell; RPE, retinal pigment epithelium.
*Table reproduced from* Handbook of Toxicologic Pathology, *2nd Ed. W. M. Haschek, C. G. Rousseaux and M. A. Wallig, eds. (2002) Academic Press, Vol 2, Table IX, p. 565, with permission.*

**Antidepressant drugs** such as amiodarone, chloroamitriptyline, chlorphentermine, clomipramine, imipramine, iprindole, various aminoglycosides, and other cationic amphophilic compounds interfere with the enzymatic degradation of phospholipids. Systemic administration results in accumulation of phospholipids (i.e., phospholipidosis) in retinal cells, including the RPE. Storage is within cytoplasmic inclusions, where the lipids assume a crystal-like conformation. This effect is

partially reversible upon discontinuation of treatment.

**Desferrioxamine**, an iron-chelating agent used to treat hemochromatosis, causes vision loss in humans. Retinal toxicity in rats and rabbits only can be detected by ERG and not by morphological analysis.

**Isopropylamine hydrochloride** given in high doses to rats and dogs causes retinal toxicity. The lesion is characterized by loss of photoreceptors and RPE migration into the subretinal space.

**Fluoride** administered as a sodium salt intravenously at near-lethal doses to rabbits results in fluoride concentration within the eye. These very high concentrations are toxic to the retina, leading to destruction of the RPE and the photoreceptor outer segments.

**Iodates** given at high doses by intravenous administration cause retinal damage in several species, including humans. Iodate causes degeneration of the RPE basement membrane, with cytoplasmic swelling and loss of apical microvilli; the end stage is necrosis. The blood–retinal barrier is compromised. Photoreceptors degenerate, and the choriocapillaris atrophies. The primary event in iodate retinal toxicity is RPE cell necrosis followed by photoreceptor cell apoptosis. The mechanism of toxicity is not clear, but inhibition of lysosomal enzymes may play an important pathogenic role in the RPE lesion.

**Iodoacetate**, an inhibitor of glycolysis, is highly retinotoxic. High intravenous doses of iodoacetate to rabbits cause injury of rods and also affect phagocytic activity of RPE cells. Recently, a new pig model of inherited retinal dystrophy has been devised by administering a single intravenous dose of iodoacetic acid. Marked photoreceptor degeneration arises after 2–5 weeks.

**Lead** poisoning can cause lipofuscin accumulation in RPE cells of rabbits, leading to outer retinal degeneration. The presumed mechanism is chronic oxidative stress.

**Methanol (**or its by-product **formic acid**) ingestion in humans and non-human primates can result in outer retinal toxicity. In contrast, retinal toxicity can be produced in rats only by inhibiting formate oxidation, which occurs much more rapidly in this species and thus prevents the accumulation of formic acid. Methanol toxicity in rats shows that both mitochondrial disruption and cellular atrophy occur in the outer retina.

**4,4′-methylenedianiline** is an intermediate in the production of isocyanates and polyurethanes. It causes retinal toxicity in pigmented and non-pigmented guinea pigs when inhaled, inducing degeneration of the photoreceptor inner and outer segments as well as the RPE. Retinal toxicity also occurs in cats exposed though oral or parenteral routes.

**N-ethyl-N-nitrosourea (ENU)** is an alkylating agent considered to be mutagenic. It is well known to cause congenital malformations including anophthalmia, microphthalmia, and tumors in various locations, especially the nervous system. Chronic exposure to high doses is retinotoxic in guinea pigs and rats. In rats, photoreceptors undergo degeneration early, with subsequent degeneration of RPE cells. A single high dose of ENU recently has been reported to cause outer retinal atrophy in adult BALB/c mice.

**Naphthalene** is better known to cause cataracts, but it is also retinotoxic. After oral administration to rabbits, the chief lesion is RPE degeneration.

**Nitroaniline**, a rodenticide, causes retinal toxicity in humans, rabbits, and hamsters. The changes of note following oral administration are related to degeneration in the RPE and photoreceptors.

**Organophosphates** inhibit cholinesterase and are commonly used as pesticides. Retinal degeneration and histological abnormalities of the RPE have been reported in some cases of toxicity, but this finding has been difficult to reproduce.

**Diburyl oxalate** delivered subcutaneously to rabbits induces the formation of needle-like birefringent crystals in the cytoplasm of RPE cells, as well as in other organs (e.g., kidney, heart, testes). The crystalline deposits in the RPE can be detected as white flecks on the retina by indirect ophthalmoscopy. Histologically, RPE cells exhibit varied

numbers of Pizzalato stain-positive (calcium oxalate), intracellular, needle-like crystals that often coalesce to form a single large deposit.

**Phenothiazines** tranquilizers, including derivatives such as piperidylchloro-phenothiazine, thioridazine, and chlorpromazine, can cause clinically significant retinopathy in humans. Retinal toxicity also can be induced in cats, but not in rabbits, rats, guinea pigs, or dogs. Photoreceptor cells, particularly the rod outer segments, are the target tissue. The main lesion is degeneration of the outer segments of photoreceptor leading to thinning of the photoreceptor layer. The RPE cells undergo secondary hypertrophy via cytoplasmic accumulation of lipofuscin, melanolysosomes, and curvilinear bodies. Atrophy of the RPE layer is seen in the end-stage lesion. Phenothiazines bind to melanin and accumulate within the uvea and RPE. Phototoxicity has been postulated as a mechanism for inducing the retinal lesion. Chlorpromazine specifically also has the potential to cause cataract.

**Chloroquine** and **hydroxychloroquine** are used as antimalarial drugs and for the treatment of extraintestinal amebiasis and autoimmune diseases (rheumatoid arthritis and lupus erythematosus). Chloroquine retinal toxicity occurs in humans, causing vision dysfunction. Chloroquine retinopathy is more severe over time and with high doses. In fully developed cases, a depigmented lesion surrounded by a pigmented ring ("bull's eye" depigmentation) is present at the macula. Several animal models of chloroquine-induced retinal toxicity have been developed, including the rat, cat, dog, rabbit, pig, and non-human primate. Cytoplasmic accumulation of membranous phospholipid inclusions occurs in retinal ganglion cells, photoreceptors, and the RPE. The RPE cells largely remain intact, but eventually the photoreceptor outer segments degenerate. Chloroquine is thought to inhibit lysosomal degradation. There is a very high affinity of chloroquine for melanin, and this is thought to be an important pathogenic mechanism. However, the significance of this binding is in fact not well understood.

**Taurine** is an amino acid that is concentrated in the photoreceptors, and is essential for retinal function. One critical RPE function is to transport taurine to the photoreceptors. Taurine is an essential amino acid for cats, so taurine depletion (by dietary insufficiency) in this species causes outer segment degeneration and loss of photoreceptor cells. The resulting functional defect is a reduced ERG. Guanidinoethyl sulfonate (GES) is an inhibitor of taurine uptake, and GES toxicity leads to a reduction in retinal taurine concentration and causes degenerative changes in the retina.

## 13. OPTIC NERVE

### 13.1. Structure, Function, and Cell Biology

The term "optic nerve" is a misnomer, since this structure actually is a central nervous system (CNS) tract. The optic nerve is mostly composed of the axons from the retinal ganglion cells that are projected centripetally within the inner nerve fiber layer of the retina, before converging at the optic nerve head and then turning caudally to project toward the brain. The central area of the optic nerve head is depressed, and is supported by a thickening of the retinal inner limiting membrane (called the supporting meniscus of Kuhnt). As the nerve passes thought the scleral canal it transverses an open meshwork of collagenous beams or plates continuous with the sclera (termed the lamina cribrosa). This connective tissue meshwork also contains elastin and lends support for the nerve tissue. Of the commonly used laboratory animals, the mouse is the only one that does not have a distinct lamina cribrosa. The rat exhibits single bundles of collagen forming a delicate lamina cribrosa, while non-human primates, pigs, dogs, and cats possess a robust lamina cribrosa comparable to humans (Figure 53.31). That said, the composition and structure of the lamina cribrosa is similar in primates and rats. In glaucoma, physical distortion of the globe resulting from elevated IOP leads to outward bowing of the lamina cribrosa and physical distortion and misalignment of the laminar plates, with resulting compression of axons.

The canine and feline optic nerve and retina receive their blood supply from the short

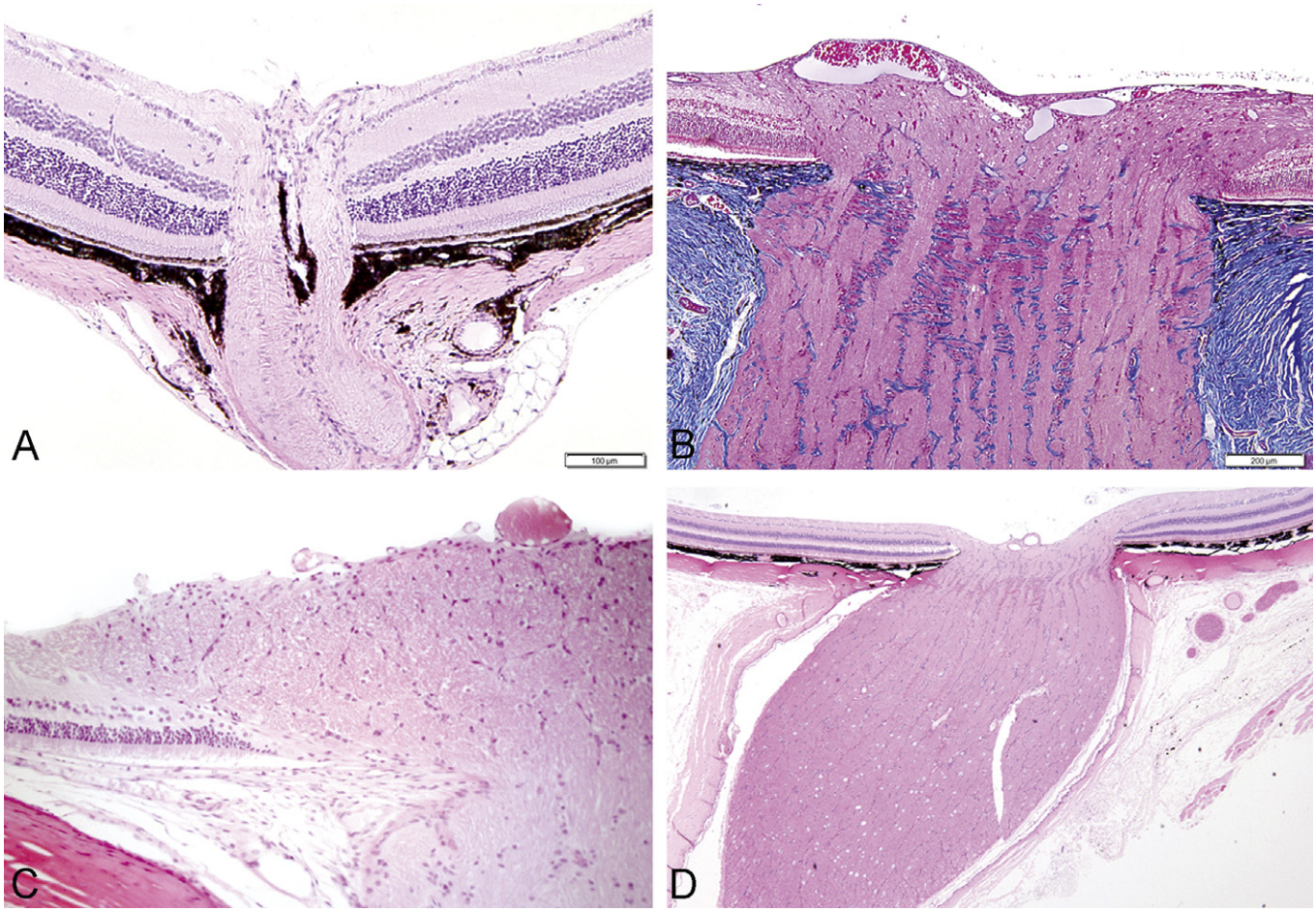


FIGURE 53.31 Normal architecture of the optic nerve. (A) Mouse optic nerve, demonstrating the absence of the lamina cribrosa. The presence of pigmented cells within the optic nerve head is a normal variation. (B) Dog optic nerve, highlighting (in blue) the many parallel collagenous beams of the lamina cribrosa. (C) Rabbit optic nerve, showing that the thick optic nerve head is composed of a large concentration of ganglion cell axons that form the retinal medullary ray. (D) Non-human primate optic nerve, resembling that of humans, has a prominent lamina cribrosa and a central retinal artery that can be observed as a circular profile on the inner aspect of the optic nerve head. (A, D) H&E, 12.5×; (B) Masson's trichrome, 100×; (C) H&E, 200×.

posterior ciliary arteries. In dogs, a small dark spot within the center of the optic nerve head is known as the physiologic pit, which is considered to be a remnant of the hyaloid artery. An exaggeration of the normal thickening of glial cells over the optic nerve (called Bergmeister's papilla) is also considered to represent a remnant of the hyaloid artery.

Before reaching the lamina cribrosa the nerve fibers are insulated by the processes of the retinal astrocytes, but after leaving the eye they are myelinated by oligodendrogliocytes. In dogs, myelination of retinal ganglion cell axons in the optic nerve begins at the optic chiasm and extends to the optic nerve head, with variable myelination extending within the peripapillary nerve fiber layer; this divergence accounts for the very irregular shape of the optic nerve head seen in many dogs. In humans, cats, non-human primates, and rodents, myelination stops at the lamina cribrosa, so the optic nerve head appears relatively small, dark, and round. There is no difference in the number of myelinated fibers in the optic nerve when comparing male vs females or right vs left globe, but the degree of myelination varies significantly among species. As an example, the difference between

primates and mice is 10-fold. The extent of optic nerve myelination also diverges substantially among different mouse strains.

As a component of the CNS, the optic nerve is covered by the three meningeal sheaths. The pia mater covers the surface of the nerve and forms interdigitations and septations throughout the neuropil that separates the axons into discrete nerve bundles. The subdural and arachnoid spaces communicate directly with their counterparts inside the cranium.

The optic nerve extends from the back of the globe to the floor of the cranial cavity, where the two nerves intersect at the optic chiasm. The degree of crossover in the chiasm varies among species, from relatively little (e.g., dog) to more than 50% (e.g., non-human primates). The axons synapse in the visual relay center within the lateral geniculate body of the midbrain.

## 13.2. Evaluation of Toxicity

Many different methods are available to evaluate optic nerve function and morphology, and can be applied to toxicology studies. Like the retina, direct observation of the optic nerve by fundoscopy is an essential component of toxicity-testing protocols. The same guidelines and inherited problems that affect the retina and dictate the choice of direct vs indirect ophthalmoscopy also apply to the optic nerve (see above). Similarly, fundus photography is an important component of most ocular toxicity investigations, allowing follow-up of lesions over time and more reliable comparisons among animals. Fluorescein angiography (FA), while principally a diagnostic technique for retinal lesions, can also be useful for evaluating abnormalities of the optic nerve vasculature. The fluorescein signal will be seen in association with the optic nerve at a late phase of the test, after choroidal and retinal vessels have already been viewed (Figure 53.23).

Electrophysiological evaluations of retinal and optic nerve functions are complementary. The Visual Evoked Potential (VEP) is a measure of the brain's electrical response to a light signal to the eye. As such, it is a measure of optic nerve function. The only test truly available for animal studies is the flash VEP, which simply measures brain wave activity in response to a flash of light to the entire retina. It is a crude measure of the ability of the optic nerve to transmit a signal to the brain. Pattern VEP is capable of estimating visual acuity, which is very useful, but it requires a trained animal (or human) to record a response. Imaging by OCT is also useful in assessing the optic nerve in live animals.

The analysis of neuronal loss in animal models of optic nerve and retinal damage is a fundamental requirement in studies of ocular toxicity. Several approaches to quantifying survival of retinal ganglion cells or their axons in the optic nerve have been used. Since quantifying retinal ganglion cells can be very time-consuming and poses some technical challenges, quantification of axons in the optic nerve is a commonly used alternative. Cross-sections of optic nerve are imaged by light microscopy or transmission electron microscopy, and counts of axon profiles can be obtained by manual or automated techniques. Manual counting of axons is also time-consuming, especially in the relatively large nerves of non-human primates. For this reason, some investigators prefer qualitative or semi-quantitative grading systems whereby optic nerve sections can be evaluated more rapidly. More detailed information on such techniques may be obtained using the sources in the Suggested Reading list.

### *Animal Models of Primary Optic Nerve Disease*

Optic neuritis with secondary demyelination is commonly associated with to multiple sclerosis (MS) in humans. Animal models of demyelinating optic neuritis are achieved by inducing experimental allergic encephalomyelitis (EAE) via subcutaneous administration of various CNS antigens – whole brain homogenate, proteolipid protein (PLP), myelin basic protein (MBP), or myelin oligodendrocyte glycoprotein (MOG) – into pre-sensitized animals. The resulting lesion is a T cell-mediated inflammatory response directed against oligodendrocyte-derived myelin, leading to encephalomyelitis and optic neuritis characterized by loss of myelin sheath, edema, lymphoplasmacytic infiltration, and blood–brain barrier disruption. The EAE pattern can be induced in non-human primates, rats, mice, and guinea pigs.

Dominant optic atrophy (DOA) is the most common inherited optic neuropathy in humans.

Common morphological changes include marked thinning of the retinal ganglion cell layer in the retina with ganglion cell degeneration and demyelination of the optic nerve. It is associated with mutation of the OPA1 gene. Two mouse models of DOA that result from engineered haploinsufficiency at the OPA1 locus are B6; C3-*Opa1*$^{q285stop}$ and B6;C3-*Opa1*$^{329\text{-}355del}$. These mice have lesions with a broad correlation to the human disease phenotype, and have provided valuable insight on the pathophysiology of visual loss.

Leber's hereditary optic neuropathy (LHON) is a maternally inherited neurodegenerative disease of humans that has been linked to mitochondrial dysfunction. LHON is the most common cause of blindness in otherwise normal young men. The key histopathologic findings are pronounced neuronal cell body and axonal degeneration, with associated demyelination and atrophy observed from the optic nerves to the lateral geniculate bodies. Experimental data indicate impaired glutamate transport, oxidative stress, and increased mitochondrial reactive oxygen species (ROS) within retinal ganglion cells, and support an apoptotic mechanism of cell death. Two mouse models of LHON have been developed, one using intravitreal injection of rotenone (a pesticide that inhibits mitochondrial complex I) and another using intraocular injection of an adeno-associated virus vector expressing ribozyme targeted against superoxide dismutase 2 mRNA.

Traumatic optic nerve lesions are usually the result of severe blunt trauma to the head. Animal models (generally rats and mice) of traumatic optic nerve injury usually involve surgical transection or crushing of the optic nerve. Typical structural lesions include classic Wallerian degeneration of the distal axons (i.e., those closest to the optic chiasm), but, unlike the Wallerian lesion in genuine peripheral nerves, the axons of the optic nerve will not regenerate once they have degenerated. The primary goal of these models is to provide a test system for neuroprotective and neuroregenerative drugs.

## 13.3. Response to Injury

The optic nerve responds to injury in a limited number of ways, and the majority of them are similar to responses in other areas of the CNS (see *Nervous System*, *Chapter 52*). Increased pressure within the cranium can result in clinically apparent swelling and rostral displacement of the optic nerve head into the eye, a protrusion known as *papilledema*. Gliosis is a common but non-specific reaction of the optic nerve neuropil to many different insults, and can be a sign of early disease. Liquefactive necrosis (malacia) of the optic nerve occurs in association with ischemic (e.g., retrobulbar hemorrhage secondary to blood collection) or inflammatory insults. Necrosis is one of the initial optic nerve alterations seen in acute cases of glaucoma, and also is very common in suppurative intraocular inflammation that involves the retina and extends into the optic nerve. As in other parts of the CNS, liquefaction of the optic nerve leads to infiltration with macrophages ("gitter cells"), many of which may contain eosinophilic intracytoplasmic debris believed to be myelin. As a consequence of optic nerve head necrosis in association with high intraocular pressure seen in glaucoma, the optic nerve collapses at the lamina cribrosa and the residual nerve tissue is displaced caudally into the sclera (an effect called *optic nerve cupping*). In some cases, a focal loss of optic nerve neuropil allows the vitreous to prolapse into the optic nerve trunk to form a cavitated lesion that is termed *Schnabel's cavernous atrophy*. This process is usually associated with glaucoma in dogs, and is thought to be an age-related change in humans.

Axonal degeneration occurs in several circumstances in the optic nerve. Loss of ganglion cells, and consequently their axons, secondary to glaucoma is probably the most common cause. On the other hand, lesions in the orbital or intracranial portions of the optic nerve can cause Wallerian degeneration with consequent axon loss and ganglion cell death. Among these lesions are trauma leading to optic nerve crush, severance, or avulsion, and also compression caused by tumors, periosteal proliferation at the optic foramen (where the nerve enters the calvarium), or granulomatous inflammation. Primary dysmyelination and demyelination affecting the optic nerve are rare in animals, but multiple mouse models of both processes have been developed to study human diseases like Pelizaeus-Merzbacher disease (PMD) and MS.

The final stage of optic nerve lesions is characterized by axonal atrophy and varying degrees of

fibrosis. At this point, optic nerve function is irreversibly lost.

### 13.4. Mechanism of Toxicity

Toxic reactions of the optic nerve are often secondary to disease processes occurring in the retina (especially involving the retinal ganglion cells) or CNS. Here, we describe the toxic events that primarily affect the optic nerve.

Congenital optic nerve disease has been reproduced in mouse models by targeted disruption of the sonic hedgehog (*shh*) gene by genetic manipulation or by exposing pregnant dams during early gestation (approximately gestational day 9.5) to the *Veratrum* alkaloid cyclopamine, which inhibits *shh* gene transduction. Affected offspring will develop cyclopia (a single or two fused eyes), holoprosencephaly (a common forebrain rather than twin cerebral hemispheres), and optic nerve aplasia (see *Embryo and Fetus*, *Chapter 62*). Optic nerve aplasia and hypoplasia are also observed in ZRDCT-An mice and in netrin-$1^{-/-}$ mice. Coloboma, a congenital abnormality in which there is segmental aplasia of optic nerve, retina, and choroid, is found in many mouse mutations. Among them are Microphthalmia (*Mitf*$^{mi}$), Belly spot and tail (*Bst*), Coloboma (*Cm*) and Total cataract and microphthamia (*Tcm*). The variety of these mutations exposes the complexity of the molecular mechanisms involved in specifying the formation and remodeling of the developing optic nerve.

Multiple toxic substances are capable of producing optic neuritis in humans and laboratory animals. The common morphological appearance of such lesions is demyelination and degeneration of axons in the optic nerve with secondary degeneration of retinal ganglion cells and, in severe cases, associated degenerative lesions in the white matter of the brain. Examples include hexachlorophene (humans and rats); arsanilic acid (humans and pigs); carbon disulfide (humans, rabbits and mice); thallium (humans); chloramphenicol (humans); clioquinol (humans, dogs and cats); cyanides (humans and rats); ethylene glycol (humans); and methanol (humans). No common mechanism of action has been found to explain the involvement of the optic nerve in the inflammation induced by these agents.

Drug-induced optic neuritis has also been described in humans and animals. The most commonly implicated drugs are the antimicrobials ethambutol (humans, monkeys, rats and rabbits), which is used frequently to treat tuberculosis; linezoid (humans), a Gram-positive bactericidal; amiodarone (humans), which is employed in the treatment of cardiac arrhythmias; and the erectile dysfunction drugs sidenafil, tadalafil, and vedenafil (humans). Again, no common molecular mechanism has been determined to explain the presence of optic nerve inflammation following exposure to these agents.

## 14. GLAUCOMA

The glaucomas represent a large, diverse group of pressure-dependent neurodegenerative disorders that result in loss of normal function and integrity of the retinal ganglion cells and their axons in the optic nerve, and ultimately lead to loss of vision. Glaucoma is the leading cause of irreversible blindness in humans worldwide. The most consistently recognized feature of glaucoma in animals is elevated intraocular pressure (IOP). Since elevated IOP is also considered a primary risk factor for glaucoma in humans, the current pharmacological therapies for treating glaucoma aim to lower IOP.

Glaucomas can be broadly dived into three categories: developmental, open angle, and closed angle disease. This classification scheme is based on clinical and histopathological evaluation; the word "angle" refers to the iridocorneal angle in the anterior chamber (see Section 9, Uvea and Filtration Apparatus, above). Many of the critical events in the pathogenesis of the glaucomas in animals remain poorly understood.

### 14.1. Evaluation of Toxicity

The measurement of the IOP is central to the evaluation of glaucoma. It has been demonstrated that the extent and duration of elevated IOP in a variety of glaucoma models is positively correlated with degree of ganglion cell loss, optic nerve damage, and functional visual deficit. The gold standard technique for measuring IOP is the fluid manometer using a pressure transducer following cannulation of the anterior chamber. Although very accurate, this technique demands a surgical intervention under general anesthesia

which might influence the IOP. To circumvent this problem, reliable non-invasive methods of tonometry (as described above) are widely used in animals with larger eyes (e.g., primates, dogs, cats, and rabbits). In rats and mice the small size of the globe represents a barrier to classical tonometric techniques, but a recently developed method termed *impact-induced tonometry* (Tonolab tonometer, TioLat, Helsinki, Finland) has been shown to be suitable for measuring IOP in conscious rodents except when the values are likely to be fairly low.

Functional retinal and optic nerve changes can be assessed by multifocal ERG (mERG), flash ERG, pattern ERG, and VEP. More information on these methods may be found in the Suggested Reading list. Evaluation of the toxic effects of elevated IOP on the optic nerve and retina was discussed above.

### *Animal Models of Glaucoma*

Animal models of glaucoma are essential in understanding the factors that determine the susceptibility of the retina and optic nerve to pressure-induced damage, and in developing therapeutic interventions to stop and even reverse the disease. A number of spontaneous animal models of glaucoma have been described, but these are of limited value in understanding the human disease since the mechanisms of elevated IOP significantly differ among species. A comprehensive description of all models of glaucoma is not within the scope of this chapter, so this list reviews the most important models (grouped by species).

#### NON-HUMAN PRIMATES

The most extensively used glaucoma model in non-human primates (NHPs) is produced by argon or diode laser photocoagulation of the trabecular meshwork. Treated animals develop sustained, moderately increased IOP beginning a few days after the treatment; the increase can last for weeks to more than a year. These animals present with decreased aqueous outflow (less by 80–90%) and optic-nerve cupping similar to that observed in humans with glaucoma. Non-laser-based NHP models have been developed by injecting autologous, fixed red blood cells, ghost blood cells, or latex microspheres (diameter, 10 μm) into the anterior chamber, resulting in elevated IOP that lasts for up to 4 days. Finally, a maternally inherited form of glaucoma similar to primary open angle glaucoma in humans has been described in rhesus monkeys from a colony at the University of Puerto Rico. The advantage of this latter model is that it could potentially be used not only to study the pathophysiology of the disease but also to investigate the inheritance patterns of the disease.

#### RATS

Rodent models of glaucoma have been developed in order to provide a more affordable system for investigating the cellular biology of pressure-induced optic neuropathy and potential neuroprotective strategies. Translimbal photocoagulation of the trabecular meshwork with diode laser bursts is considered the most reliable model in the rat. Following treatment, IOP is increased for at least 3 weeks, peaking at about 40 mmHg. The animals develop axonal loss in the optic nerve of 50% within 9 weeks. Other more technically challenging and time-consuming models in rats depend on hyperosmotic saline injection into the anterior chamber, cauterization of the episcleral (vortex) veins, and intracameral injection of India ink followed by photocoagulation.

#### MICE

Following the improvement of the techniques for measuring IOP in small globes, several mouse models of glaucoma have been developed. Limbal photocoagulation by laser treatment induces elevated IOP that lasts 2–12 weeks with a mean IOP about 1.5-fold higher than that measured in control animals. This model is associated with glaucomatous optic nerve damage. As in rats, limbal injection of saline can produce a loss of 20% of optic nerve axons after 8 weeks. Another well-established model is spontaneous glaucoma in DBA/2J which develops secondary to anterior chamber anomalies that resemble pigmentary dispersion glaucoma in humans. Among the anterior chamber changes are pigment dispersion, iris atrophy, and anterior synechia; with the chronic rise in IOP, retinal and optic nerve degeneration will occur. While the DBA/2J strain model was discovered retrospectively, transgenic and knockout models of glaucoma have been developed proactively. Of note are mice bearing mutated myocilin (*Myoc*) in the trabecular meshwork. Mutations in

*MYOC* are associated with severe glaucoma in humans but cause only moderate increases in IOP in mice. Despite the small increase in IOP, *Myoc*-mutant mice develop degeneration of peripheral ganglion cells and the optic nerve. Multiple mice models of congenital glaucoma have been generated. Examples include *Cyp1b1* (cytochrome P450, family 1, subfamily b, polypeptide 1), and *Foxc1* and *Foxc2* knockout mice. Characteristically, these mice present with anterior segment abnormalities (e.g., collapse of the iridocorneal angle and a narrowed anterior chamber) that resemble congenital glaucoma in humans.

## 14.2. Response to Injury

Increased IOP causes global enlargement of the eye (buphthalmos). A number of secondary changes develop subsequently, including corneal stromal edema and neovascularization; multiple breaks in Descemet's membrane (termed Haab's striae); scleral atrophy at the limbus, which can evolve to a staphyloma (i.e., outward bulging of the thin atrophic sclera); collapse of the ciliary cleft; and atrophy of the iris, ciliary body, and trabecular meshwork. In some cases, animals can develop cataracts and lens luxation due to stretching and breaking of the lens zonular ligaments. One of the central histological features of glaucoma is the loss of ganglion cells in the inner retina.

The mechanisms of optic nerve and retinal damage in the glaucomas remain subject to debate. Of the many proposed mechanisms, the most popular hypotheses are given here:

- Elevated IOP leads to deformation of the optic nerve axons at the lamina cribrosa and blockade of anterograde and retrograde axonal transport. This stoppage, in turn, leads to death of retinal ganglion cells due to an interruption in the supply of neurotrophic factors from the CNS.
- Elevated IOP deforms the lamina cribrosa, resulting in decreased vascular perfusion of the optic nerve head microcirculation. Ischemia produces a loss of axonal integrity and subsequent death of retinal ganglion cells.
- Elevated IOP leads to optic nerve infarction and subsequent gliosis.
- Retinal ganglion cell loss may also be due to the pathologic release of glutamate from within the damaged retina, which initiates "excitotoxic" neurodegeneration.
- Decreased choroidal perfusion causes segmental retinal degeneration affecting both inner and outer retina.

Any or all of these proposed mechanisms might play a role, depending on the species and also the underlying pathophysiology of the different glaucoma syndromes. In dogs, the retinal atrophy can affect all retinal layers and is usually more prominent in the non-tapetal (ventral) than in the tapetal (dorsal) retina. This phenomenon is called tapetal sparing, and it is a typical feature of dog glaucomas.

Necrosis of the optic nerve is an early feature of glaucoma, and it often is followed by malacia, gliosis and the formation of a deep cup. In species other than the dog, the development of gliosis and optic nerve cupping follows a less precipitous course. In glaucomatous optic neuropathy, there is a loss of large-diameter optic nerve axons and consequent optic nerve atrophy (Figure 53.32).

## 14.3. Mechanism of Toxicity

Elevated IOP can be considered a significant toxic effect of some drugs. These drugs can directly increase IOP, or they can cause intraocular damage that will lead to secondary glaucoma. Parasympatholytic drugs such atropine, homatropine, and scopolamine can paralyze the ciliary muscles and increase IOP in humans, dogs, and cats. Systemic or topical administration of corticosteroids can increase IOP in humans. It is believed that corticosteroids affect metabolism by the trabecular meshwork cells, impairing their ability to degrade glycosaminoglycans and phagocytize debris that can then be deposited to obstruct the aqueous outflow. This toxic reaction is rare in animals, with only transient elevation of IOP having been observed in rabbits treated with almost lethal systemic doses of corticosteroids and one report of an increase in IOP in a cat treated with dexamethasone. Viscoelastic substances injected into the anterior chamber during intraocular surgeries (to protect the corneal endothelium) have been implicated in the induction of significant postoperative increase in IOP in humans and dogs.

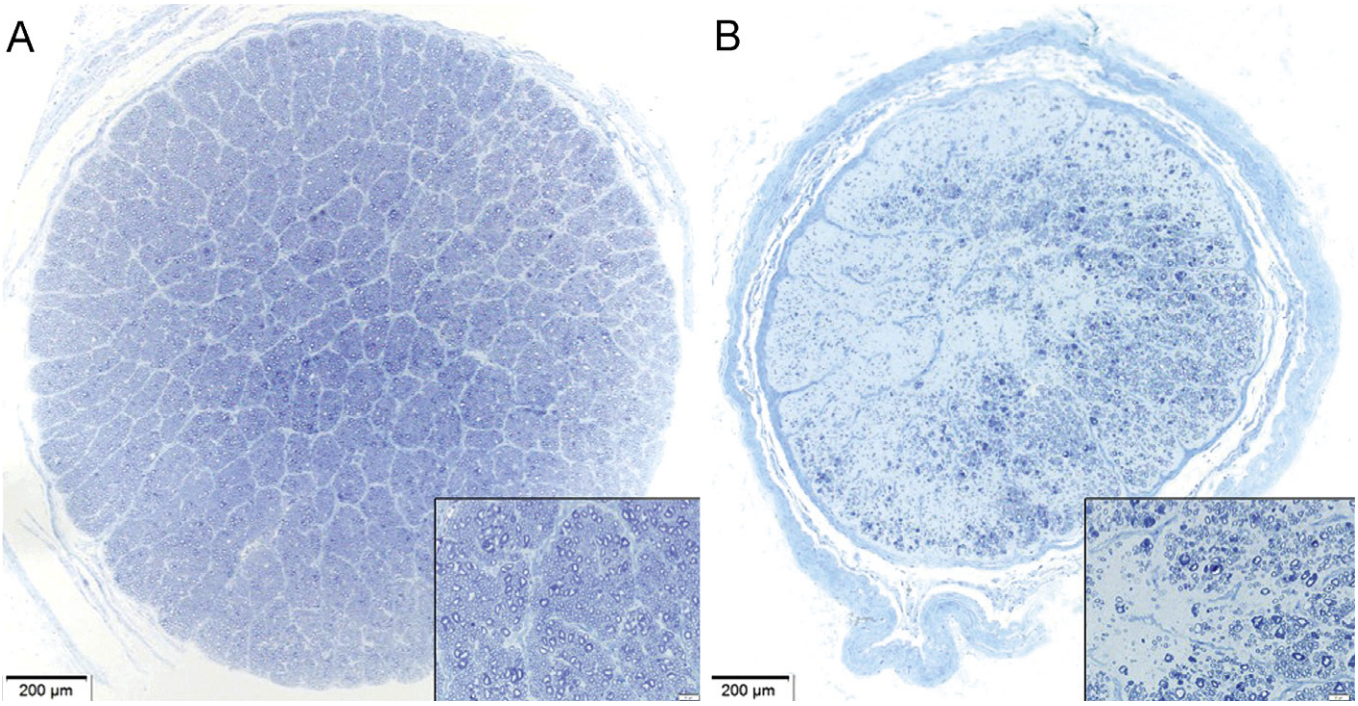


FIGURE 53.32 Optic nerve pathology resulting from congenital glaucoma in a cat. Transverse sections of the orbital portion of the optic nerve. (A) Control animal, showing the appropriate number of axons highlighted by their thick myelin sheaths. (B) Congenital glaucoma of 36-month-old cat, with marked atrophy of the optic nerve characterized by a smaller overall size of the nerve trunk and multifocal to coalescing areas of axon degeneration and fibrosis. (A, B) Toluidine blue, 100×, insets 600×.

## 15. SUMMARY

The critical nature of vision as a sensory modality for humans renders ocular toxicology pathology a critical component of non-clinical safety assessment. In many respects, analysis of the eye presents many unique challenges to toxicologic pathologists. Distinctive features of the eye include many interspecies differences in anatomy, and the need for special processing techniques to preserve small and/or delicate structures. In-life evaluations provide an equal or better assessment to pathology endpoints for some ocular conditions; indeed, in some cases routine pathology parameters will not reveal that a toxicant has produced an adverse effect. Toxic effects to structures and functions in human eyes may be modeled with some success using many spontaneous, induced, and genetically engineered animal models. Mechanisms of ocular toxicity in animals often are mirrored in humans for those parts of the eye that occur across species.

## GLOSSARY

**Accommodation** Adjustment (in the shape of the lens) to increase optical power and maintain a clear image (i.e., focus) as objects are viewed at a closer distance.

**Age-related macular degeneration (AMD)** A group of conditions in aged humans that leads to deterioration of the macula, resulting in loss of sharp central vision. It is often associated with retinal neovascularization.

**Angle, iridocorneal** Junction of the anterior surface of the iris and inner surface of the cornea, where aqueous fluid filters out of the eye.

**Anterior chamber** Fluid-filled intraocular space between the iris and the innermost corneal surface (endothelium).

**Anterior ocular segment** The part of the eye rostral to the crystalline lens, including the cornea, anterior chamber, iris, and ciliary body.

**Aphakia** Absence of the lens.

**Aqueous (also aqueous fluid or aqueous humor)** Clear, thin fluid that fills the anterior and posterior chambers. Produced by the ciliary processes. Nourishes the cornea, iris, and lens, and maintains intraocular pressure (IOP).

**Astigmatism** Optical defect in which refractive power is not uniform in all directions. Light rays entering the eye are bent unequally, which prevents formation of a sharply

focused image on the retina. Slight uncorrected astigmatism may not cause symptoms, but a large amount may result in significant blurring and headache.

**Blepharitis** Inflammation of the eyelids.

**Bowman's layer** Acellular homogenous layer of the most superficial corneal stroma, situated between the epithelium and the stroma. Thought to be responsible for epithelium adhesion.

**Bruch's membrane** Innermost layer of the choroid, composed of the basal lamina of retinal pigmented epithelial (RPE) cells, a central layer of collagen and elastic fibers, and the basal lamina of the blood vessels in the choriocapillaris.

**Cataract** Opacity or cloudiness of the lens, which may prevent a clear image from forming on the retina.

**Central vision** The region of the eye providing the best vision; used for reading and discriminating fine detail and color. Results from stimulation of the fovea and the macular area.

**Chalazion** Inflamed meibomian gland. Sometimes called an *internal hordeolum*.

**Choroid** Vascular layer of the eye lying between the retina and the sclera. Provides nourishment to outer layers of the retina.

**Ciliary body** Part of the uvea that connects the iris to the choroid. Produces aqueous humor.

**Ciliary muscle** Smooth muscle of the ciliary body stroma that functions in visual accommodation by controlling the suspension of the lens and thereby its curvature.

**Cone** Light-sensitive retinal receptor cell that provides sharp visual acuity and color discrimination.

**Conjunctiva** Transparent mucous membrane covering the outer surface of the rostral eye (except the cornea) and lining the inner surfaces of the eyelids.

**Conjunctivitis** Inflammation of the conjunctiva.

**Cornea** Transparent front part of the eye that covers the iris, pupil, and anterior chamber and provides most of an eye's optical power.

**Descemet's membrane** Basement membrane produced by the endothelial (i.e., inner epithelial) layer of the cornea, which is localized between the posterior (deep) border of the corneal stroma and the corneal endothelium. It is composed of laminin, fibronectin, and type IV collagen.

**Diabetic retinopathy** Spectrum of retinal changes accompanying long-standing diabetes mellitus. Characterized by abnormal new blood vessels (neovascularization) and fibrous tissue.

**Dilated pupil** Enlarged pupil, resulting from contraction of the dilator muscle or relaxation of the iris sphincter.

**Drusen** Small, white, hyaline deposits on Bruch's membrane associated with age and age-related macular degeneration.

**"Dry eye" syndrome** See Keratoconjunctivitis sicca (KCS).

**Ectropion uvea** Outward turning of the free edges of the iris, usually secondary to contraction of a fibrovascular membrane.

**Ectropion** Outward turning of the upper or lower eyelid so that the lid margin does not rest against the eye, but falls away. Can create corneal exposure with excessive drying, tearing, and irritation.

**Endothelium** Layer of low cuboidal cells that covers the inner aspect of the cornea.

**Entropion uvea** Inward turning of the free edges of the iris, usually secondary to a contraction of fibrovascular membrane.

**Entropion** Inward turning of the upper or lower eyelid so that the lid margin rests against and rubs the eye. Can create corneal irritation due to trauma from hairs impacting the cornea.

**Extraocular muscles** Striated muscles that move the globe (lateral rectus, medial rectus, dorsal [superior] rectus, ventral [inferior] rectus, dorsal [superior] oblique, ventral [inferior] oblique).

**Eyelids** Structures covering the front of the eye, which protect it, limit the amount of light entering the pupil, and distribute tear film over the exposed corneal surface.

**Farsightedness** See hyperopia.

**Fluorescein angiography** Technique used for visualizing and recording the location and size of retinal, choroidal, and iris blood vessels.

**Fovea** Central pit in the macula that produces the sharpest vision. Contains a high concentration of cones and no retinal blood vessels.

**Fundus** Interior posterior surface of the globe; includes the retina and optic disc.

**Glaucoma** Group of diseases characterized by increased intraocular pressure (IOP). Chronic elevations in IOP can result in compression and eventual atrophy to the retina and optic nerve fibers.

**Gonioscopy** Clinical examination of the anterior chamber angle through a goniolens (a special type of contact lens).

**Hyperopia ("farsightedness")** Focusing defect in which an eye is underpowered. Thus, light rays coming from a distant object converge to a focal point after passing through the retina, thereby blurring vision.

**Hyphema** Accumulation of blood in the anterior chamber.

**Intraocular pressure (IOP)** 1. Fluid pressure inside the eye. 2. The assessment of pressure inside the eye with a tonometer.

**Iris** Most anterior part of the uvea. Pigmented tissue lying behind the cornea that gives color to the eye (e.g., blue eyes) and controls the amount of light entering the eye by varying the size of the pupillary opening.

**Keratectomy** Surgical removal of corneal tissue.

**Keratoconjunctivitis sicca (KCS)** Corneal and conjunctival dryness due to deficient tear production. Also termed "dry eye" syndrome.

**Keratoconus** Degenerative corneal disease characterized by generalized thinning and cone-shaped protrusion of the central cornea, usually in both eyes. Hereditary cause of blurred vision.

**Lacrimal gland** Almond-shaped gland that produces tears. Located at the dorsomedial margin of the orbit, above the sclera.

**LASIK** Acronym for "laser *in situ* keratomileusis." Type of refraction-correcting surgery in which the cornea is reshaped to change its optical power.

**Lens (or crystalline lens)** Transparent, biconvex intraocular tissue that helps bring the light to a focus on the retina.

**Lenticular** Referring to the lens.

**Limbus** Thin rim at which the cornea meets the sclera.

**Macula** Small central area of the retina surrounding the fovea; area of acute central vision.

**Macular degeneration** Disease of the macula that results in the loss of central vision.

**Mydriasis** Pupillary dilation.

**Myopia ("nearsightedness")** Focusing defect in which the eye is overpowered. Light rays coming from a distant object converge to a focal point before reaching the retina, thus blurring vision.

**Nearsightedness** See myopia

**Neovascularization** Abnormal formation of new blood vessels, usually in or under the retina or on the iris surface. May develop in diabetic retinopathy, blockage of the central retinal vein, or macular degeneration.

**OD** Abbreviation standing for "*oculus dextrum*," meaning right eye.

**Open-angle glaucoma** Type of glaucoma where the iridocorneal angle morphology is normal (i.e., open, not collapsed).

**Ophthalmoscope** Illuminated instrument for visualizing the interior of the eye (especially the fundus).

**Ophthalmoscopy** Examination of the internal structures of the eye using an illumination and magnification system.

**Optic disc/optic nerve head** Ocular end of the optic nerve. Denotes the points of exit of retinal nerve fibers from the eye and entrance of blood vessels into the eye.

**Optic nerve** A large bundle of axons (fibers) from retinal ganglion cells that pass from the inner surface of the retina, converge at the optic nerve head, and then project to the brain.

**Orbit** Osseous socket containing the globe, fat, extraocular muscles, nerves and blood vessels.

**OS** Abbreviation standing for "*oculus sinistrum*," meaning left eye.

**Pachymeter** Instrument used to measure the corneal thickness.

**Pachymetry** Clinical examination used to measure corneal thickness.

**Papilledema** Non-inflammatory swelling/elevation of the optic nerve, often due to increased intracranial pressure (IOP) or a space-occupying mass within the orbit.

**Photophobia** Abnormal sensitivity to, and discomfort from, light. May be associated with excessive tearing. Often due to inflammation of the iris and/or cornea.

**Posterior capsule** The thin posterior aspect of the lens capsule.

**Posterior chamber** Aqueous-filled space that holds the lens. It is delineated anteriorly by the posterior aspect of the iris and posteriorly by the anterior face of the vitreous body.

**Posterior segment** The part of the eye posterior to the lens, including the vitreous cavity and body, choroid, retina, and optic nerve.

**Ptosis** Drooping of the upper eyelid.

**Pupil** Variable-sized black, circular opening in the center of the iris that regulates the amount of light which enters the eye.

**Pupillary response** Constriction and dilation of the pupil due to stimulation by light or accommodation.

**Retina** Light-sensitive nerve tissue in the eye that converts images from the eye's optical system of photoreceptors and linked neuronal layers into electrical impulses that are sent along the optic nerve to the brain.

**Retinal detachment** Separation of the retina from the underlying retinal pigmented epithelium (RPE).

**Retinal pigmented epithelium (RPE)** Layer of epithelial cell that resides between the photoreceptor layer of the retina and the choroid.

**Retinoscope** Device for measuring an eye's refractive error, with no response required from the patient. Light is projected into the eye, and the movements of the light reflection from the eye are neutralized (eliminated) with lenses.

**Rod** Light-sensitive, specialized retinal receptor cell that works at low light levels (for "night vision" in shades of gray).

**Schirmer test** Clinical examination that measures the production of tears using a strip of porous paper placed in the conjunctival sac.

**Schlemm's canal** Circular channel deep in the corneoscleral junction (limbus) that carries aqueous fluid from the anterior chamber of the eye to the bloodstream. Present as a distinct structure in humans, non-human primates, mice, and rats.

**Sclera** Opaque, fibrous, protective outer layer of the eye that is directly continuous with the cornea.

**Slit lamp** Microscope used for clinical examination the eye; allows cornea, lens and otherwise clear fluids and tissues in the eye to be seen in layer-by-layer detail.

**Strabismus** Eye misalignment caused by extraocular muscle imbalance. The result is that one fovea is not directed at the same object as the other.

**Stroma (corneal)** The middle, thickest layer of tissue in the cornea.

**Tonometry** Measurement of intraocular pressure.

**Trabecular meshwork** Mesh-like structure inside the iridocorneal angle. Filters aqueous fluid and controls its flow into Schlemm's canal (in species that have one), prior to its leaving the anterior chamber.

**Uvea** Pigmented layer of the eye (iris, ciliary body, choroid) that contains most of the intraocular blood vessels.

**Uveitis** Inflammation of the uvea. Anterior uveitis refers to inflammation of the iris and ciliary body. Posterior uveitis refers to inflammation of the choroid, which is more commonly denominated *choroiditis*.

**Visual acuity** Assessment of the eye's ability to distinguish details and shape, using the smallest identifiable object that can be seen at a specified distance (usually 20 ft or 16 in).

**Visual field** Full extent of the area visible to an eye that is fixating straight ahead.

**Vitreous (also vitreous fluid or vitreous humor)** Transparent, colorless, gelatinous mass that fills the posterior segment (vitreous cavity) of the eye.

**Vitreous detachment** Separation of vitreous gel from retinal surface.

**Zonules/zonular ligament** Radially arranged fibers that suspend the lens from the ciliary body.

# SUGGESTED READING

## General


Barile, F.A., 2010. Validating and troubleshooting ocular *in vitro* toxicology tests. J. Pharmacol. Toxicol. Methods 61 (2), 136–145.

Bibliowicz, J., Tittle, R.K., Gross, J.M., 2011. Towards a better understanding of human eye disease: insights from the zebrafish. Danio rerio. Prog. Mol. Biol. Transl. Sci. 100, 287–330.

Caspi, R.R., 2010. A look at autoimmunity and inflammation in the eye. J. Clin. Invest. 120 (9), 3073–3083.

Chévez-Barrios, P., 2005. Frozen section diagnosis and indications in ophthalmic pathology. Arch. Pathol. Lab. Med. 129, 1626–1634.

Chiou, G.C.Y., 1999. Ophthalmic toxicology, second ed. Taylor and Francis, Philadelphia, PA. 379.

Dubielzig, R.R., Ketring, K.L., McLellan, G.J., Albert, D.M., 2010. Veterinary Ocular Pathology: A Comparative Review, first ed. Saunders Ltd, Edinburgh, UK.

Eagle, R.C., 2011. Eye Pathology: An Atlas and Text, Second ed. Lippincott Williams & Wilkins, Philadelphia.

Eter, N., 2010. Molecular imaging in the eye. Br. J. Ophthalmol. 94 (11), 1420–1426.

Fraunfelder, F., Fraunfelder, F., 2004. Adverse ocular drug reactions recently identified by the National Registry of Drug-Induced Ocular Side Effects. Ophthalmology 111 (7), 1275–1279.

Fraunfelder, F.T., Fraunfelder, F.W., Chambers, W.A., 2008. Clinical Ocular Toxicology: Drug-Induced Ocular Side Effects, first ed. Saunders, Philadelphia, PA.

Gellatt, K.N., 2007. Veterinary Pathology. Blackwell, Ames, IA. 4ed.

Glass, A.S., Dahm, R., 2004. The zebrafish as a model organism for eye development. Ophthalmic Res. 36 (1), 4–24.

Gross, J.M., Perkins, B.D., 2008. Zebrafish mutants as models for congenital ocular disorders in humans. Mol. Reprod. Dev. 75 (3), 547–555.

Hu, D.N., Savage, H.E., Roberts, J.E., 2002. Uveal melanocytes, ocular pigment epithelium, and Müller cells in culture: *in vitro* toxicology. Int. J. Toxicol. 21 (6), 465–472.

Ikeda, Y., Takahashi, S., Kimura, J., Cho, Y.M., Imaida, K., Shirai, S., 1999. Anophthalmia in litters of female rats treated with the food-derived carcinogen, 2-amino-1-methyl-6-phenylimidazo [4, 5-b] pyridine. Toxicol. Pathol. 27 (6), 628–631.

Jancevski, M., Foster, C.S., 2010. Anterior Segment Optical Coherence Tomography. Semin. Ophthalmol. 25 (5–6), 317–323.

Latendresse, J.R., Warbrittion, A.R., Jonassen, H., Creasy, D.M., 2002. Fixation of testes and eyes using a modified Davidson's fluid: comparison with Bouin's fluid and conventional Davidson's fluid. Toxicol. Pathol. 30 (4), 524–533.

Leblanc, B., Jezequel, S., Davies, T., Hanton, G., Taradach, C., 1998. Binding of drugs to eye melanin is not predictive of ocular toxicity. Regul. Toxicol. Pharmacol. 28, 124–132.

Lee, S.S., Hughes, P., Ross, A.D., Robinson, M.R., 2010. Biodegradable implants for sustained drug release in the eye. Pharm. Res. 27 (10), 2043–2053.

Maeda, N., 2010. Optical coherence tomography for corneal diseases. Eye & Contact Lens 36 (5), 254–259.

Montezuma, S.R., Vavvas, D., Miller, J.W., 2009. Review of the Ocular Angiogenesis Animal Models. Semin. Ophthalmol. 24 (2), 52–61.

Niederkorn, J.Y., 2006. See no evil, hear no evil, do no evil: the lessons of immune privilege. Nat. Immunol. 7 (4), 354–359.

Smith, R.S., Smith, R.S., 2002. Systematic evaluation of the mouse eye, first ed. CRC Press, Boca Raton, FL.

Short, B.G., 2008. Safety evaluation of ocular drug delivery formulations: techniques and practical considerations. Toxicol. Pathol. 36 (1), 49–62.

Stein-Streilein, J., 2005. A privileged view of NKT cells and peripheral tolerance through the eye. Ocul. Immunol. Inflamm. 13 (2–3), 111–117.

Stone, R.A., Khurana, T.S., 2010. Gene profiling in experimental models of eye growth: clues to myopia pathogenesis. Vision Res. 50 (23), 2322–2333.

Streilein, J.W., 2003. Ocular immune privilege: therapeutic opportunities from an experiment of nature. Nat. Rev. Immunol. 3 (11), 879–889.

Tsonis, P.A., 2008. Animal Models in Eye Research, first ed. Academic Press, Amsterdam, The Netherlands.

Zhang-Hoover, J., Stein-Streilein, J., 2007. Therapies based on principles of ocular immune privilege. Chem. Immunol. Allergy 92, 317–327.


## Lacrimal System and Precorneal Tear Film


Barabino, S., Dana, M.R., 2004a. Animal models of dry eye: a critical assessment of opportunities and limitations. Invest. Ophthalmol. Vis. Sci. 45 (6), 1641–1646.

Barabino, S., Chen, W., Dana, M.R., 2004b. Tear film and ocular surface tests in animal models of dry eye: uses and limitations. Exp. Eye Res. 79 (5), 613–621.

Chen, H.B., Yamabayashi, S., Ou, B., Tanaka, Y., Ohno, S., Tsukahara, S., 1997. Structure and composition of rat

precorneal tear film. A study by an *in vivo* cryofixation. Invest. Ophthalmol. Vis. Sci. 38 (2), 381–387.

Ding, C., Parsa, L., Nandoskar, P., Zhao, P., Wu, K., Wang, Y., 2010. Duct system of the rabbit lacrimal gland: structural characteristics and role in lacrimal secretion. Invest. Ophthalmol. Vis. Sci. 51 (6), 2960–2967.

Green-Church, K.B., Butovich, I., Willcox, M., Borchman, D., Paulsen, F., Barabino, S., et al., 2011. The International Workshop on Meibomian Gland Dysfunction: Report of the Subcommittee on Tear Film Lipids and Lipid–Protein Interactions in Health and Disease. Invest. Ophthalmol. Vis. Sci. 52 (4), 1979–1993.

Gumus, K., Crockett, C.H., Rao, K., Yeu, E., Weikert, M.P., Shirayama, M., et al., 2011. Noninvasive assessment of tear stability with the tear stability analysis system in tear dysfunction patients. Invest. Ophthalmol. Vis. Sci. 52 (1), 456–461.

Holly, F.J., 1993. Diagnostic methods and treatment modalities of dry eye conditions. Int. Ophthalmol. 17 (3), 113–125.

Knop, E., Knop, N., Millar, T., Obata, H., Sullivan, D.A., 2011. The International Workshop on Meibomian Gland Dysfunction: Report of the Subcommittee on Anatomy, Physiology, and Pathophysiology of the Meibomian Gland. Invest. Ophthalmol. Vis. Sci. 52 (4), 1938–1978.

Paulsen, F.P., Berry, M.S., 2006. Mucins and TFF peptides of the tear film and lacrimal apparatus. Prog. Histochem. Cytochem. 41 (1), 1–53.

Schechter, J.E., Warren, D.W., Mircheff, A.K., 2010. A lacrimal gland is a lacrimal gland, but rodents and rabbits are not human. Ocul. Surf. 8 (3), 111–134.

Schrader, S., Mircheff, A., Geerling, G., 2008. Animal models of dry eye. Dev. Ophthalmol. 41, 298–312.

Tiffany, J., 2008. The normal tear film. Dev. Ophthalmol. 41, 1–20.

Wang, J., Fonn, D., Simpson, T.L., Jones, L., 2003. Precorneal and pre-and postlens tear film thickness measured indirectly with optical coherence tomography. Invest. Ophthalmol. Vis. Sci. 44 (6), 2524–2528.

## Cornea and Conjunctiva

Bundoc, V.G., Keane-Myers, A., 2003. Animal models of ocular allergy. Curr. Opin. Allergy Clin. Immunol. 3 (5), 375.

Collin, S.P., Collin, H.B., 1998. A comparative study of the corneal endothelium in vertebrates. Clin. Exp. Optom. 81 (6), 245–254.

Eggeling, P., Pleyer, U., Hartmann, C., Rieck, P.W., 2000. Corneal endothelial toxicity of different lidocaine concentrations. J. Cataract Refract. Surg. 26 (9), 1403–1408.

Ellenberg, D., Azar, D.T., Hallak, J.A., Tobaigy, F., Han, K.Y., Jain, S., et al., 2010. Novel aspects of corneal angiogenic and lymphangiogenic privilege. Prog. Retin. Eye Res. 29 (3), 208–248.

Fraunfelder, F., 2006. Corneal toxicity from topical ocular and systemic medications. Cornea 25 (10), 1133.

Groneberg, D., Bielory, L., Fischer, A., Bonini, S., Wahn, U., 2003. Animal models of allergic and inflammatory conjunctivitis. Allergy 58 (11), 1101–1113.

Jester, J.V., Molai, A., Petroll, W.M., Parker, R.D., Carr, G.J., Cavanagh, H.D., et al., 2000. Quantitative characterization of acid-and alkali-induced corneal injury in the low-volume eye test. Toxicol. Pathol. 28 (5), 668–678.

Marquart, M.E., 2011. Animal Models of Bacterial Keratitis. J. Biomed. Biotechnol. 2011, 680642.

Maurer, J.K., Molai, A., Parker, R.D., Li, L., Carr, G.J., Petroll, W.M., Cavanagh, H.G., Jester, J.V., 2001a. Pathology of Ocular Irritation with Acetone, Cyclohexanol, Parafluoroaniline, and Formaldehyde in the Rabbit Low-Volume Eye Test. Toxicol. Pathol. 29 (2), 187–199.

Maurer, J.K., Molai, A., Parker, R.D., Li, L., Carr, G.J., Petroll, W.M., Cavanagh, H.G., Jester, J.V., 2001b. Pathology of ocular irritation with bleaching agents in the rabbit low-volume eye test. Toxicol. Pathol. 29 (3), 308–319.

Maurer, J.K., Parker, R.D., 2000. Microscopic changes with acetic acid and sodium hydroxide in the rabbit low-volume eye test. Toxicol. Pathol. 28 (5), 679–687.

Newkirk, K.M., Chandler, H.L., Parent, A.E., Young, D.C., Colitz, C.M.H., Wilkie, D.A., et al., 2007. Ultraviolet radiation-induced corneal degeneration in 129 mice. Toxicol. Pathol. 35 (6), 817–824.

Parikh, C., Edelhauser, H., 2003. Ocular surgical pharmacology: corneal endothelial safety and toxicity. Curr. Opin. Ophthalmol. 14 (4), 178.

Pauly, A., Brignole-Baudouin, F., Labbé, A., Liang, H., Warnet, J.M., Baudouin, C., 2007. New tools for the evaluation of toxic ocular surface changes in the rat. Invest. Ophthalmol. Vis. Sci. 48 (12), 5473–5483.

Peng, Y., Ang, M., Foo, S., Lee, W.S., Ma, Z., Venkatraman, S.S., Wong, T.T., 2011. Biocompatibility and Biodegradation Studies of Subconjunctival Implants in Rabbit Eyes. PLoS ONE 6 (7), 1–11.

Reichl, S., Koolln, C., Hahne, M., Verstraelen, J., 2011. *In vitro* cell culture models to study the corneal drug absorption. Expert Opin. Drug Metab. Toxicol. 7 (5), 559–578.

Schein, O.D., 1992. Phototoxicity and the cornea. J. National. Med. Assoc. 84 (7), 579–583.

Steven, P., Gebert, A., 2009. Conjunctiva-associated lymphoid tissue – current knowledge, animal models and experimental prospects. Ophthalmic Res. 42 (1), 2–8.

Vinardell, M., Mitjans, M., 2008. Alternative methods for eye and skin irritation tests: an overview. J. Pharm. Sci. 97 (1), 46–59.

York, M., Steiling, W., 1998. A critical review of the assessment of eye irritation potential using the Draize rabbit eye test. J. Appl. Toxicol. 18 (4), 233–240.

Zheng, X., Ohashi, Y., 2002. Understanding corneal endotheliitis: An animal model approach. Int. Ophthalmol. Clin. 42 (1), 151.

## Uvea

Bodaghi, B., Rao, N., 2008. Relevance of animal models to human uveitis. Ophthalmic Res. 40 (3-4), 200–202.

Caspi, R.R., Silver, P.B., Luger, D., Tang, J., Cortes, L.M., Pennesi, G., Mattapallil, M.J., Chan, C.C., 2008. Mouse models of experimental autoimmune uveitis. Ophthalmic Res. 40 (3-4), 169–174.

Curnow, S.J., Murray, P.I., 2006. Inflammatory mediators of uveitis: cytokines and chemokines. Curr. Opin. Ophthalmol. 17 (6), 532.

Do, C.W., Civan, M.M., 2009. Species variation in biology and physiology of the ciliary epithelium: similarities and differences. Exp. Eye Res. 88 (4), 631–640.

Johnson, D.H., 2005. Trabecular meshwork and uveoscleral outflow models. J. Glaucoma. 14 (4), 308–310.

Sinha, D.P., Cartwright, M.E., Johnson, R.C., 2006. Incidental mononuclear cell infiltrate in the uvea of cynomolgus monkeys. Toxicol. Pathol. 34 (2), 148–151.

Smith, J.R., Hart, P.H., Williams, K.A., 1998. Basic pathogenic mechanisms operating in experimental models of acute anterior uveitis. Immunol. Cell Biol. 76 (6), 497–512.

Wildner, G., Diedrichs-Möhring, M., Thurau, S.R., 2008. Rat models of autoimmune uveitis. Ophthalmic Res. 40 (3-4), 141–144.

## Lens

Augusteyn, R.C., 2008. Growth of the lens: *in vitro* observations. Clin. Exp. Optom. 91 (3), 226–239.

Graw, J., 2009. Mouse models of cataract. J. Genet. 88 (4), 469–486.

Shearer, T.R., Ma, H., Fukiage, C., Azuma, M., 1997. Selenite nuclear cataract: review of the model. Mol. Vis. 23, 3–8.

Yoshizawa, K., Oishi, Y., Nambu, H., Yamamoto, D., Yang, J., Senzaki, H., Miki, H., Tsubara, A., 2000. Cataractogenesis in neonatal Sprague-Dawley rats by N-methyl-N-nitrosourea. Toxicol. Pathol. 28 (4), 555–564.

## Retina

Baehr, W., Frederick, J.M., 2009. Naturally occurring animal models with outer retina phenotypes. Vision Res. 49 (22), 2636–2652.

Barnett, J.M., Yanni, S.E., Penn, J.S., 2009. The development of the rat model of retinopathy of prematurity. Doc. Ophthalmol. 120 (1), 3–12.

Bringmann, A., Wiedemann, P., 2012. Müller Glial Cells in Retinal Disease. Ophthalmologica 227 (1), 1–19.

Caine, R., Albert, D.M., Lahav, M., Bullock, J., 1975. Oxalate retinopathy: an experimental model of a flecked retina. Invest. Ophthalmol. 14 (5), 359–363.

Dalke, C., Graw, J., 2005. Mouse mutants as models for congenital retinal disorders. Exp. Eye Res. 81 (5), 503–512.

Fletcher, E.L., Jobling, A.I., Vessey, K.A., Luu, C., Guymer, R., Baird, P., 2011. Animal models of retinal disease. Prog. Mol. Biol. Transl. Sci. 100, 211–286.

Goldstein, M., Zemel, E., Loewenstein, A., Perlman, I., 2006. Retinal toxicity of indocyanine green in albino rabbits. Invest. Ophthalmol. Vis. Sci. 47 (5), 2100–2107.

Grossniklaus, H.E., Kang, S.J., Berglin, L., 2010. Animal models of choroidal and retinal neovascularization. Prog. Retin. Eye Res. 29 (6), 500–519.

Kiuchi, K., Yoshizawa, K., Shikata, N., Moriguchi, K., Tsubura, A., 2002. Morphologic characteristics of retinal degeneration induced by sodium iodate in mice. Curr. Eye Res. 25 (6), 373–379.

Labriola, L.T., Jeng, D., Fawzi, A.A., 2012. Retinal Toxicity of Systemic Medications. Int. Ophthalmol. Clin. 52 (1), 149.

Li, J., Tripathi, R.C., Tripathi, B.J., 2008. Drug-induced ocular disorders. Drug Saf. 31 (2), 127–141.

Maurice, D., 2001. Review: practical issues in intravitreal drug delivery. J. Ocul. Pharmacol. Ther. 17 (4), 393–401.

Mecklenburg, L., Schraermeyer, U., 2007. An overview on the toxic morphological changes in the retinal pigment epithelium after systemic compound administration. Toxicol. Pathol. 35 (2), 252–267.

Michaelides, M., Stover, N.B., Francis, P.J., Weleber, R.G., 2001. Toxicity Associated With Hydroxychloroquine and Chloroquine Risk Factors, Screening, and Progression Despite Cessation of Therapy. Arch. Ophthalmol. 129 (1), 30–39.

Penha, F.M., Rodrigues, E.B., Maia, M., Dib, E., Fiod Costa, E., Furlani, B.A., Nunes Moraes Filho, M., Dreyfuss, J.L., Bottós, J., Farah, M.E., 2010a. Retinal and Ocular Toxicity in Ocular Application of Drugs and Chemicals – Part I: Animal Models and Toxicity Assays. Ophthalmic Res. 44 (2), 82–104.

Penha, F.M., Rodrigues, E.B., Maia, M., Furlani, B.A., Regatieri, C., Melo, G.B., Magalhães Jr., O., Manzano, R., Farah, M.E., 2010b. Retinal and Ocular Toxicity in Ocular Application of Drugs and Chemicals – Part II: Retinal Toxicity of Current and New Drugs. Ophthalmic Res. 44 (4), 205–224.

Penha, F.M., Rodrigues, E.B., Furlani, B.A., Dib, E., Melo, G.B., Farah, M.E., 2011. Toxicological considerations for intravitreal drugs. Expert Opin. Drug Metab. Toxicol. 7 (8), 1021–1034.

Perlman, I., 2009. Testing retinal toxicity of drugs in animal models using electrophysiological and morphological techniques. Doc. Ophthalmol. 118 (1), 3–28.

Puthussery, T., Taylor, W.R., 2010. Functional changes in inner retinal neurons in animal models of photoreceptor degeneration. Retin. Degener. Dis. 664, 525–532.

Rakoczy, P.E., Yu, M.J.T., Nusinowitz, S., Chang, B., Heckenlively, J.R., 2006. Mouse models of age-related macular degeneration. Exp. Eye Res. 82 (5), 741–752.

Ramkumar, H.L., Zhang, J., Chan, C.C., 2010. Retinal ultrastructure of murine models of dry age-related macular degeneration (AMD). Prog. Retin. Eye Res. 29 (3), 169–190.

Rao, G.N., 1991. Light intensity-associated eye lesions of Fischer 344 rats in long-term studies. Toxicol. Pathol. 19 (2), 148–155.

Rivas, M.A., Vecino, E., 2009. Animal models and different therapies for treatment of retinitis pigmentosa. Histol. Histopathol. 24 (10), 1295.

Scott, P.A., Kaplan, H.J., Sandell, J.H., 2011. Anatomical evidence of photoreceptor degeneration induced by iodoacetic acid in the porcine eye. Exp. Eye Res. 93 (4), 513–527.

Tehrani, R., Ostrowski, R.A., Hariman, R., Jay, W.M., 2008. Ocular toxicity of hydroxychloroquine. Semin. Ophthalmol. 23 (3), 201–209.

Torriglia, A., Valamanesh, F., Behar-Cohen, F., 2010. On the retinal toxicity of intraocular glucocorticoids. Biochem. Pharmacol. 80 (12), 1878–1886.

Yoshizawa, K., Kuro-Kuwata, M., Sasaki, T., Lai, Y.C.C., Kanematsu, S., Miki, H., et al., 2011. Retinal degeneration induced in adult mice by a single intraperitoneal injection of N-ethyl-N-nitrosourea. Toxicol. Pathol. 39 (4), 606–613.

Youssef, P., Sheibani, N., Albert, D., 2010. Retinal light toxicity. Eye 25 (1), 1–14.

Zeiss, C., 2010. Animals as models of age-related macular degeneration: an imperfect measure of the truth. Vet. Pathol. 47 (3), 396–413.

## Optic Nerve

Bernstein, S.L., Johnson, M.A., Miller, N.R., 2011. Nonarteritic anterior ischemic optic neuropathy (NAION) and its experimental models. Pro. Retin. Eye Res. 30 (3), 167–187.

Chan, K.C., Fu, Q., So, K., Wu, E.X., 2007. Evaluation of the visual system in a rat model of chronic glaucoma using manganese-enhanced magnetic resonance imaging. Engineering in Medicine and Biology Society, EMBS 29th Annual International Conference of the IEEE. 2007, 67–70.

Girkin, C.A., 2004. Relationship between structure of optic nerve/nerve fiber layer and functional measurements in glaucoma. Curr. Opin. Ophthalmol. 15 (2), 96–101.

Heywood, R., 1982. Histopathological and laboratory assessment of visual dysfunction. Environ. Health Perspect. 44, 35–45.

Holder, G., 2004. Electrophysiological assessment of optic nerve disease. Eye 18 (11), 1133–1143.

Kiosawa, I., 1996. Age-related changes in visual function and visual organs of rats. Exp. Anim. 45 (2), 103–114.

Levin, L.A., 2004. Extrapolation of animal models of optic nerve injury to clinical trial design. J. Glaucoma 13 (1), 1–5.

Levkovitch-Verbin, H., 2004. Animal models of optic nerve diseases. Eye 18 (11), 1066–1074.

May, C.A., 2008. Comparative anatomy of the optic nerve head and inner retina in non-primate animal models used for glaucoma research. Open Ophthalmol. J. 9 (2), 94–101.

Melamud, A., Kosmorsky, G.S., Lee, M.S., 2003. Ocular ethambutol toxicity. Mayo Clin. Proc. 78 (11), 1409–1411.

Morrison, J.C., Cepurna, Ying Guo, W.O., Johnson, E.C., 2011. Pathophysiology of human glaucomatous optic nerve damage: Insights from rodent models of glaucoma. Exp. Eye Res. 93 (2), 156–164.

Salgado, C., Vilson, F., Miller, N.R., Bernstein, S.L., 2011. Cellular Inflammation in Nonarteritic Anterior Ischemic Optic Neuropathy and Its Primate Model. Arch. Ophthalmol. 129 (12), 1583.

Salinas-Navarro, M., Alarcón-Martínez, L., Valiente-Soriano, F.J., Jiménez-López, M., Mayor-Torroglosa, S., Avilés-Trigueros, M., Villegas-Perez, M.P., Vidal-Sanz, M., 2010. Ocular hypertension impairs optic nerve axonal transport leading to progressive retinal ganglion cell degeneration. Exp. Eye Res. 90 (1), 168–183.

Sanfilippo, P.G., Cardini, A., Hewitt, A.W., Crowston, J.G., Mackey, D.A., 2009. Optic disc morphology-Rethinking shape. Prog. Retin. Eye Res. 28 (4), 227–248.

Vidal-Sanz, M., Salinas-Vavarro, M., Nadal-Nicolas, F.M., Alarcon- Martinez, L., Valiente-Soriano, F.J., de Imperial, J.M., Aviles- Trigueros, M., Agudo-Barriuso, M., Villegas-Perez, M.P., 2012. Understanding glaucomatous damage: Anatomical and functional data from ocular hypertensive rodent retinas. Prog. Retin. Eye Res. 31 (1), 1–27.

Williams, P., Morgan, J., Votruba, M., 2011. Mouse models of dominant optic atrophy: What do they tell us about the pathophysiology of visual loss? Vision Res. 51 (2), 229–234.

Xu, J., Sun, S.W., Naismith, R.T., Snyder, A.Z., Cross, A.H., Song, S.K., 2008. Assessing optic nerve pathology with diffusion MRI: from mouse to human. NMR Biomed. 21 (9), 928–940.

You, Y., Klistorner, A., Thie, J., Graham, S.L., 2011. Latency delay of visual evoked potential is a real measurement of demyelination in a rat model of optic neuritis. Invest. Ophthalmol. Vis. Sci. 52 (9), 6911–6918.

Zhang, X., Jones, D., Gonzalez-Lima, F., 2002. Mouse model of optic neuropathy caused by mitochondrial complex I dysfunction. Neurosci. Lett. 326 (2), 97–100.

## Glaucoma

Goldblum, D., Mittag, T., 2002. Prospects for relevant glaucoma models with retinal ganglion cell damage in the rodent eye. Vision Res. 42 (4), 471–478.

Johnson, T.V., Tomarev, S.I., 2010. Rodent models of glaucoma. Brain Res. Bull. 81 (2–3), 349–358.

McKinnon, S.J., Schlamp, C.L., Nickells, R.W., 2009. Mouse models of retinal ganglion cell death and glaucoma. Exp. Eye Res. 88 (4), 816–824.

Morrison, J.C., 2005. Elevated intraocular pressure and optic nerve injury models in the rat. J. Glaucoma. 14 (4), 315.

Rasmussen, C.A., Kaufman, P.L. Primate glaucoma models. J. Glaucoma 14(4), 311–314

Salmon, J.F., Kanski, J.J., 2004. Glaucoma. A colour manual of diagnosis and treatment, third ed. Butterworth-Heinemann Medical, Edinburgh, UK. 168.

Tombran-Tink, J., Barnstable, C.J., Shields, B.M., 2008. Mechanisms of the Glaucomas: Disease Processes and Therapeutic Modalities, first ed. Humana Press, Totowa, NJ.